GEM TN-92-139

Higgs to Gamma Gamma Task Force Meeting - SSCL

August 4, 1992

Abstract:

Attendees, minutes and presentations of the GEM $H^0 \rightarrow \gamma\gamma$ Task Force Meeting held at the SSC Laboratory on August 4, 1992.

$H^0 \to \gamma\gamma$ Task Force Meeting

August 4, 1992

Abstract

Transparencies of the $H^0 \to \gamma\gamma$ Task Force meeting held on August 4, 1992 at the SSC Laboratory are presented.

Minutes of the meeting

Gena Mitselmakher started meeting with a discussion of the goals of this group. There are two deadlines for the presentation of the results. The first is early in september - before the GEM decision on calorimeter choice. The final deadline is the GEM presentation for the PAC meeting in November. Gena suggested to incorporate all the experience of $H^0 \to \gamma\gamma$ studies including those done for the LHC.

Renyuan Zhu presented a two hour talk on his results in $H^0 \to \gamma\gamma$ studies (see enclosed transparencies). He made comments on the both PAC questions:

a) Recent experimental data agree well with PYTHIA predictions. Thus the factor of 5 uncertainty in jet background cannot be justified

b) simple calculation shows that random vertex choice will be correct in more than 50% of cases.

Several comments were made during Renyan's talk:

Harvey Newman mentioned that RD3 collaboration get the 0.6% constant term in liquid argon calorimeter resolution for the semi-projective accordion. Yuri Kamyshkov quoted published RD3 value of 0.3% for the non-projective accordion.

Frank Paige suggested to use different significance calculation for the $H^0 \to \gamma\gamma$ search. He quoted Sally Dawson advise to use the 1.5 K-factor in H^0cross-section as the simulated background effectively includes such a factor.

Harvey Newman noted that at the LHC bremstrahlung dominates the background.

Frank Paige noted that Figure 2 from Renyuan's presentation looks too clean. There should be some particles compensating the 32 GeV mean p_T of the H^0. Renyuan acknowledged that the shown event was selected from 10 events sample to demonstrate that H^0 events are clean comparative to the background events.

Tomasz Skwarnicki pointed out that Renyuan's cuts to reduce the "irreducible" background are irrelevant as they do not improve the significance. Renyuan acknowledged that some of these cuts are from acceptance and trigger requirements. Others are not optimized and that the Task Force should optimize cuts.

Tomasz also noted that isolation cuts may change the $M_{\gamma\gamma}$ distribution from the background events. (Renyuan assumed this mass distribution to be the same as parton-parton mass distribution.)

Harvey Newman encouraged Task Force to study more carefully the pileup issues. He warned that the pileup noise cancellation reported by Cleland may not work for real pulses.

Gena Mitselmakher stated that the factor of 5 in background uncertainty quoted by PAC was used in Aachen studies of 1990. This factor should be better now.

Tomasz Skwarnicki presented preliminary results of his $H^0 \rightarrow \gamma\gamma$ studies (see enclosed transparencies). Using different isolation algorithm he get a factor of 7 better rejection of the background in $\gamma - jet$ events. The significance of the H^0 signal is similar to the Renyuan values. This may indicate the discrepancy in their results.

Sasha Vanyashin made a comment that the 40 GeV cut on gamma with higher p_T do not reduce the $\gamma - jet$ background but will cut the $jet - jet$ background (see enclosed transparencies).

Kostya Shmakov presented his results on GEANT MC studies on vertex selection from calorimeter pointing (see enclosed transparencies). He got a 20% better significance than in a case with random vertex choice.

Howard Gordon presented the status of the noise calculations for the liquid calorimeter option (see enclosed transparencies).

Gena Mitselmakher discussed plans for the Task Force. We need to understand better the difference from SDC and LHC experiments.

Harvey Newman noted that it is very difficult to compare GEM with LHC due to an uncertain cost of LHC experiments.

Renyuan Zhu mentioned the need to study more pileup noise and to address trigger questions.

Michael Danilov advised to consider $H^0 \rightarrow \gamma\gamma$ as just an example. GEM need to consider more general questions of overall calorimeter optimization, e.g., with respect to γ/π^0 separation.

Higgs → 2γ Task force meeting 8/4/92

Name	Institution	Email Address	Fax
K. McFarlane	SSCL	mcfarlan@sscvx1	214-708-6088
A. Vanyashin	SSCL	VANYASHIN@SSCVX1	214-708-6088
K. Shmakov	Oak Ridge	SHMAKO@ORPHØ1	
X. Shi	Caltech	shi@cithex.bitnet	
Y. Kamyshkov	ORNL	KAMYSHKOV@SSCVX1	
Y. Guo	SSCL	GUO@SSCVX1	
R. Shang	SSCL	shang@sscvx1.	
H. Newman	Caltech	newman@cithex.bitnet	
Chunhua Jiang	IHEP of Beijing	JiangCH@SSCVX1	
Frank Paige	SSC	PAIGE@SSCVX1	
Tomasz Skwarnicki	SSCL/SMU	TOMASZ@SSCVX1	
Andrey Golutvin	SSCL/ITEP	Golutvin@SSCVX1	
Bill Bugg	Tennessee	BUGG@SLACVM	
J. Sheer	SSCL	sheer@SSCVX1	
G. Mitselmakher	SSCL	MITSELMAKHER@SSCVX1	
M. Danilov	ITEP	DANILOV@SSCVX1	
Gary Liu	Caltech	GL@CITHEX.Caltech.Edu	

(over)

3.2 Calorimetry

The committee is concerned about the GEM approach to calorimetry, as described in the various documents submitted for the July review (GEM Baseline 1 and responses to the December 1991 PAC Report):

1) The overriding concern is the ability of GEM electromagnetic calorimetry to identify photons. The GEM group aims at excellent electromagnetic energy resolution; however, the ability to reject jet backgrounds was given insufficient emphasis in the design. An impressive and very thorough study of GEM performance, focused on $H \rightarrow \gamma\gamma$, has been described in GEM-TN-92-126, for both electromagnetic calorimeter options. The results are summarized in Tables 13 and 14 of that document. Some comments follow:

   a) Jet backgrounds
   From Table 13, we can extract the excess jet background (from γ-jet and jet-jet), above the "irreducible" background, that remains after shower isolation and shape cuts; as compared to the "irreducible" backgrounds (from $\gamma\gamma$ + irreducible γ-jet and jet-jet). The expected rates correspond to 20pb for excess jet backgrounds versus 52pb for irreducible backgrounds with BaF_2, and 77pb for excess jet backgrounds versus 58pb for irreducible backgrounds with LAr. For a Higgs mass of 90 GeV, this corresponds to 4σ and 2σ significances for BaF_2 and LAr respectively, in one SSC year. The large uncertainties (of order of a factor of 5 or more) in the jet backgrounds indicate that even these levels of significance may not be achieved.

   b) Measurement of photon direction
   The BaF_2 calorimeter has no longitudinal segmentation and therefore does not provide a measurement of the photon direction. The selection of the highest multiplicity vertex as the primary Higgs vertex has not been demonstrated to be a solution to this problem.

   From these considerations, we are concerned that the GEM baseline design may not be adequate for $H \rightarrow \gamma\gamma$, and for γ-identification in general.

2) The engineering of a 1-mm Pb LAr accordion calorimeter is difficult and a large scale prototype may well be needed to evaluate the construction method as well as a realistic performance and cost.

3) A coherent (electromagnetic + hadronic) calorimeter design with its associated performance characteristics should be presented. For a hybrid option with scintillating fiber hadronic calorimetry, issues such as calibration, radiation damage monitoring, and overall calorimeter integration and performance should be addressed, including prototype test results wherever possible.

Renyuan Zhu

H$\rightarrow \gamma\gamma$ Study for GEM

Renyuan Zhu
Caltech

GEM Meeting

Dallas, August 4, 1992

- Signal and Background;
- Main Issues:
  - Higgs Vertex;
  - Calorimeter Radius;
  - Jet Background.

Energy Resolution of BaF_2 Calorimeter

$$(\frac{\Delta E}{E})^2 = (\frac{a_0}{E})^2 + (\frac{a_1}{\sqrt{E}})^2 + b^2$$

where

- a_0 is the contribution from electrical noise, summed over detector readout channels within a few Moliere radii around the center of the lateral shower distribution;

- a_1 is the contribution from the photoelectron statistics;

- the systematic term **b** has three contributions:

$$b^2 = b_n{}^2 + b_G{}^2 + b_C{}^2$$

  - b_G represents the geometry effect, including shower leakage at the front, side and back of the detector and inactive material between cells;

  - b_n represents physics noise, including fluctuations and uniformity of response from active media etc.;

  - b_C represents intercalibration error.

Energy Resolution of BaF_2 Calorimeter

E (GeV)	5	10	20	50	100	200	500
Thermal Noise	0.4	0.2	0.1	0.04	0.02	0.01	0.004
P.E.	0.2	0.14	0.1	0.063	0.045	0.03	0.02
b_G	0.60	0.43	0.32	0.30	0.30	0.30	0.36
b_C	0.40	0.40	0.40	0.40	0.40	0.40	0.40
Total	0.85	0.63	0.53	0.51	0.50	0.50	0.54

Event Acceptance

Dead Space:

- BaF_2 $|\eta| = 0 - 0.0525$ and $|\eta| = 1.308 - 1.428$;
- LAr $|\eta| = 1.18 - 1.39$.

Process	BaF_2(O)	BaF_2(P)	LAr(O)	LAr(P)	$\bar{\eta}$
$H \rightarrow \gamma\gamma$	0.95	0.86	0.87	0.83	0.49
$Ht\bar{t} \rightarrow \gamma\gamma\mu X$	0.86	0.77	0.77	0.74	0.16
$Ht\bar{t} \rightarrow \gamma\gamma eX$	0.93	0.81	0.79	0.74	0.16
$H \rightarrow ZZ^{\star} \rightarrow 4e$	0.91	0.75	0.73	0.67	0.45
$H \rightarrow ZZ \rightarrow 4e$	0.90	0.74	0.74	0.68	0.50

$$GA = \left(\frac{5. - \Delta\eta(dead)}{5.}\right)^{\#\ e's\ and\ \gamma's\ to\ detect}$$

Significance

- High Statistics:

$$S = \frac{N_S}{\sqrt{N_B}} = \frac{\int \mathcal{L}dt\ A_S\ RA\ 0.683\sigma_{H\to\gamma\gamma}}{\sqrt{\int \mathcal{L}dt\ A_B\ RA\ 2\sigma_{M_{\gamma\gamma}}\ R_B}} \propto \sqrt{\frac{RA\int \mathcal{L}dt}{\sigma_{M_{\gamma\gamma}}}}$$

- Low Statistics:

$$P_n(\lambda) = \frac{\lambda^n e^{-\lambda}}{n!}$$

where λ is the expected value, i.e. N_S for the signal and N_B for the background.

The probability of signal events caused by background fluctuation is:

$$Prob = \sum_{n=0}^{\infty} [P_n(N_B + N_S) \times \sum_{m=n}^{\infty} P_m(N_B)]$$

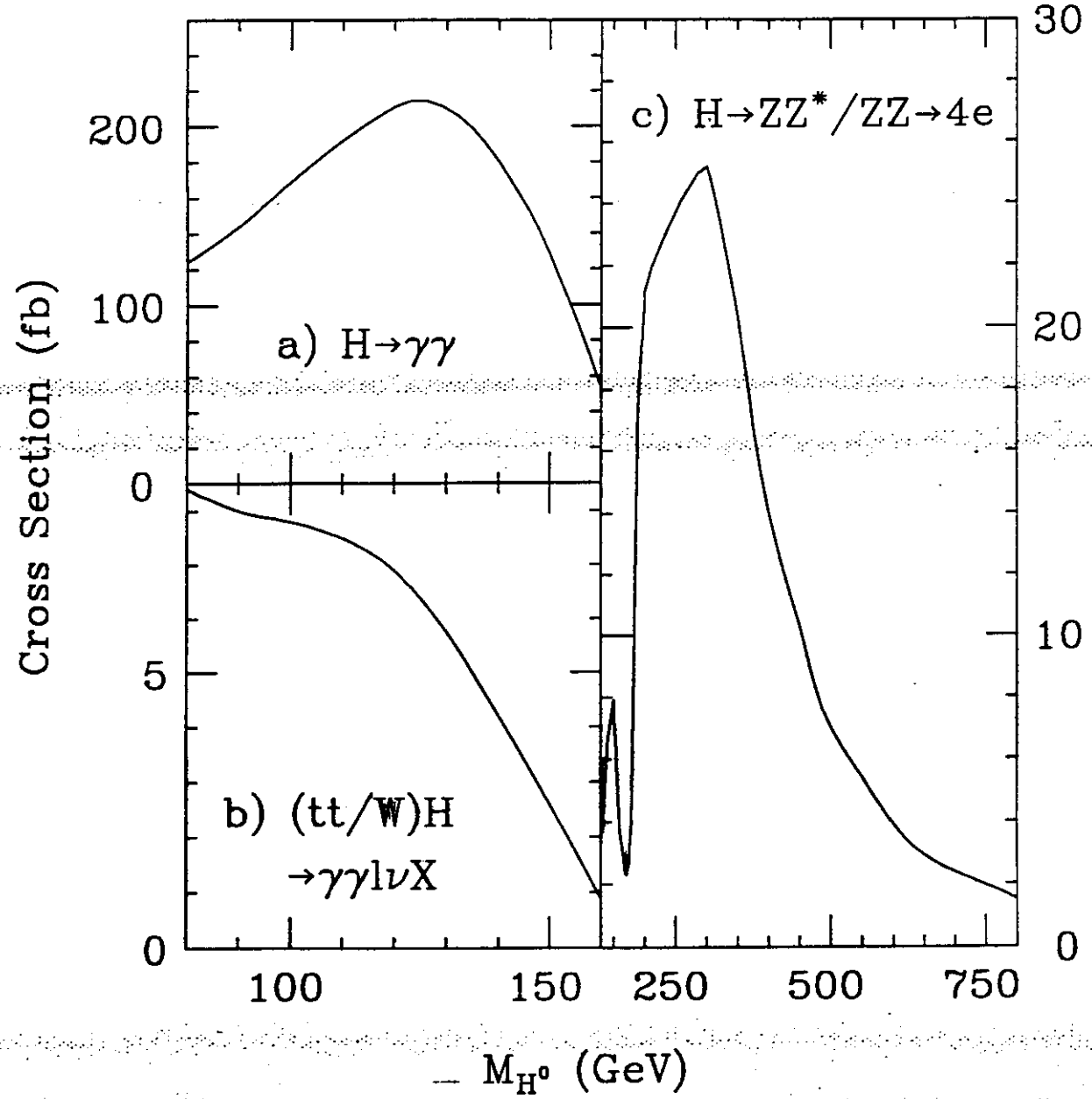
Cross Section (fb)
200
100
0
5
0
30
20
10
0
a) H→γγ
b) (tt/W)H
→γγlνX
c) H→ZZ*/ZZ→4e
100
150
250
500
750
M_H° (GeV)

Cross-Section (fb) and Events/SSCY

M_H	$\sigma_{H(\gamma\gamma)}$	$N_{\gamma\gamma}$	$\sigma_{\ell H(\gamma\gamma)}$	$N_{l\gamma\gamma}$	$\sigma_{H(4e)}$	N_{4e}
80	124	510	8.4	18		
90	144	610	8.0	20		
100	169	730	7.8	21		
120	211	990	6.9	18		
140	180	880	4.2	14	6.5	27
150	128	630	2.6	8	7.9	39
160	52.6	270	0.87	3	3.7	16
170					2.3	14

$H^0 \to \gamma\gamma$ Signal/Background

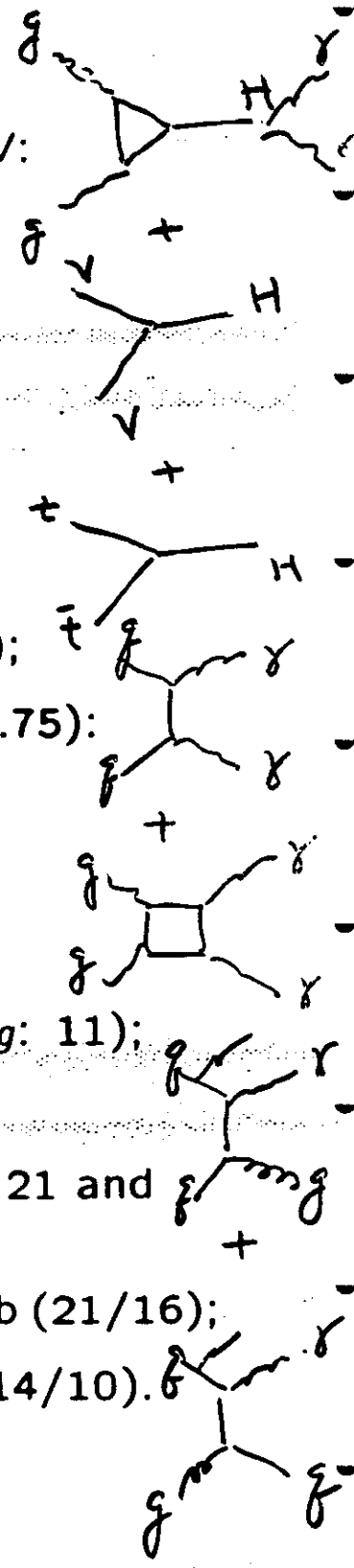

- Signal: 0.05–0.2 pb for $M_H \in (80,160)$GeV:
  - $|\eta_\gamma| < 2.5$;
  - $E_T > 20$ GeV;
  - $|\cos\theta^*_\gamma| < 0.9 \Rightarrow$ reduce gg $\to \gamma\gamma$;
  - $|\eta_{\gamma\gamma}| < 3 \Rightarrow$ reduce qq $\to \gamma\gamma$.
- Direct Photon Background:
  - 276 pb (gg$\to \gamma\gamma$: 198 and qq $\to \gamma\gamma$ 78);
  - After selection and isolation (5 GeV, 0.75): 32 pb for $M_{\gamma\gamma} \in (75, 165)$ GeV.
- QCD Background:
  - 2jets: 2 mb; $\to$
  - γ-jet: 237nb ($qg \to \gamma q$: 226 and $qq \to \gamma g$: 11);
  - After isolation: 23 and 20 pb (50/73);
  - After shower shape analysis (5 mrad): 21 and 16 pb (28/29);
  - After preradiator (2 mrad): 19 and 16 pb (21/16);
  - Irreduciable (single γ): 14 and 10 pb (14/10).

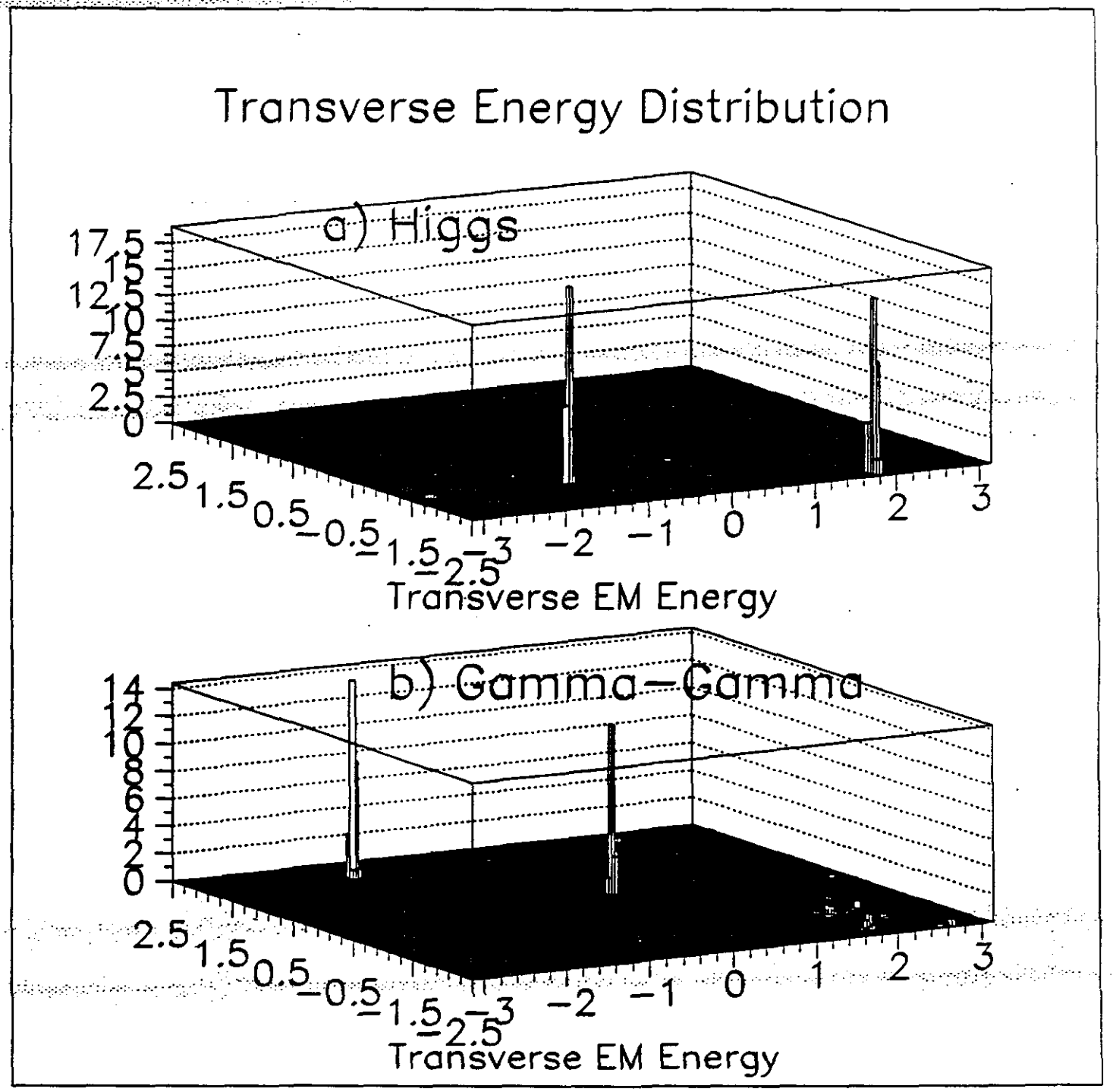

Figure 2: Transverse energy distributions in EMC for two typical events from signal process of H→ $\gamma\gamma$ (a) and irreducible background process $\gamma\gamma$ (b).

Events Selection ($H \to \gamma\gamma$)

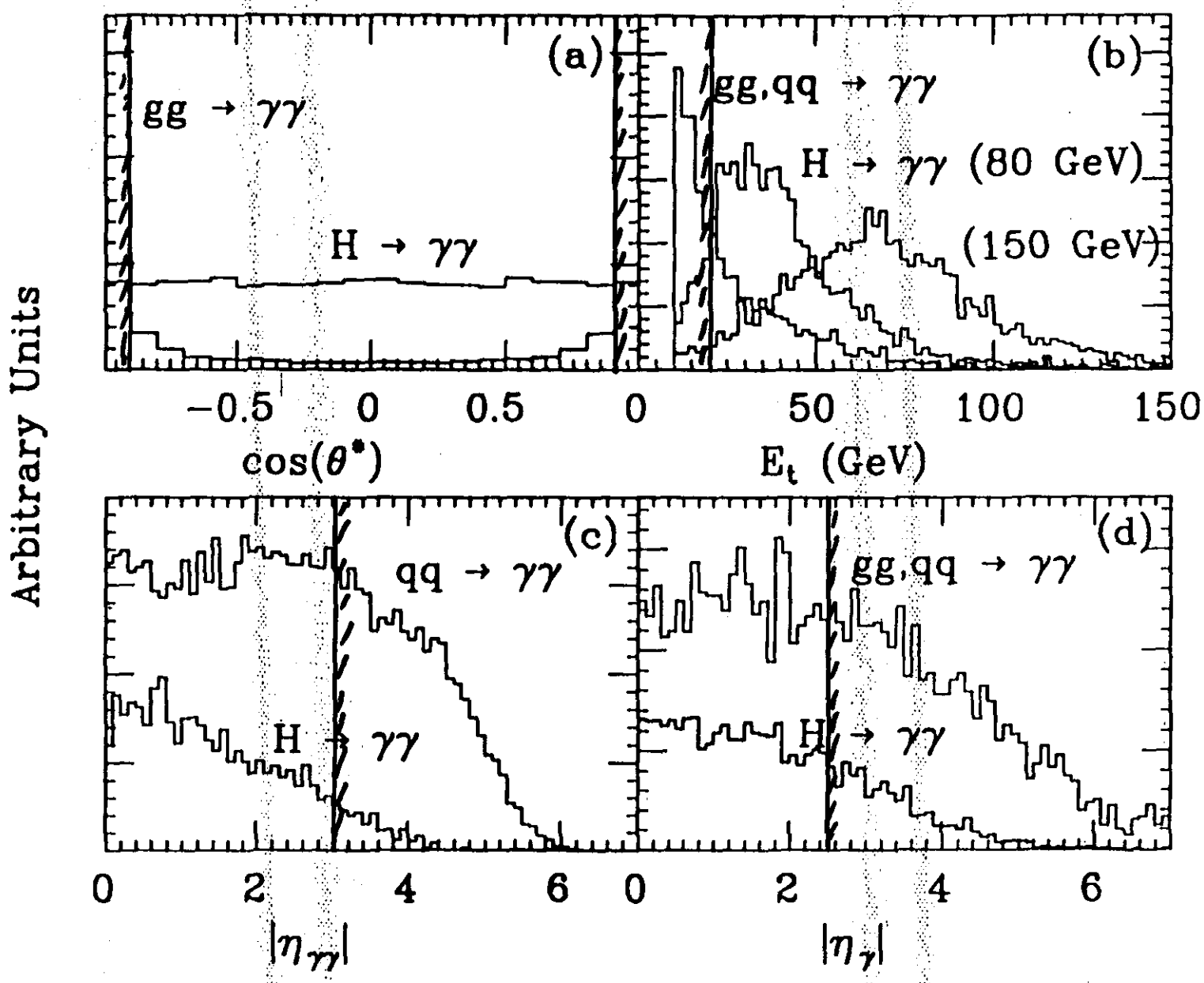

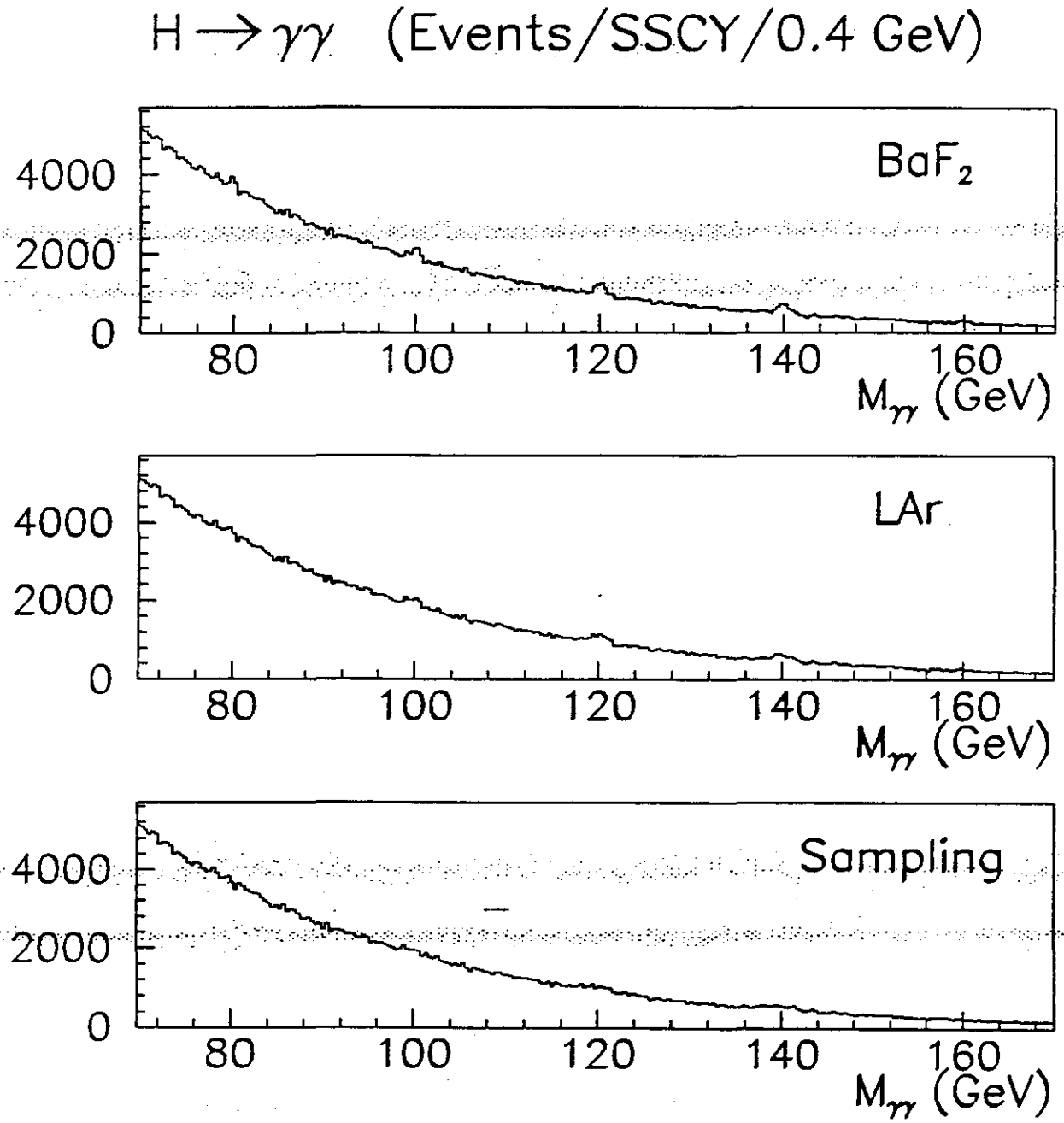
H → γγ (Events/SSCY/0.4 GeV)
BaF2
LAr
Sampling
4000
2000
0
80
100
120
140
160
Mγγ (GeV)

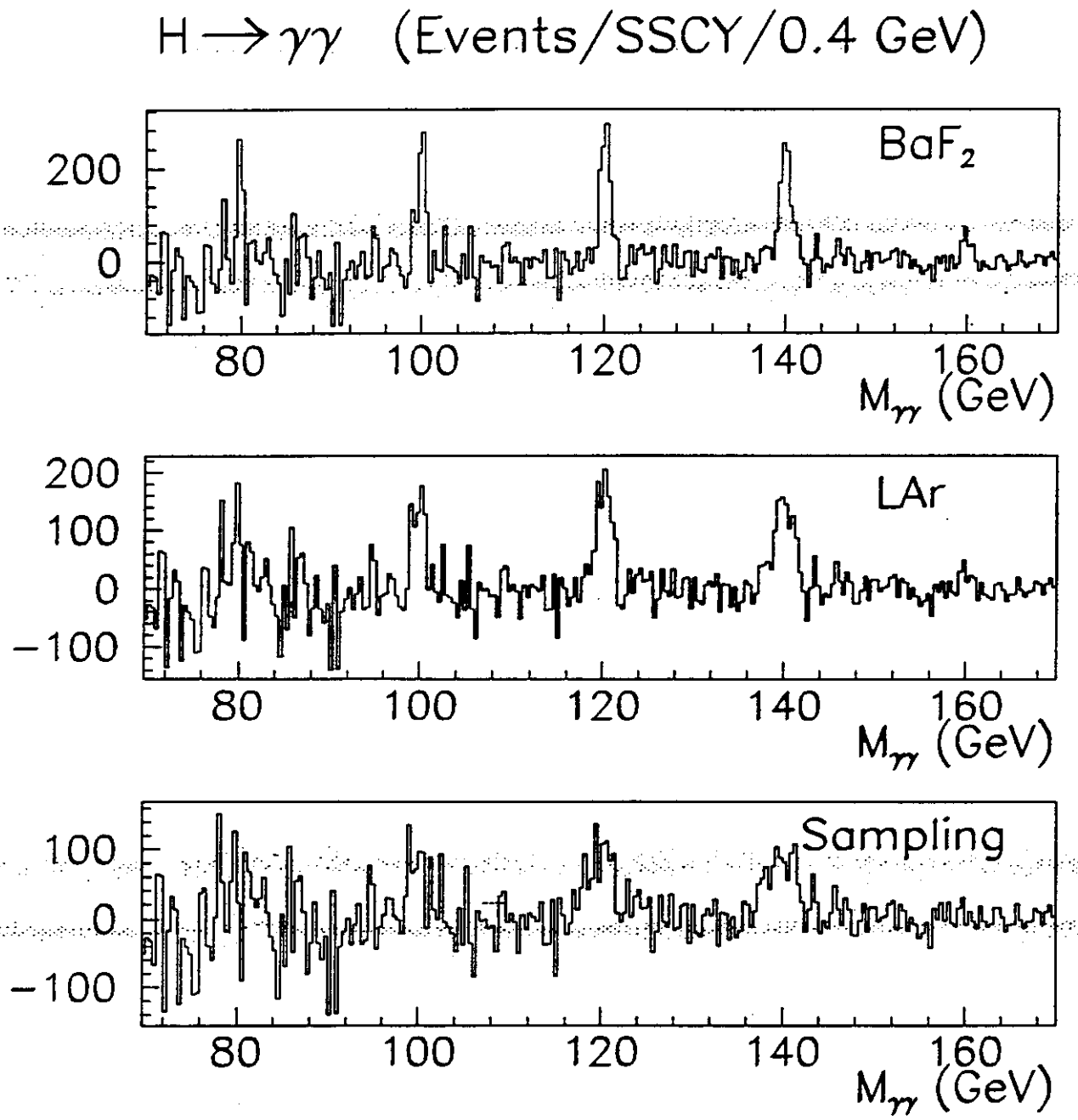
H → γγ (Events/SSCY/0.4 GeV)
BaF2
200
0
80
100
120
140
160
Mγγ (GeV)
LAr
200
100
0
−100
80
100
120
140
160
Mγγ (GeV)
Sampling
100
0
−100
80
100
120
140
160
Mγγ (GeV)

$H^0 \rightarrow \gamma\gamma$ Significance

with Irreducible Background in One SSCY

$\Delta E/E$ (%)			$2/\sqrt{E} \oplus 0.5$		$7.5/\sqrt{E} \oplus 0.5$		$15/\sqrt{E} \oplus 1.0$	
M_H (GeV)	$\sigma_{\gamma\gamma}$ (fb)	N_S	$\sigma_{M_{\gamma\gamma}}$ (GeV)	S	$\sigma_{M_{\gamma\gamma}}$ (GeV)	S	$\sigma_{M_{\gamma\gamma}}$ (GeV)	S
80	124	360	0.34	4.6	0.66	3.2	1.3	2.3
90	144	430	0.37	6.1	0.70	4.5	1.4	3.2
100	169	510	0.40	8.6	0.73	6.3	1.45	4.5
120	211	690	0.45	14	0.77	11	1.5	7.7
140	180	620	0.53	16	0.89	12	1.7	8.9
150	128	450	0.58	13	0.95	10	1.9	7.3
160	52.6	190	0.65	5.9	1.1	4.7	2.0	3.4

Significance of $H \rightarrow \gamma\gamma$

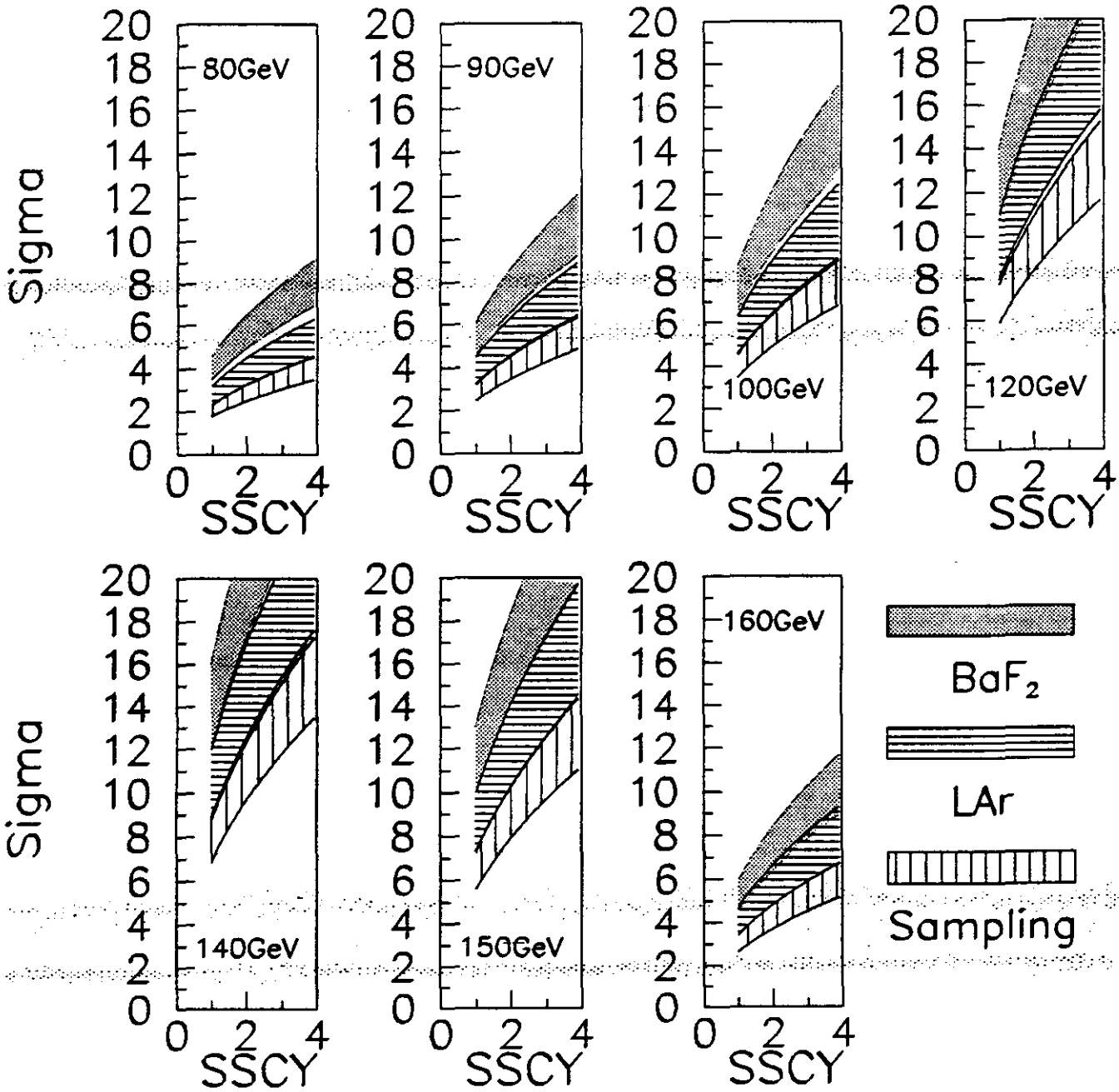

Ratio of H$\rightarrow \gamma\gamma$ Peak Width

as Function of a and b

a	2.0	3.0	5.5	7.5	10	15
M_H = 80 GeV						
b=0.5	1.0	1.1	1.5	1.9	2.4	3.4
b=.75	1.4	1.5	1.7	2.1	2.6	3.6
b=1.0	1.8	1.8	2.1	2.4	2.8	3.8
b=1.5	2.6	2.6	2.8	3.1	3.4	4.2
b=2.0	3.4	3.5	3.6	3.8	4.1	4.8
M_H = 150 GeV						
b=0.5	1.0	1.1	1.3	1.6	2.0	2.8
b=.75	1.4	1.5	1.7	1.9	2.3	3.0
b=1.0	1.8	1.9	2.0	2.2	2.5	3.2
b=1.5	2.6	2.7	2.8	3.0	3.2	3.7
b=2.0	3.6	3.6	3.7	3.8	4.0	4.4

Ratio of H$\rightarrow \gamma\gamma$ Peak Width

as Function of δx, a and b.

δx (mm)		0.5	1.0	1.5	2.0	2.5	3.0
a=2	b=0.5	0.97	1.0	1.0	1.1	1.1	1.2
a=5.5	b=0.5	1.5	1.5	1.5	1.6	1.6	1.6
a=7.5	b=0.5	1.9	1.9	1.9	1.9	2.0	2.0
a=15	b=3.7	3.8	3.8	3.8	3.8	3.8	3.8

as Function of δz, a and b.

δz (mm)		1.0	2.0	3.0	5.0	10.	50.
a=2	b=0.5	1.0	1.0	1.1	1.1	1.5	5.4
a=5.5	b=0.5	1.5	1.5	1.6	1.6	1.9	5.5
a=7.5	b=0.5	1.9	1.9	1.9	2.0	2.2	5.6
a=15	b=1.0	3.8	3.8	3.8	3.8	3.9	6.5

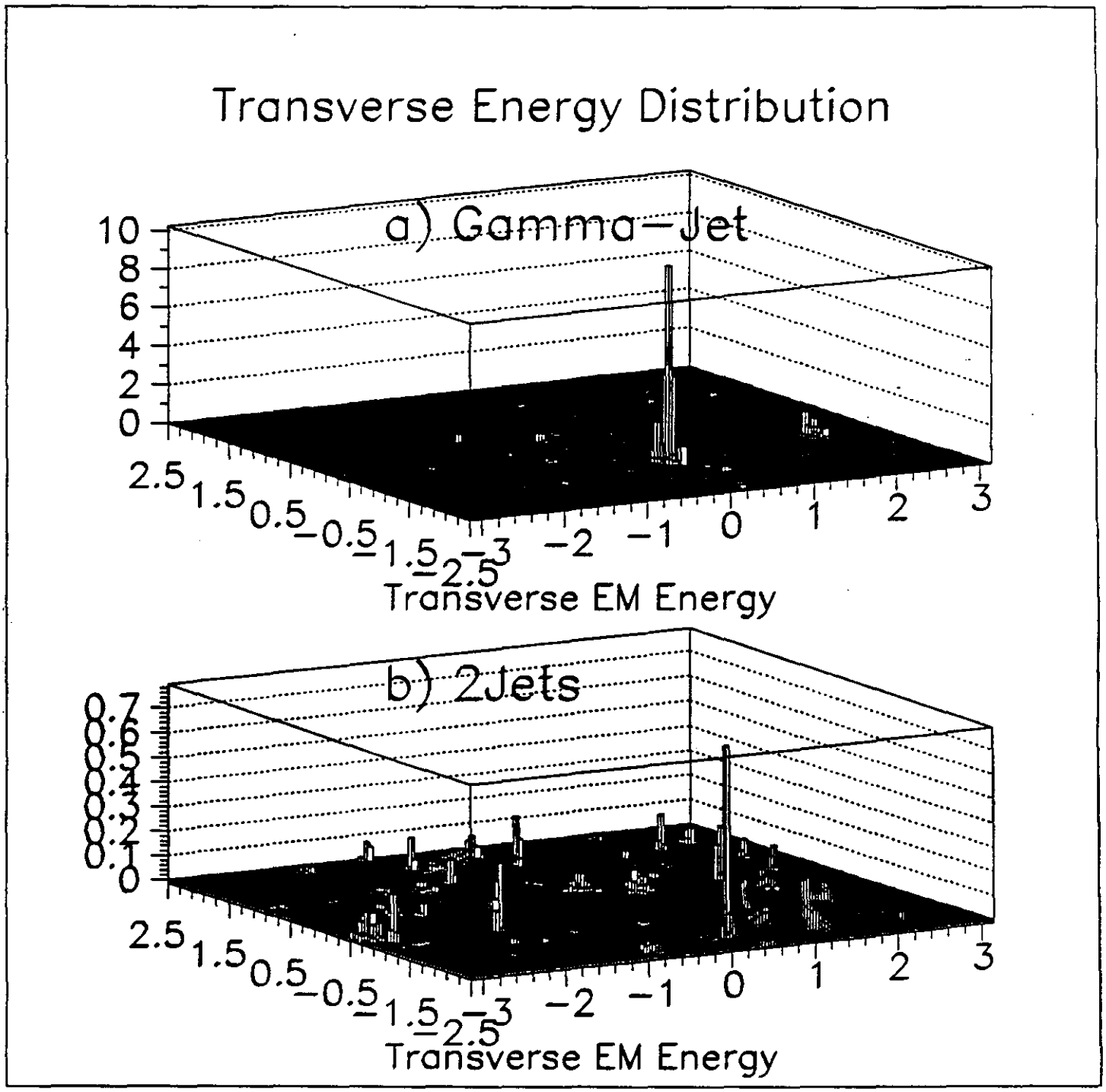

Figure 5: Transverse energy distributions in EMC for two typical events from background processes: (a) γ-jet and (b) 2jets.

Isolation Cut

- Generate 2jets or γ-jet with PYTHIA5.5, deposit all EM energy and part of hadron energy (from GEANT) in calorimeter cells with parametrized shower spread. Record cell numbers hitted by charged track with 8 kG field.

- Search through all cells ($\Delta\eta \times \Delta\phi$=0.04 x 0.04) to identify all cells hit by photons only, find E_T^{cell}.

- Charge Veto: if there is a charged track hitting neighboring 8 cells $\Rightarrow$ **Reject**;

- Define the sum of E_T^{cell}'s of these 9 cells ($\sum_{9cells} E_T^{cell}$) as the E_T^{photon};

- Isolation Veto: if the sum of the transverse energies in a cone of radius R ($R=\sqrt{\Delta\eta^2+\Delta\phi^2}$), excluding the E_T^{photon}, is larger than 10% of the E_T^{photon} plus an isolation energy cut (E_T^{cut}).

$$\sum_{r<R} E_T - E_T^{photon} \geq (E_T^{cut} + 0.1 E_T^{photon}) \Rightarrow \textbf{Reject};$$

- Option: use only cells with transverse energy larger than 3 standard deviations of combined thermal and pile-up noise:
  150 MeV for BaF_2 + Spaghetti, and 250 MeV for L.Ar.

Isolation Rejection Factor (10^{-4})

- 2jets: 2 mb (gg: 1.54; gq: 0.44 and qq: 0.043), 12% quark jets and 88% gluon jets.

E_T^{cut}	R=0.45	R=0.60	R=0.75
5 GeV	5.3	4.1	3.1
10 GeV	8.8	6.8	6.2
15 GeV	13	10	8.6
20 GeV	16	14	13

- γ-jet: 237nb (γq: 226 and γg: 11), 95% quark jets and 5% gluon jets.

E_T^{cut}	R=0.45	R=0.60	R=0.75
5 GeV	16	13	9.6
10 GeV	30	26	22
15 GeV	40	34	32
20 GeV	54	47	43

- Result:
  10^{-3} for quark jets and 2.2×10^{-4} for gluon jets.

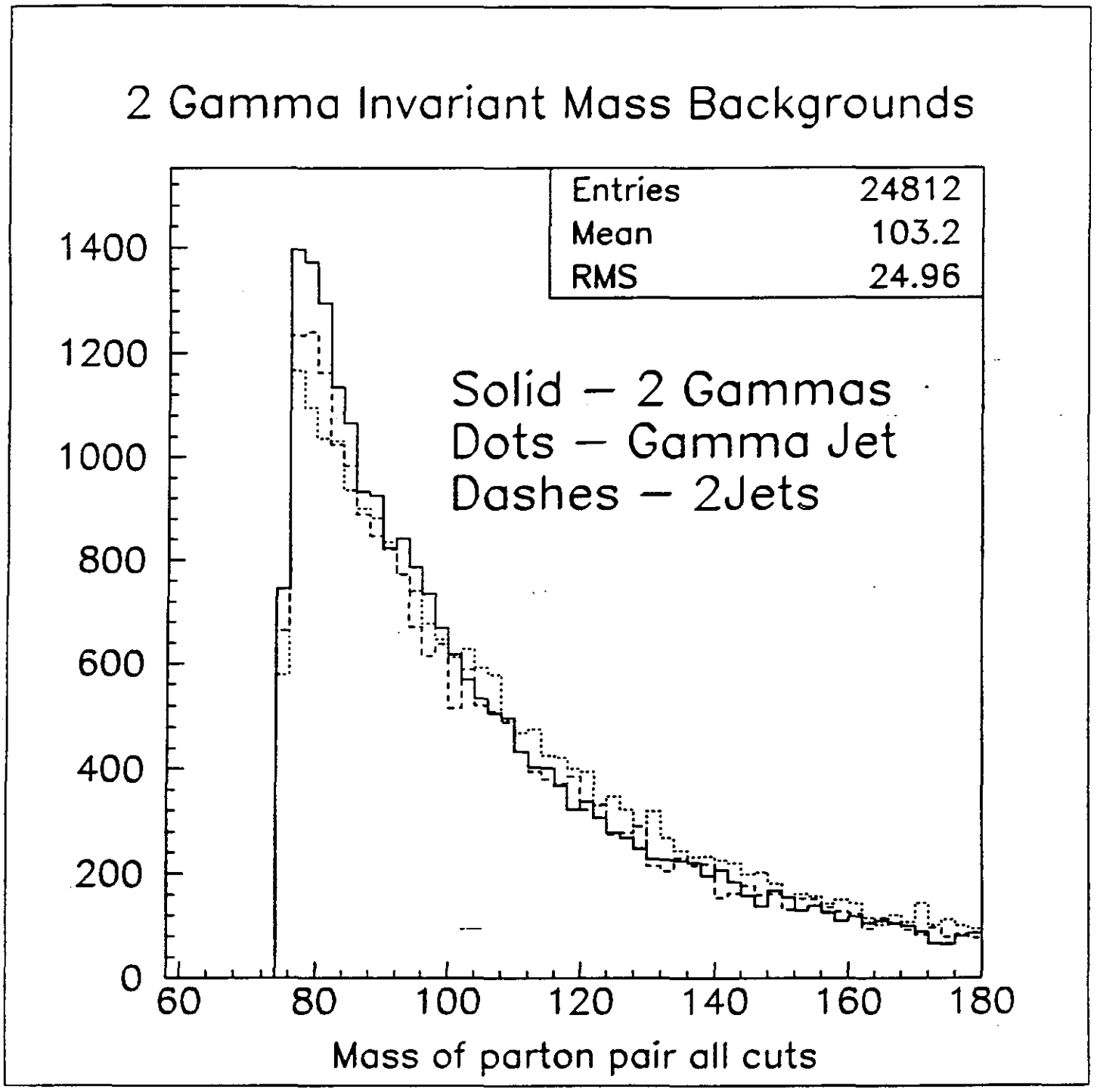

Figure 6: Comparison of parton invariant mass spectra from three QCD processes: $\gamma\gamma$, γ-jet and 2jets.

QCD Background Rejection

Shower Shape Analysis and Preradiator

- Calculate Background x-section by analyzing **isolated photon candidates** passing isolation cuts.

- Calculate $\bar{\theta}$ for each **isolated photon candidate**:

$$\bar{\theta} = \frac{\sum_i E_i \times \theta_i}{\sum_i E_i}$$

where

$$\cos\theta_i = \frac{\vec{E}_i \cdot \vec{n}}{E_i}, \quad \vec{n} = \frac{\sum_i \vec{E}_i}{|\sum_i \vec{E}_i|},$$

and $\vec{E}_1$ is the energy vector of the ith photon in the **isolated photon candidate**.

- A detailed GEANT study by **H. Yamamoto** shows that isolated photon candidates with $\bar{\theta} > 5$ mrad can be effectively rejected by using shower shape analysis.

- Assuming isolated photon candidates with $\theta_M > 2$ mrad may be rejected by using an effective preradiator.

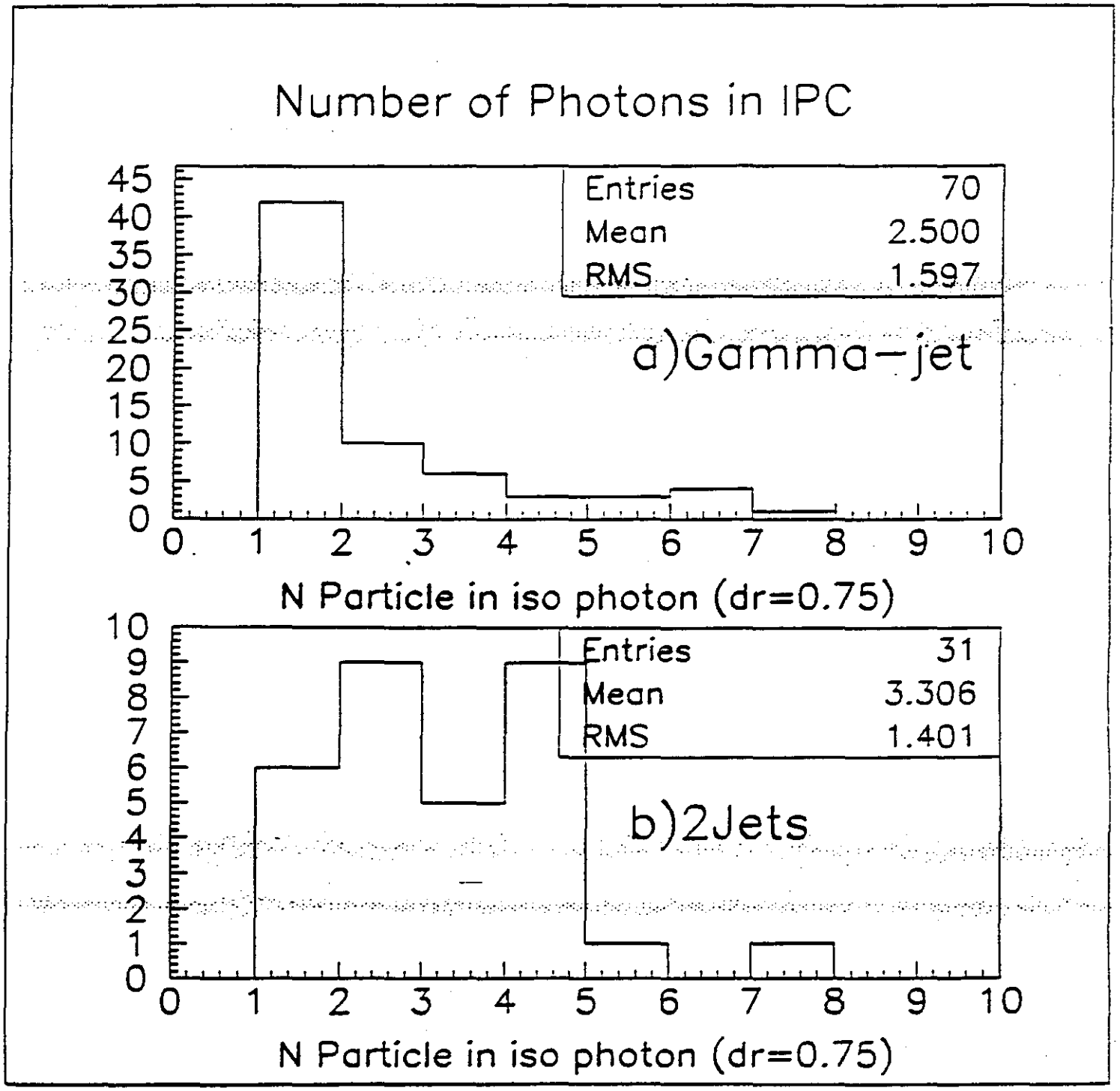

Figure 9: Distributions of photon numbers in isolated photon candidates, passing an isolation cut of R = 0.75 and E_T^{cut} = 10 GeV from 100k events each of (a) γ-jet and (b) 2jets.

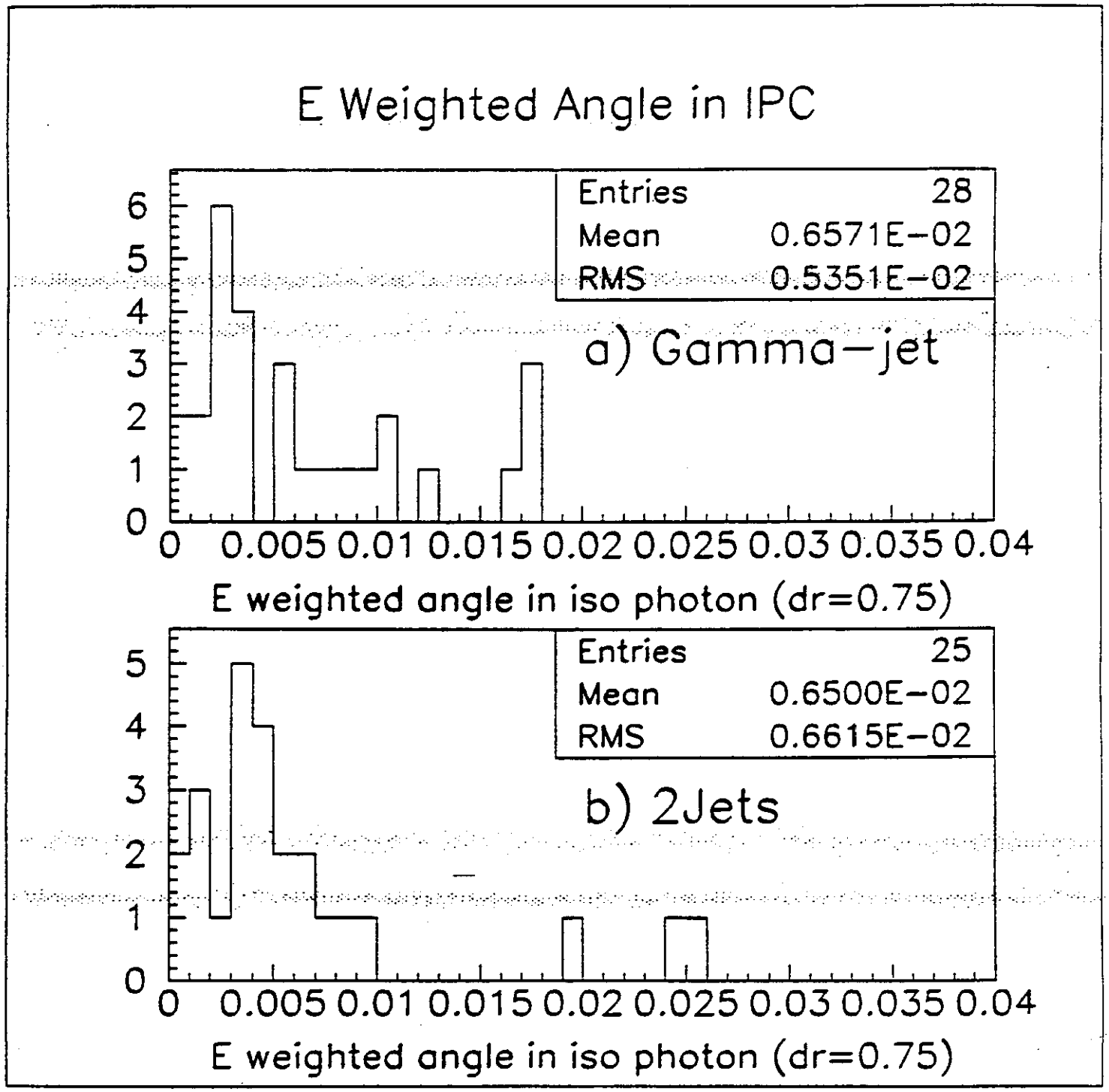

Figure 10: Distributions of $\bar{\theta}$ of isolated photon candidates, passing an isolation cut of R = 0.75 and E_T^{cut} = 10 GeV from 100k events each of (a) γ-jet and (b) 2jets.

Table 2: QCD Background Cross-Sections (pb)

After Isolation						
Process	2jets			γ-jet		
E_T^{cut}	R=0.45	R=0.60	R=0.75	R=0.45	R=0.60	R=0.75
5 GeV	140	81	46	55	45	33
10 GeV	370	220	180	100	90	76
15 GeV	780	510	360	140	120	110
20 GeV	1200	940	800	190	160	150
After Showe Shape Analysis						
Process	2jets			γ-jet		
E_T^{cut}	R=0.45	R=0.60	R=0.75	R=0.45	R=0.60	R=0.75
5 GeV	73	34	20	31	26	21
10 GeV	160	120	89	54	50	42
15 GeV	250	210	140	68	59	57
20 GeV	310	260	230	83	73	66
After Preradiator						
Process	2jets			γ-jet		
E_T^{cut}	R=0.45	R=0.60	R=0.75	R=0.45	R=0.60	R=0.75
5 GeV	20	16	13	19	17	17
10 GeV	25	20	13	24	24	19
15 GeV	34	29	20	24	24	24
20 GeV	34	34	29	26	26	26
Irreducible QCD Background						
Process	2jets			γ-jet		
E_T^{cut}	R=0.45	R=0.60	R=0.75	R=0.45	R=0.60	R=0.75
5 GeV	10	10	7.3	17	14	14
10 GeV	13	10	7.3	19	14	14
15 GeV	16	16	13	21	17	17
20 GeV	16	16	16	21	19	17

Thermal and Pileup Noise (GeV)

for two GEM Calorimeters

- pileup noise is proportional to $\sqrt{t_{integration}}$, where $t_{integration}$ is the integration time of the detector, which is 16, 32, 40 and 100 ns respectively for BaF_2, SHCAL, LAr accordion and LAr HCAL.
- pileup noise is proportional to $Area^{0.6}$, taking into account jet correlation;
- thermal noise is proportional to $Area^{0.5}$, assuming no jet correlation.

	BaF_2				LAr Accordion			
R	0.04^2	0.45	0.60	0.75	0.032^2	0.45	0.60	0.75
σ_t	0.003	0.12	0.16	0.20	0.020	0.50	0.66	0.83
σ_p	0.026	0.95	1.3	1.8	0.032	1.5	2.1	2.8
σ_{EMC}	0.026	0.96	1.3	1.8	0.038	1.6	2.2	2.9
	SHCAL–				LAr HCAL			
	0.08^2	0.45	0.60	0.75	0.08^2	0.45	0.60	0.75
σ_t	0.003	0.03	0.04	0.05	0.13	1.3	1.7	2.2
σ_p	0.068	1.1	1.5	2.0	0.12	1.9	2.7	3.5
σ_{HC}	0.068	1.1	1.5	2.0	0.18	2.3	3.2	4.1
σ_{TOT}	N/A	1.5	2.0	2.7	N/A	2.8	3.9	5.0

$H^0 \rightarrow \gamma\gamma$ Background (pb)

for Two GEM Calorimeters

	BaF_2 System				
Process	$\gamma\gamma$	γ-jet	2jets	Total	B.F.
Isol.	31	33	46	110	3.5
S.S.	31	21	20	72	2.3
P.R.	31	17	13	61	2.0
Irr.	31	14	7.3	52	1.7
	LAr System				
Process	$\gamma\gamma$	γ-jet	2jets	Total	B.F.
Isol.	31	55	140	226	7.3
S.S.	31	31	73	135	4.4
P.R.	31	19	20	70	2.3
Irr.	31	17	10	58	1.9

R(e/jet) Rejection and

Fake Electron Cross Section (pb)

2jets			
R	0.30	0.45	0.60
R(e/jet) by isolation (10^{-5})	21	12	8.1
R(e/jet) by E-p match (10^{-5})	5.6	4.0	3.0
R(γ/jet) by isolation (10^{-4})	7.4	5.3	4.1
$\sigma_{"\gamma-e"}$ (pb) $M_{"\gamma-e"} \geq 75$ GeV	22	11	6.4
$\sigma_{"e-e"}$ (pb) $M_{"e-e"} \geq 75$ GeV	0.8	0.4	0.2
γ-jet			
R	0.30	0.45	0.60
R(e/jet) by isolation (10^{-5})	22	12	9.8
R(e/jet) by E-p match (10^{-5})	3.7	3.7	3.7
R(γ/jet) by isolation (10^{-4})	21	16	13
$\sigma_{"\gamma-e"}$ (pb) $M_{"\gamma-e"} \geq 75$ GeV	1.3	1.3	1.3

$$|E_{Cal} - \bar{p}_{track}| < 5\sqrt{\sigma^2_{Cal} + \sigma^2_{track}}$$

where

$$\frac{\sigma_{Cal}}{E} = (\frac{10}{\sqrt{E}} \oplus 2)\%, \ and \ \frac{\sigma_{track}}{p^2} = 0.25\%$$

or

$$\frac{p_{track}}{E_{Cal}} \leq 0.5$$

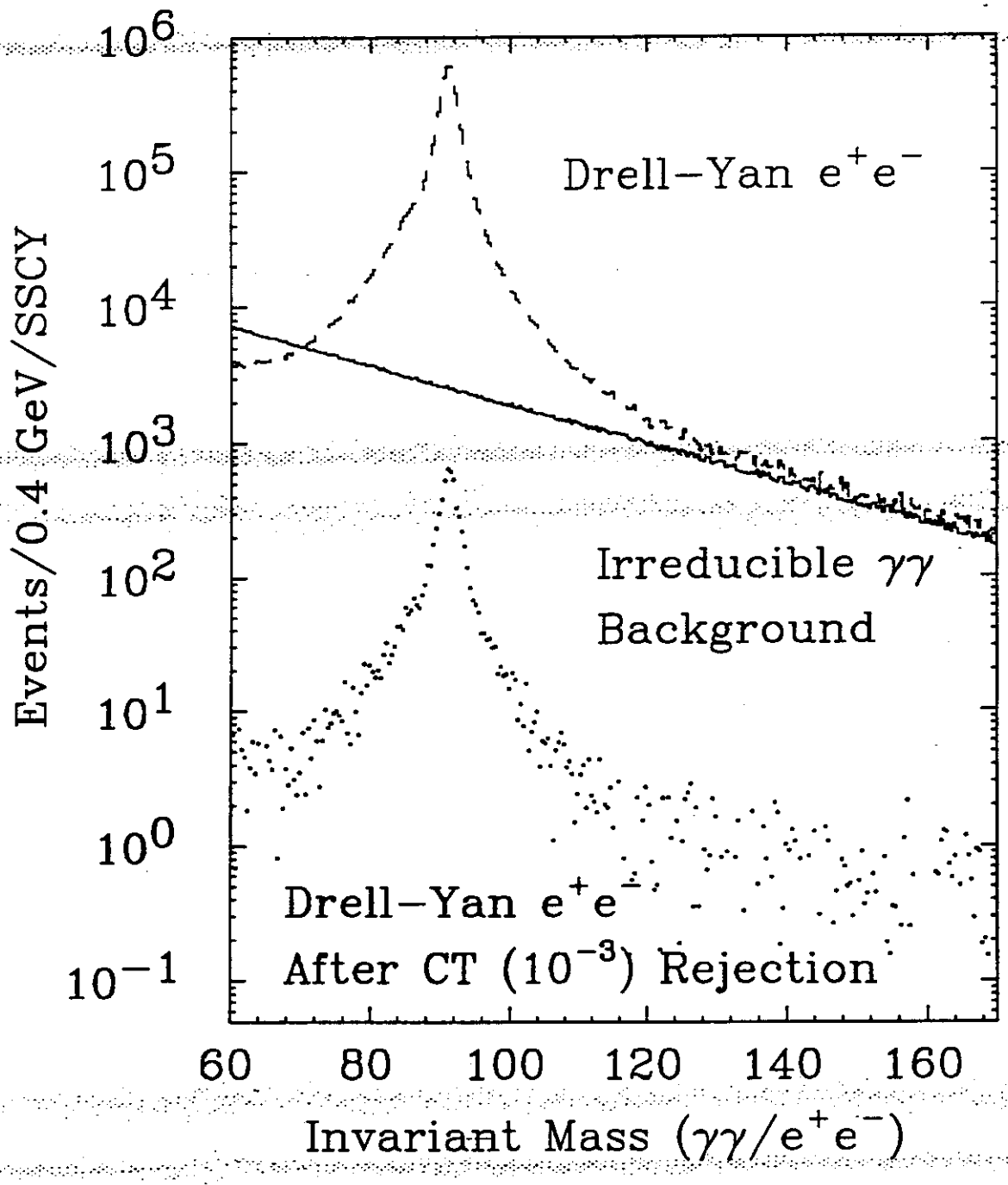
Drell−Yan e+e−
Irreducible γγ
Background
Drell−Yan e+e−
After CT (10−3) Rejection
Events/0.4 GeV/SSCY
Invariant Mass (γγ/e+e−)
10^6
10^5
10^4
10^3
10^2
10^1
10^0
10^−1
60
80
100
120
140
160

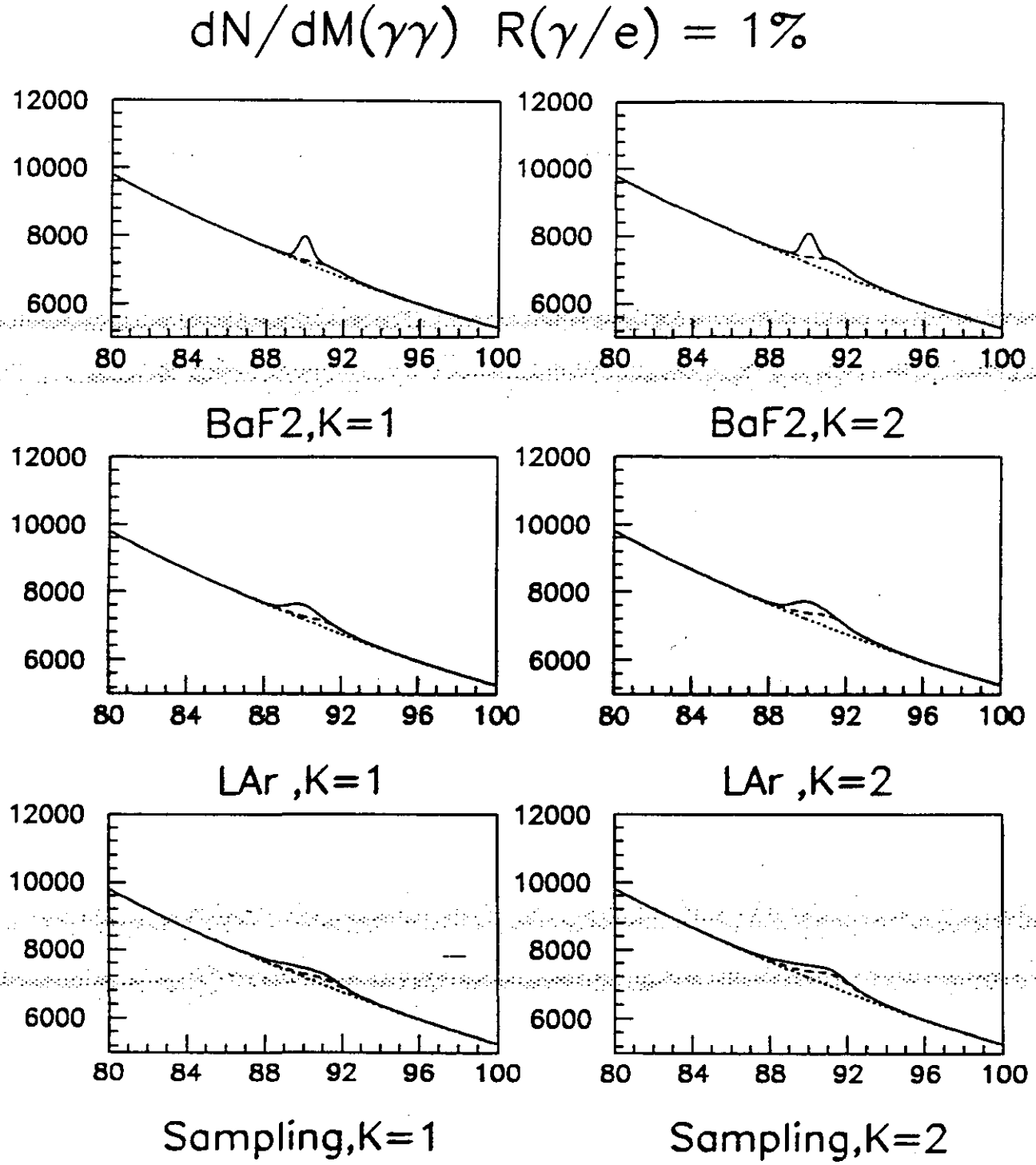
dN/dM(γγ) R(γ/e) = 1%
12000
10000
8000
6000
80
84
88
92
96
100
BaF2,K=1
BaF2,K=2
LAr ,K=1
LAr ,K=2
Sampling,K=1
Sampling,K=2

$H^0 \rightarrow \gamma\gamma$ Significance

with QCD Jets Background in One SSCY

M_H (GeV)	BaF_2 System			LAr System		
	S.S.	P.R.	Irr.	S.S.	P.R.	Irr.
80	3.0	3.3	3.5	1.5	2.1	2.3
90	4.0	4.3	4.7	2.1	3.0	3.3
100	5.7	6.1	6.6	3.0	4.2	4.6
120	9.2	9.9	11	5.2	7.3	8.0
140	11	11	12	5.7	7.9	8.7
150	8.6	9.2	10	4.8	6.6	7.3
160	3.9	4.2	4.5	2.2	3.1	3.4

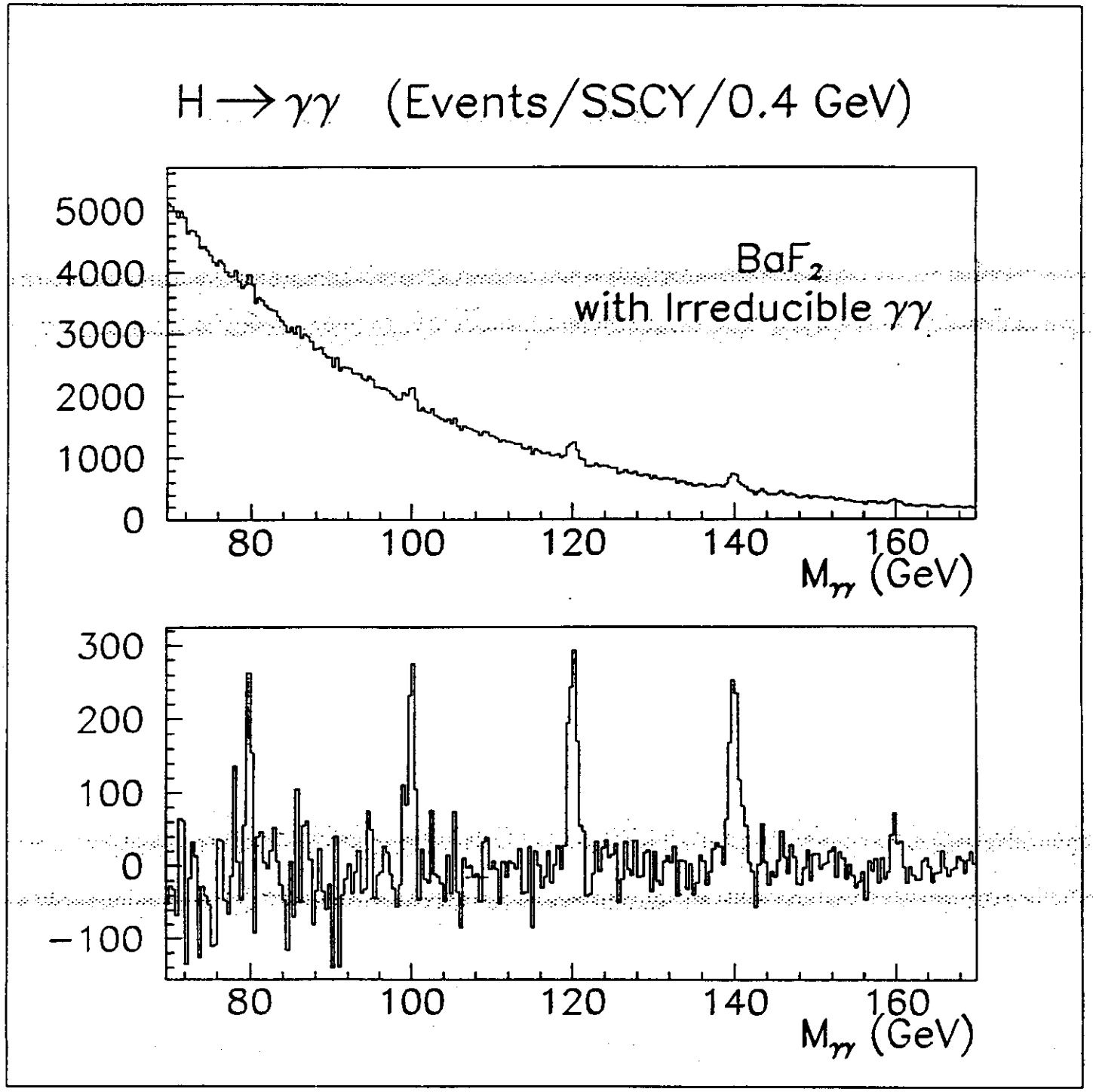
H → γγ (Events/SSCY/0.4 GeV)
5000
4000
3000
2000
1000
0
BaF2
with Irreducible γγ
80
100
120
140
160
Mγγ (GeV)
300
200
100
0
−100
80
100
120
140
160
Mγγ (GeV)

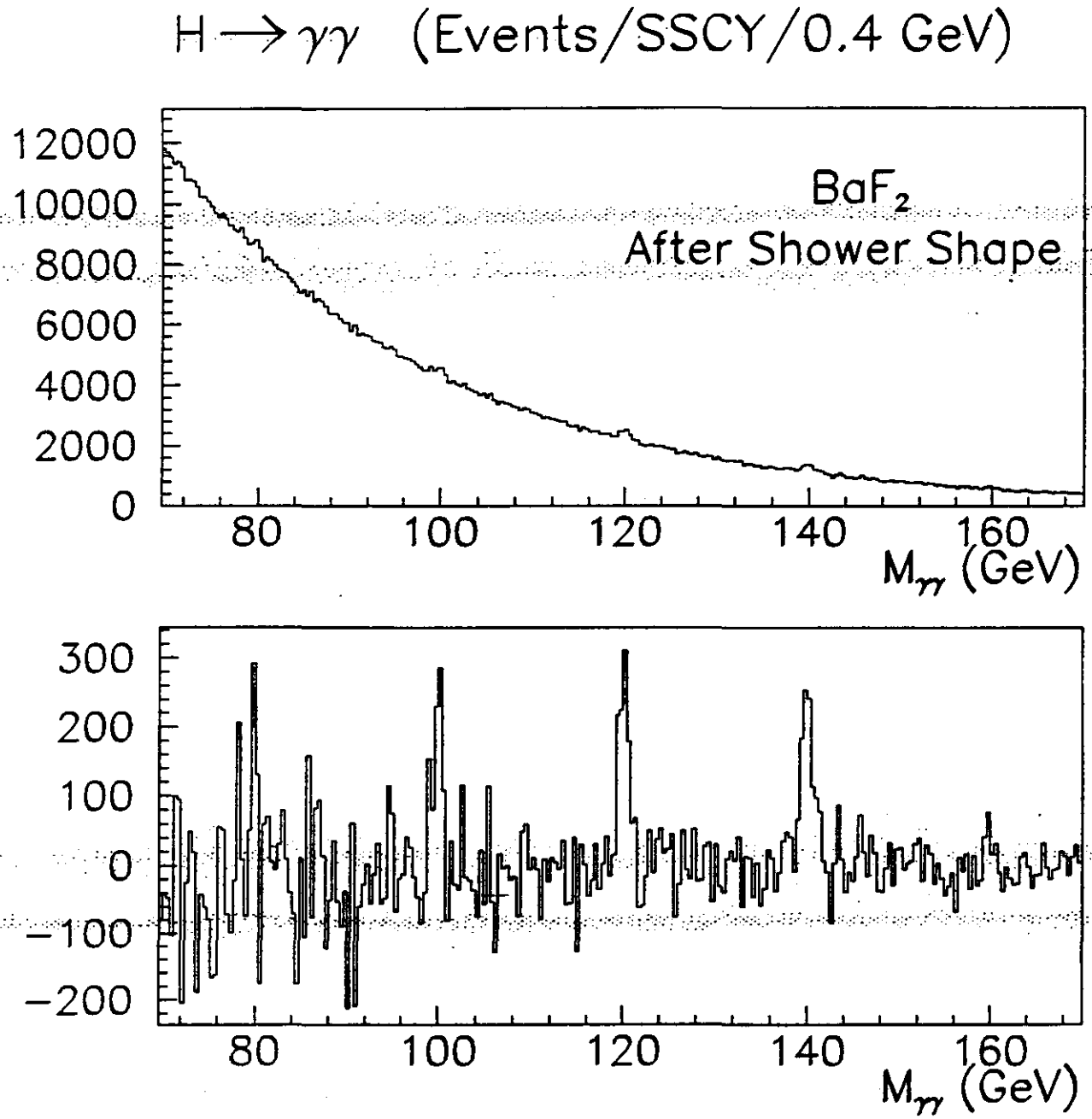
H → γγ (Events/SSCY/0.4 GeV)
BaF2
After Shower Shape
12000
10000
8000
6000
4000
2000
0
80
100
120
140
160
Mγγ (GeV)
300
200
100
0
−100
−200
80
100
120
140
160
Mγγ (GeV)

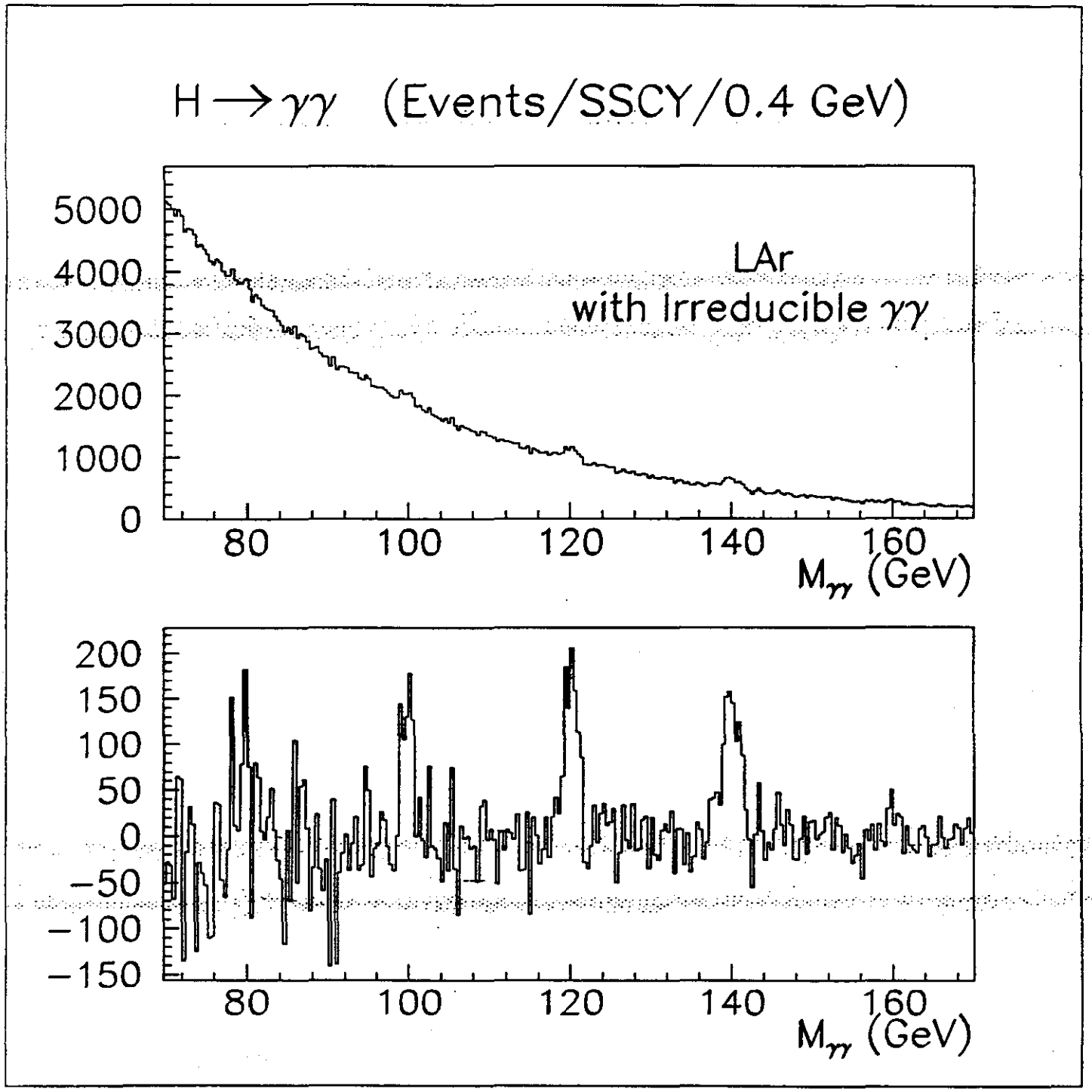
H → γγ (Events/SSCY/0.4 GeV)
5000
4000
3000
2000
1000
0
LAr
with Irreducible γγ
80
100
120
140
160
M_γγ (GeV)
200
150
100
50
0
−50
−100
−150
80
100
120
140
160
M_γγ (GeV)

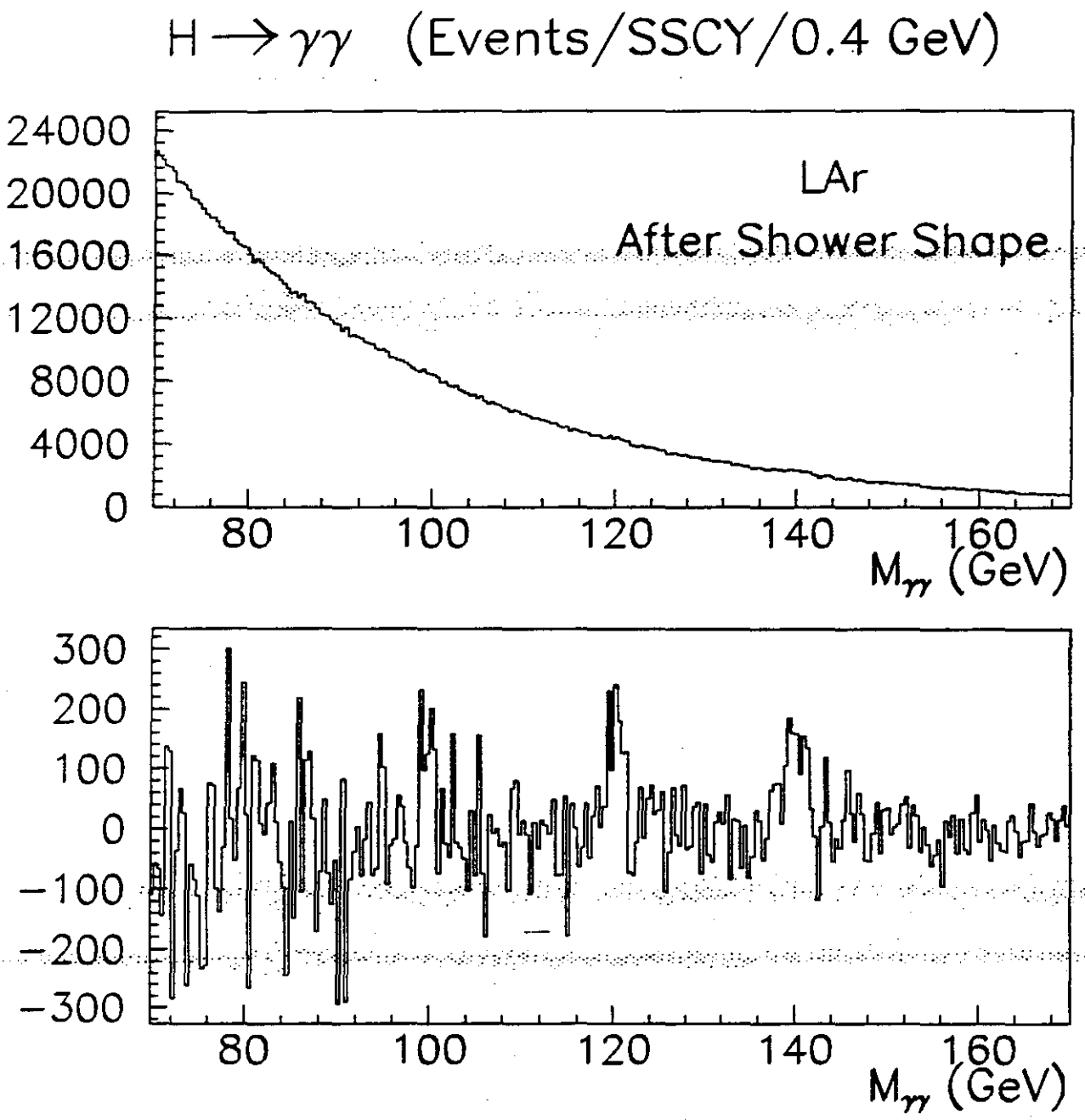
H → γγ (Events/SSCY/0.4 GeV)
LAr
After Shower Shape
24000
20000
16000
12000
8000
4000
0
80
100
120
140
160
M_γγ (GeV)
300
200
100
0
−100
−200
−300
80
100
120
140
160
M_γγ (GeV)

On Vertex Determination in H$\rightarrow \gamma\gamma$ Searches
Response to Dr. D. Froidevaux

Ren-yuan Zhu and Hiro Yamamoto

Lauritsen Laboratory
California Institute of Technology
Pasadena, CA 91125

July 14, 1992

1 Introduction

In GEM's recent physics report to the PAC (GEM-92-126), we pointed out that based upon our analysis using PYTHIA program the primary Higgs event vertex for H$\rightarrow \gamma\gamma$ searches at the SSC can be determined by using underlying event topology with a probability of 85%.

A question was raised by Dr. D. Froidevaux concerning the reliability of this analysis, and specially the Monte Carlo program used in this analysis. Dr. D. Froidevaux's question was based on experimental data that the W production is not much different from the minimum bias event.

After a brief study on this issue, we conclude:

- The W production data published by UA1, UA2 and CDF agree well with PYTHIA predictions;
- The higher p_T of Higgs production, compared with W production, predicted by PYTHIA, has solid theoretical backup: while W is produced through $q\bar{q}'$ annihilation, the Higgs is produced through gluon-gluon fusion or W/Z-W/Z fusion. Here, gluon-gluon coupling is larger than quark-gluon coupling, so Higgs gets more recoil than W, and W/Z mass in the propagator produces high p_T.
- Theoretical calculations including high order corrections predict that the p_T of Higgs at the SSC energy is over 50 GeV, and the PYTHIA's prediction is consistent with this result.

In this note, we discuss the facts and analysis, which leads to above conclusions.

2 PYTHIA vs Experiment Data

PYTHIA's predictions for the W production has been compared with the UA1 and UA2 data. The comparison is published in Z. Phys. C32 67 (1986), which shows PYTHIA's predictions agree with data.

We compared PYTHIA with the CDF data (for the W-boson mass measurement) published in PR D43 2070 (1991). Figure 1 shows this comparison. While Figure (a) and (b) are the transverse energy of the W boson and the scalar E_T sum of the underlying event measured by CDF, Figure 1(c) and (d) are corresponding predictions calculated with PYTHIA 5.6.

Since we do not know the exact experimental cuts used in CDF data analysis, Figure 1(c) plots the p_T of W's without any event selection cut, and Figure 1(d) plots the scalar sum of E_T (Σ E_T) of all partons produced in the rapidity range of ± 3.5. It is clear from Figure 1 that the data agree reasonablly well with PYTHIA's predictions. Also, PYTHIA tends to give softer distributions, which may be explained by data selection cuts and/or detector effects.

The detailed comparison between PYTHIA and minimum bias events are given in CERN 90-10 (LHC Workshop) 155.

3 W vs 80 GeV Higgs

Figure 2 shows the p_T distributions of W and 80 GeV Higgs produced at three center of mass energies of 1.8 TeV, 16 TeV and 40 TeV. This is a measure of the transverse motion of the underlying event. Figure 3 shows the Σ E_T of partons in the rapidity range ± 3.5 for the same sets of events. This is a measure of the multiplicity of hadrons of the underlying event. In each plot the average value is also listed.

As one can see from the average values in these plots, the $< p_T >$ and $< \Sigma\, E_T >$ in the Higgs events are larger than that in the W production at the same center of mass energy. This difference can be easily understood by diffrent production mechanism of W and Higgs. While W is produced by q-$\overline{q'}$ annihilation, the Higgs is produced by either gluon-gluon fusion or W/Z-W/Z fusion processes. In corresponding figures of

Fig.2 and Fig.3, the contributions from gluon-gluon fusion process are shown in gray area, and their corresponding average values ($< p_T >_{gg}$ and $< \Sigma\ E_T >_{gg}$) are also listed.

The $< p_T >_{gg}$ and $< \Sigma\ E_T >_{gg}$ for the Higgs production are around a factor of two larger than those in the W production. This can be understood by the difference of gluon-gluon and quark-gluon coupling, where the average number of partons radiated from the incident partons is different by a factor of 9/4.

The cross section of W/Z-W/Z fusion in Higgs production is around 25% of the total production cross sections at the SSC energy. The W/Z fusion process tends to give a higher $< p_T >$ and $< \Sigma\ E_T >$ because p_T in this process is determined by the W and Z mass which appears in a form of propagator.

4 Energy Dependence

The $< p_T >$ and $< \Sigma\ E_T >$ show a mild energy dependence. This is determined by perturbative QCD, which everyone relies on to predict phenomena at SSC energy.

5 Conclusion

In this note, we have shown that a big difference exists between the W production at Tevatron energy and the Higgs production at SSC energy. The reasons are:

1. The number of partons in the Higgs production by gluon-gluon fusion is twice larger than that in the W production;
2. The p_T of Higgs from W/Z-W/Z fusion is larger than the typical p_T produced by QCD radiation;
3. The mild energy dependence is predicted by the perturbative QCD.

The theoretical calculations (calculations done analytically, not by thousands of lines of Monte Carlo codes) predicts that the p_T of Higgs at SSC energy is over 50 GeV, which is consistent with or larger than the prediction of PYTHIA.

In summary, we believe that the difference between Fig.2(a) and (f) and/or Fig.3(a) and (f) are understandable, and the prediction is as reliable as other physics

quantities at the SSC energies predicted by perturbative QCD based Monte Carlo programs.

Note, we used the default mode for the Higgs production (MSTP(82) = 1) of PYTHIA in our analysis. According to Sjostrand, this prediction is conservative. We also used MINBIAS event of ISEJET to generate minimum bias events, so our estimation by using ISAJET might be a under estimation. The result obtained by using PYTHIA (85%) thus is more appropriate to use.

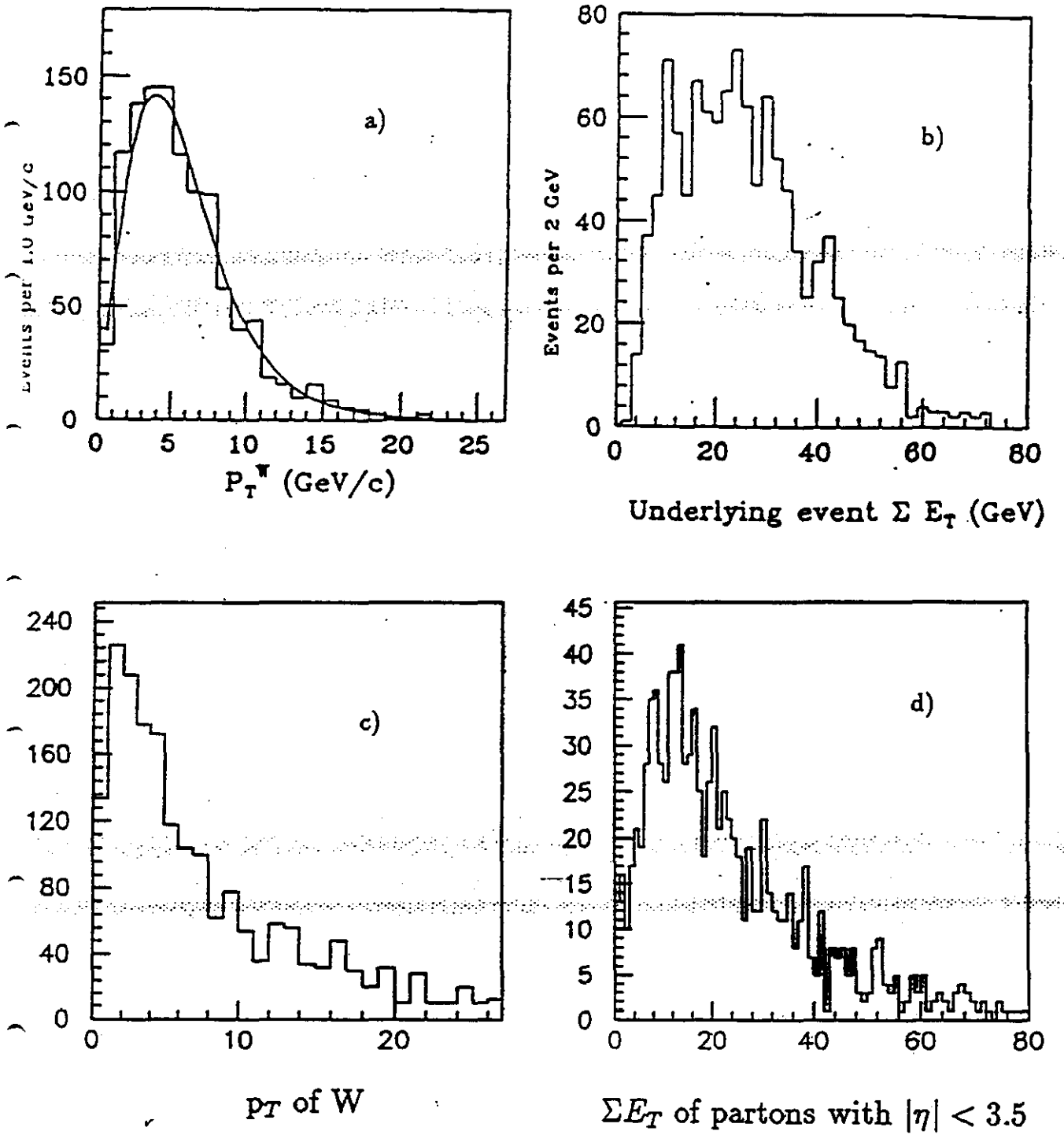

Fig.1 CDF W production data vs PYTHIA prediction

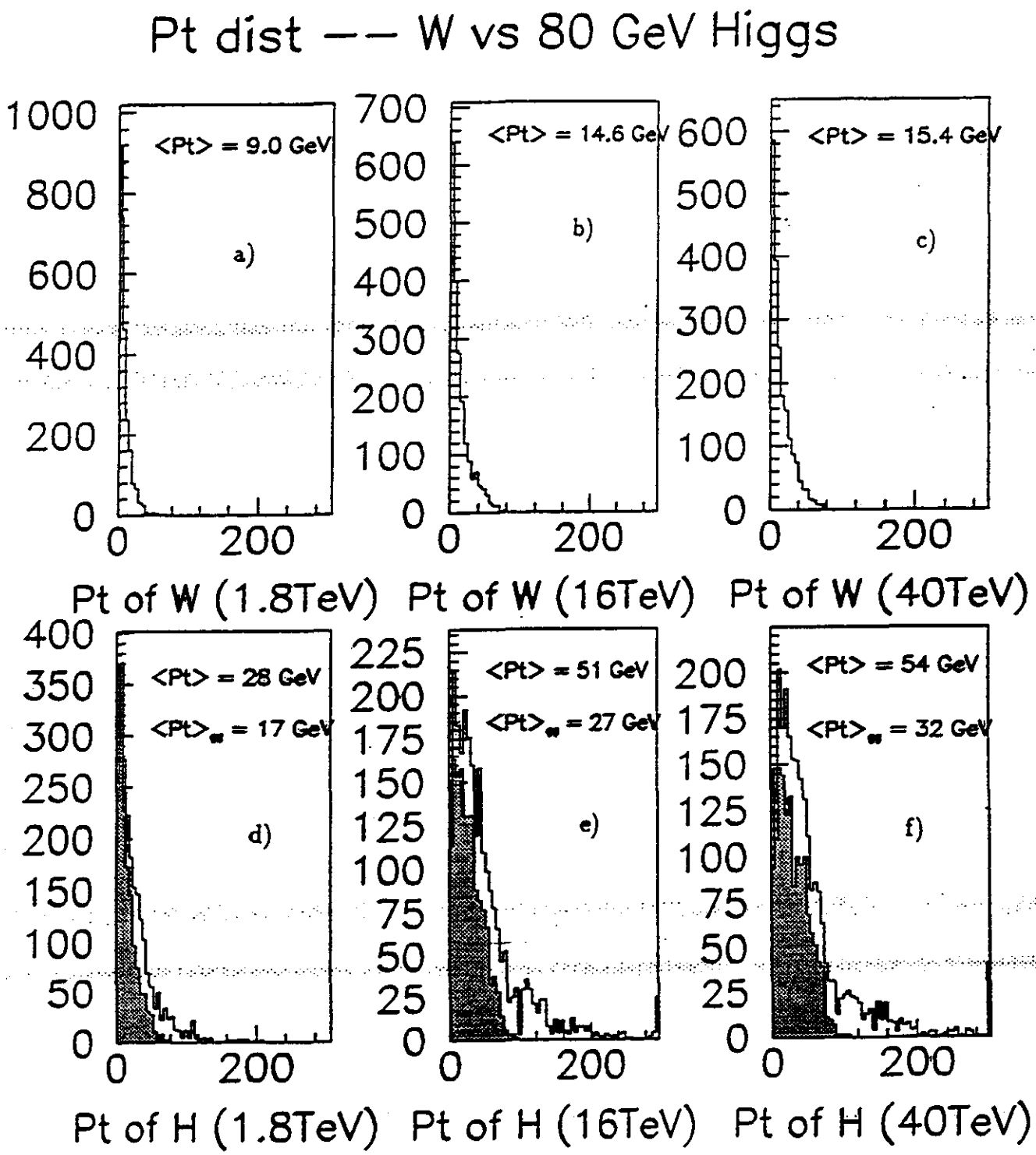

Fig.2 P_t distribution of W and 80 GeV Higgs

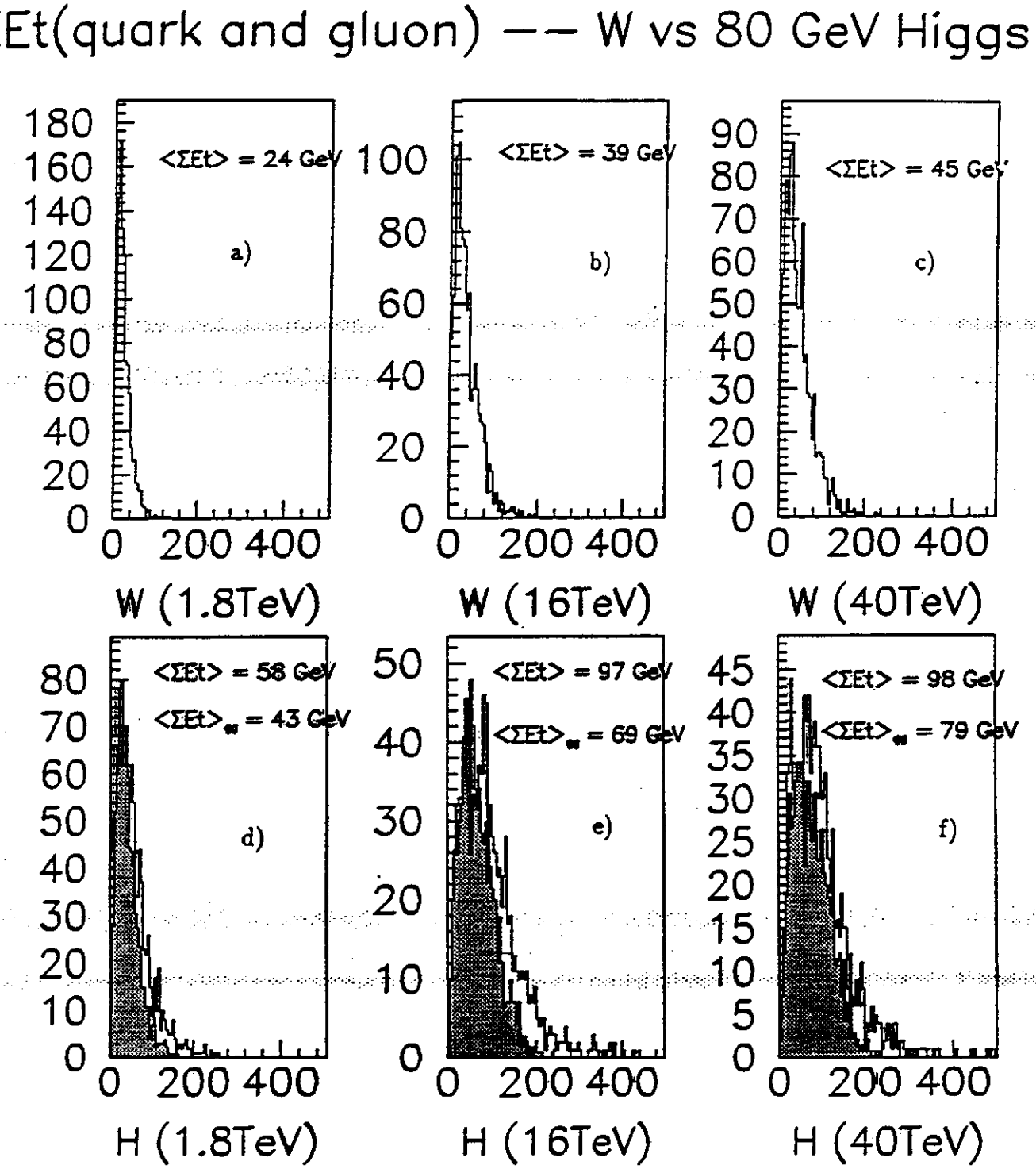

Fig.3 ΣE_t(q and g) in W and Higgs production

Determination of Higgs Vertex @10^{33}

- High p_T of Higgs production can be used to distinguish vertices from MBE: 85% according to PYTHIA.

- If Higgs is produced with qq annihilation: 74%

- Bottom Line: Random Selection of Higgs Vertex.

# of MBE	0	1	2	3	4
Probability	0.20	0.32	0.26	0.14	0.06
$P_{Correct}$	0.20	0.16	0.087	0.035	0.012

Conclusion: > 50% probability, you have a correct primary vertex.

- **Do not understand PAC's comment.**

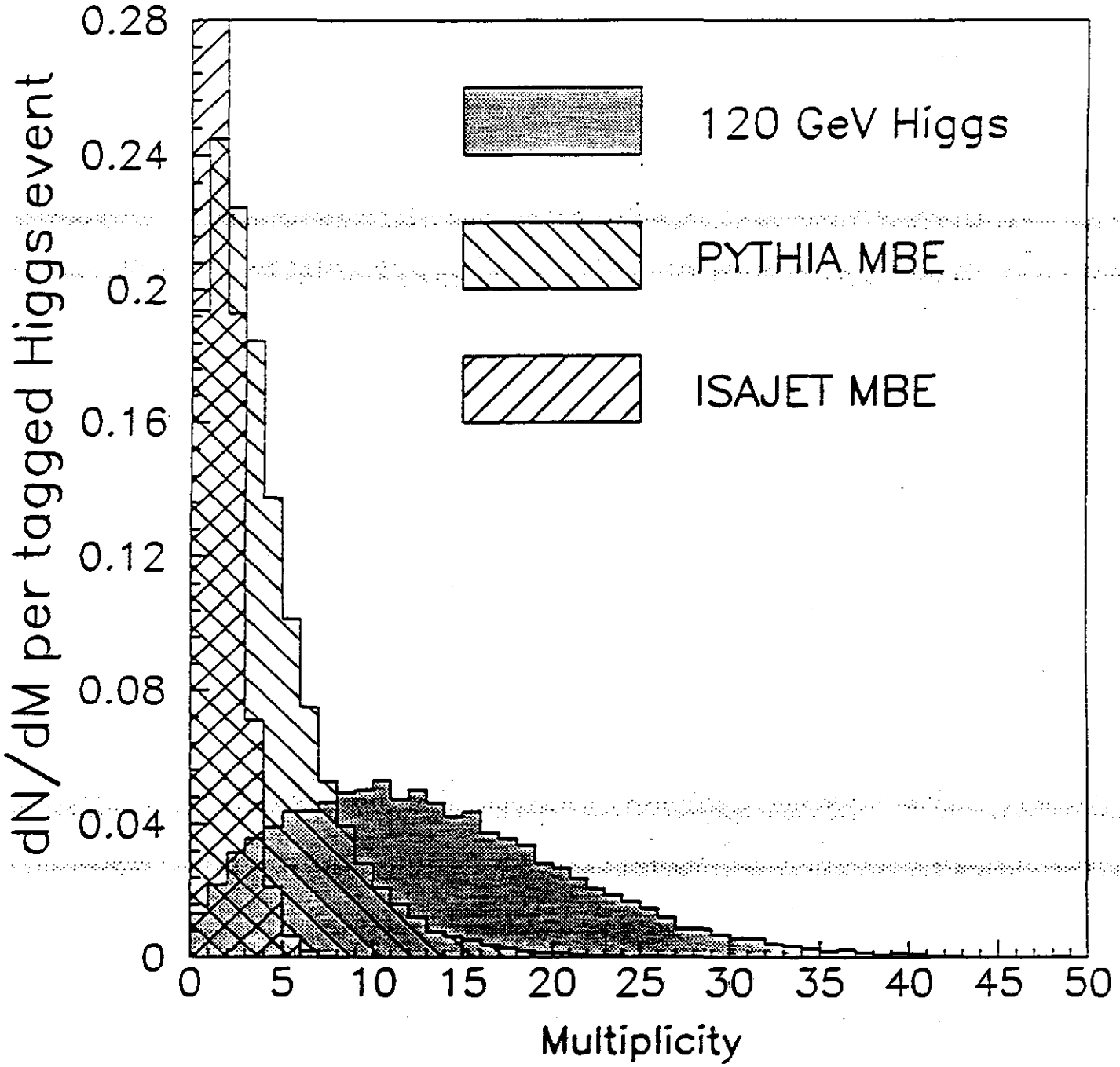

Figure 7: Charge multiplicity distributions after $p_T > 1$ GeV and $|\eta| < 2.5$ cuts for a 120 GeV Higgs signal and minimum bias events backgrounds generated by using PYTHIA and ISAJET programs.

Vertex with high charge multiplicity

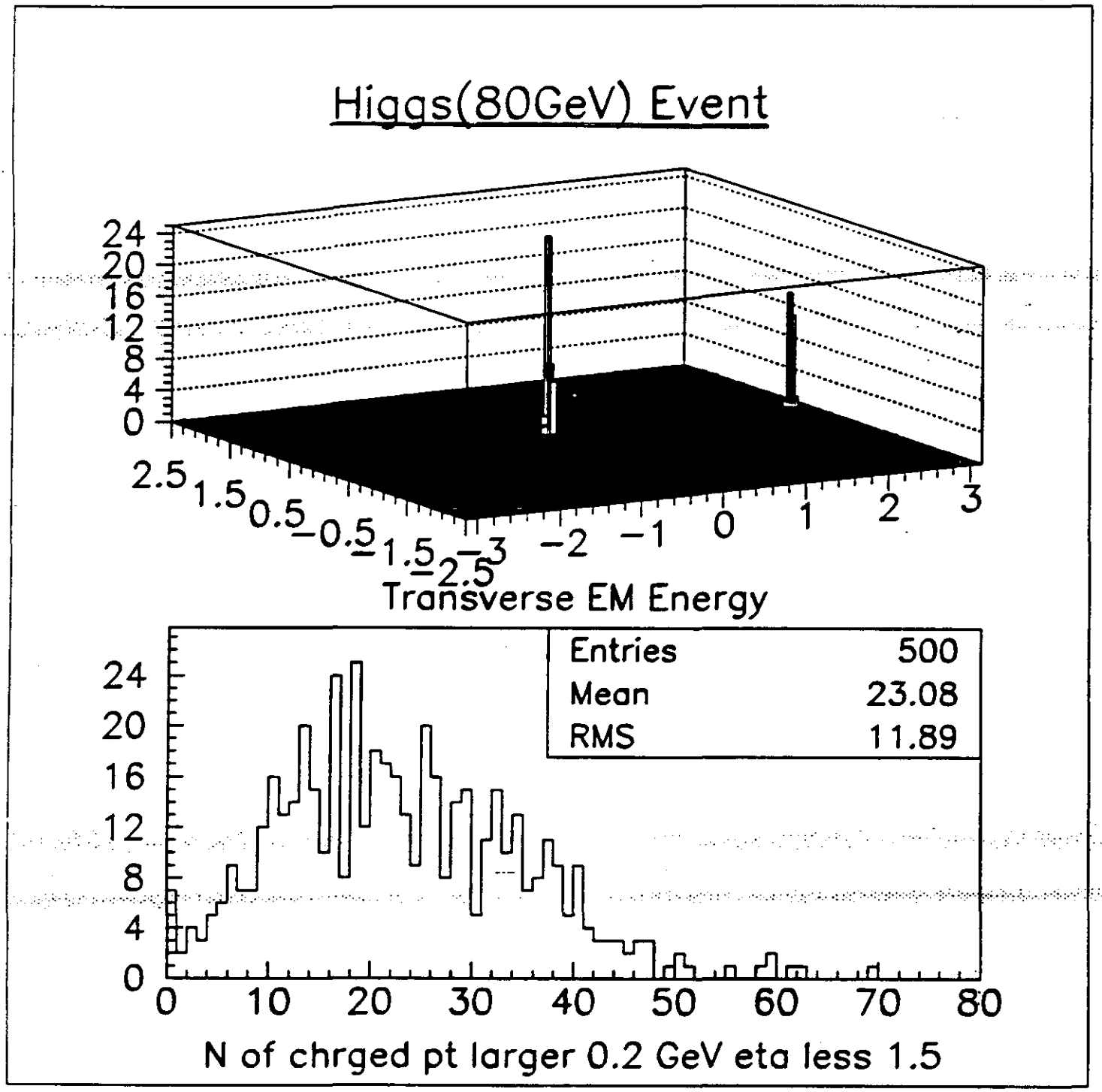

Vertex' with low charge multiplicity

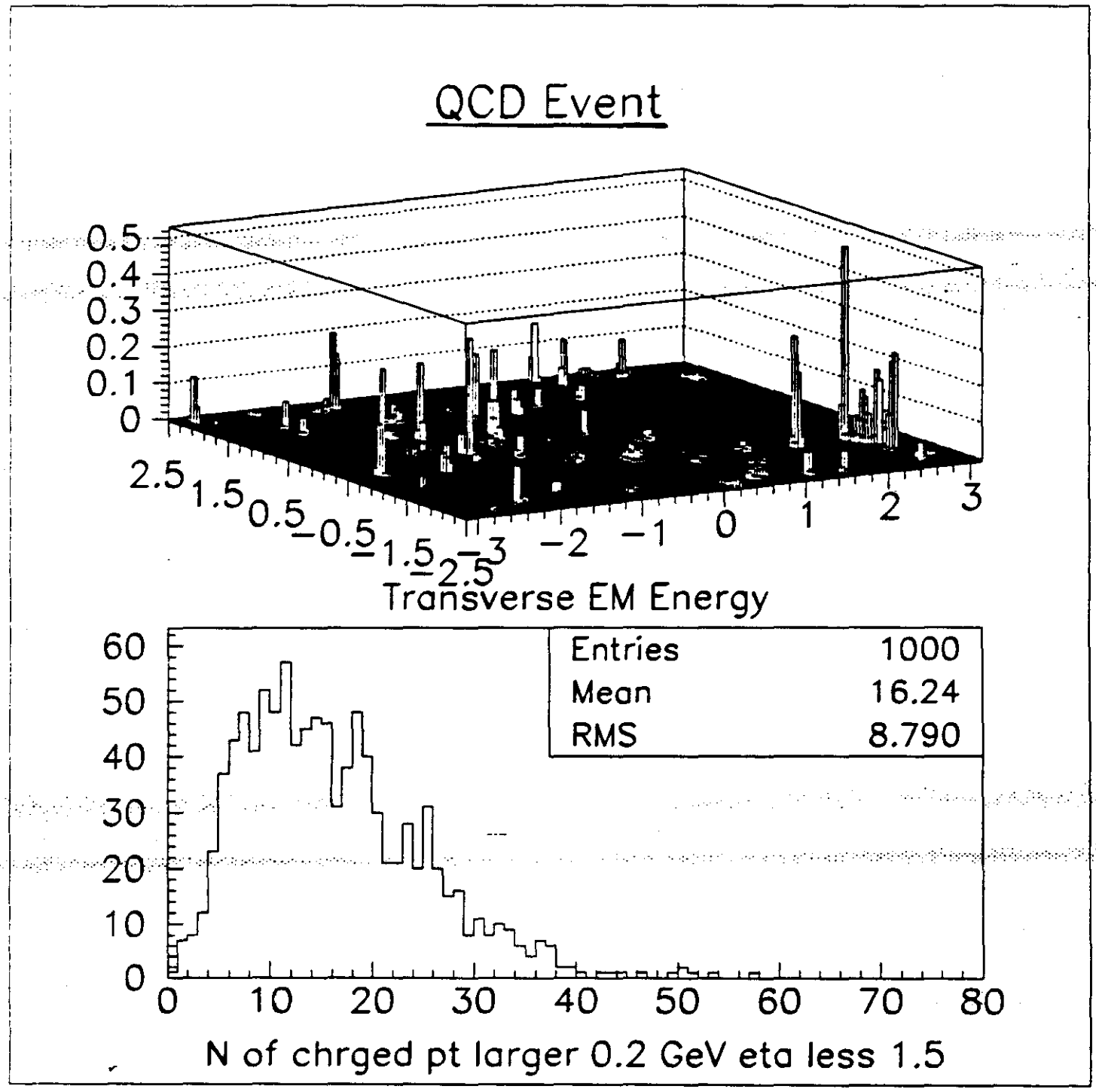

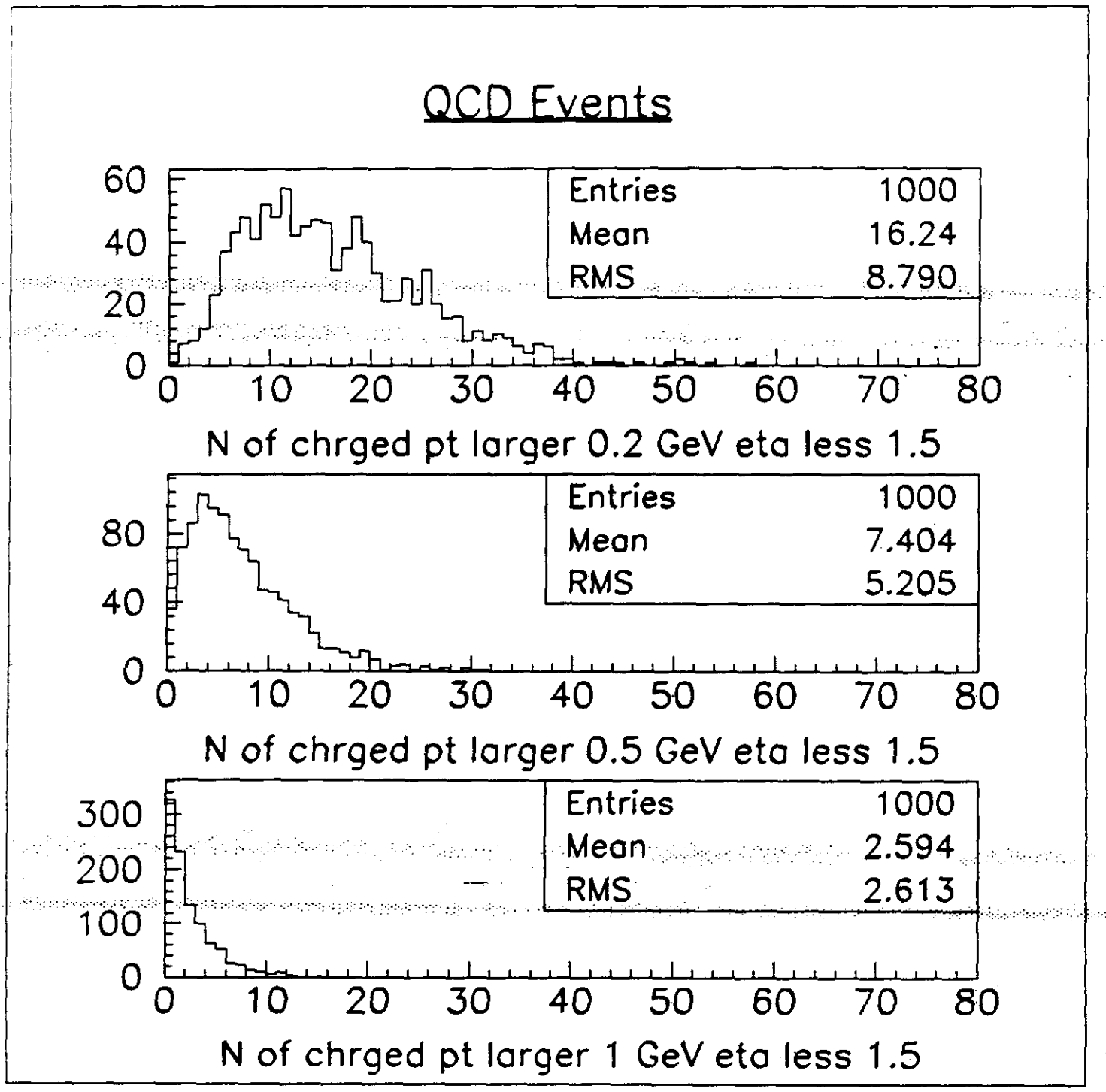
QCD Events
Entries 1000
Mean 16.24
RMS 8.790
N of chrged pt larger 0.2 GeV eta less 1.5
Entries 1000
Mean 7.404
RMS 5.205
N of chrged pt larger 0.5 GeV eta less 1.5
Entries 1000
Mean 2.594
RMS 2.613
N of chrged pt larger 1 GeV eta less 1.5

Higgs(80GeV) to 2 Photons

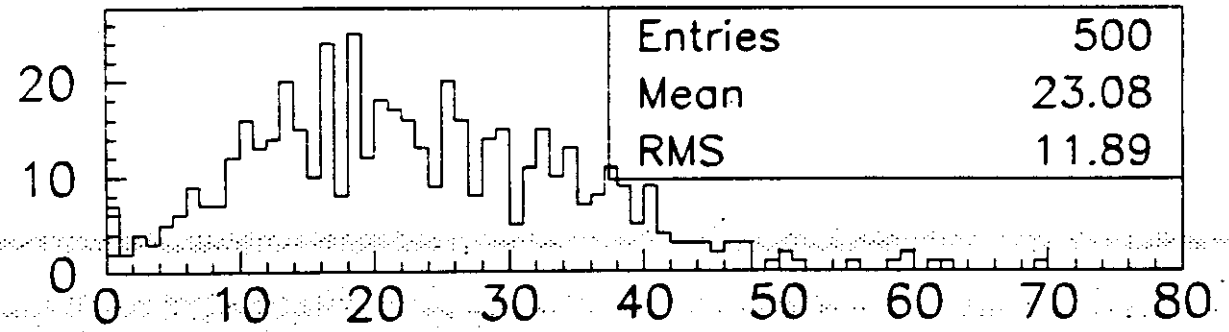

N of chrged pt larger 0.2 GeV eta less 1.5

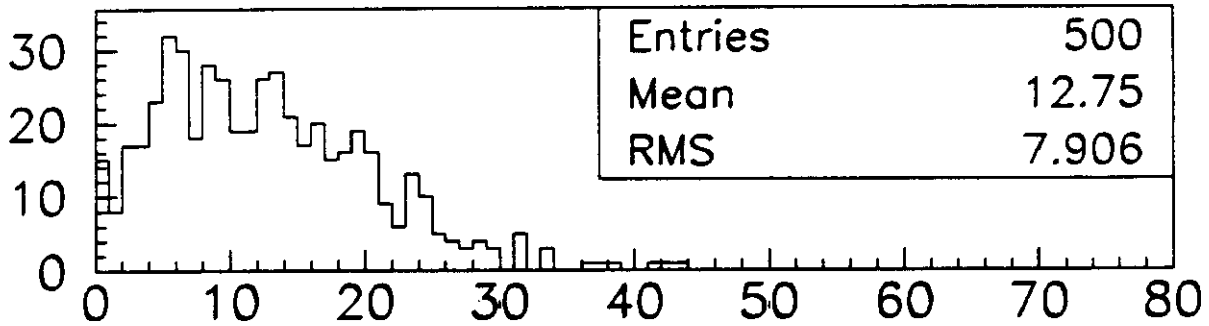

N of chrged pt larger 0.5 GeV eta less 1.5

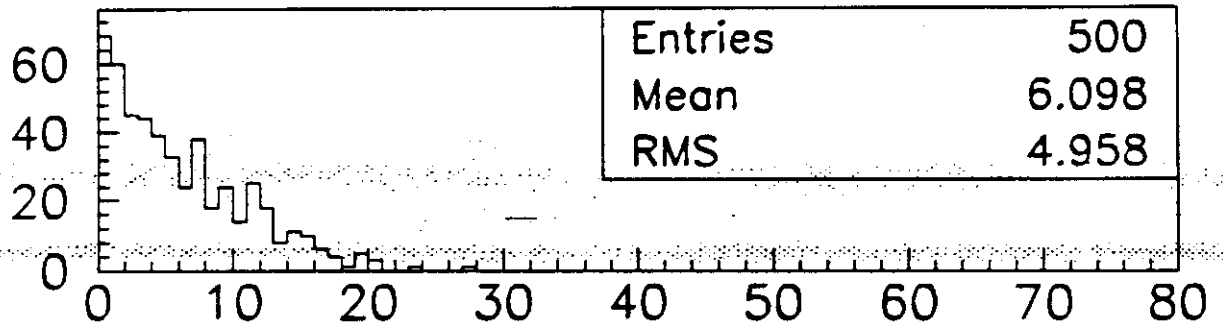

N of chrged pt larger 1 GeV eta less 1.5

Jet Backghround

- CDF Data:
  - Single γ: Data agree qualitatively with NLO QCD calculation of Owens *et al.* **PL B234** (1990) 127, except at $p_T < 20$ GeV.
  - Double γ: Data are factor of 2–4 higher than NLO QCD calculation of Owens *et al.* **FSU-HEP-920320** (1992), however, jet background of 2jets and γ-jet are not included in the comparison, which should be factor of 1.7 of NLO QCD.
- L3 Data:
  Data is 14% higher than JETSET 7.3 with $E_\gamma >$ 5 GeV, and agrees with $_\gamma > 20$ GeV. Note the background from jet has been scheled by 1.88 $\rightarrow$ Data is 15-20% higher than JETSET.
- **Do not understand PAC's comment on factor of 5.**

CDF/PUB/JET/PUBLIC 1757
For Proceedings of the
XXVII Recontre de Moriond,
Les Arcs, France, 1992.
FERMILAB-CONF-92/146-E

QCD Physics at CDF

The CDF Collaboration*

Presented by Robert M. Harris†
Fermi National Accelerator Laboratory
Batavia, Illinois 60510

ABSTRACT

We present measurements of jet production and isolated prompt photon production in $\bar{p}p$ collisions at $\sqrt{s} = 1.8$ TeV from the 1988-89 run of the Collider Detector at Fermilab (CDF). To test QCD with jets, the inclusive jet cross section ($\bar{p}p \to J + X$) and two jet angular distributions ($\bar{p}p \to JJ + X$) are compared to QCD predictions and are used to search for composite quarks. The ratio of the scaled jet cross sections at two Tevatron collision energies ($\sqrt{s} = 546$ and 1800 GeV) is compared to QCD predictions for X_T scaling violations. Also, we present the first evidence for QCD interference effects (color coherence) in third jet production ($\bar{p}p \to JJJ + X$). To test QCD with photons, we present measurements of the transverse momentum spectrum of single isolated prompt photon production ($\bar{p}p \to \gamma + X$), double isolated prompt photon production ($\bar{p}p \to \gamma\gamma + X$), and the angular distribution of photon-jet events ($\bar{p}p \to \gamma J + X$). We have also measured the *isolated* production ratio of η and π^0 mesons $(\bar{p}p \to \eta + X)/(\bar{p}p \to \pi^0 + X) = 1.02 \pm .15(stat) \pm .23(sys)$.

* The CDF collaboration: ANL - Brandeis - University of Chicago - Fermilab - INFN, Frascati - Harvard - University of Illinois - KEK - LBL - University of Pennsylvania - INFN, University of Scuola Normale Superiore of Pisa - Purdue - Rockefeller - Rutgers - Texas A&M - Tsukuba - Tufts - University of Wisconsin

† Supported by the U.S. Department of Energy, contract number DE-AC02-76CH03000.

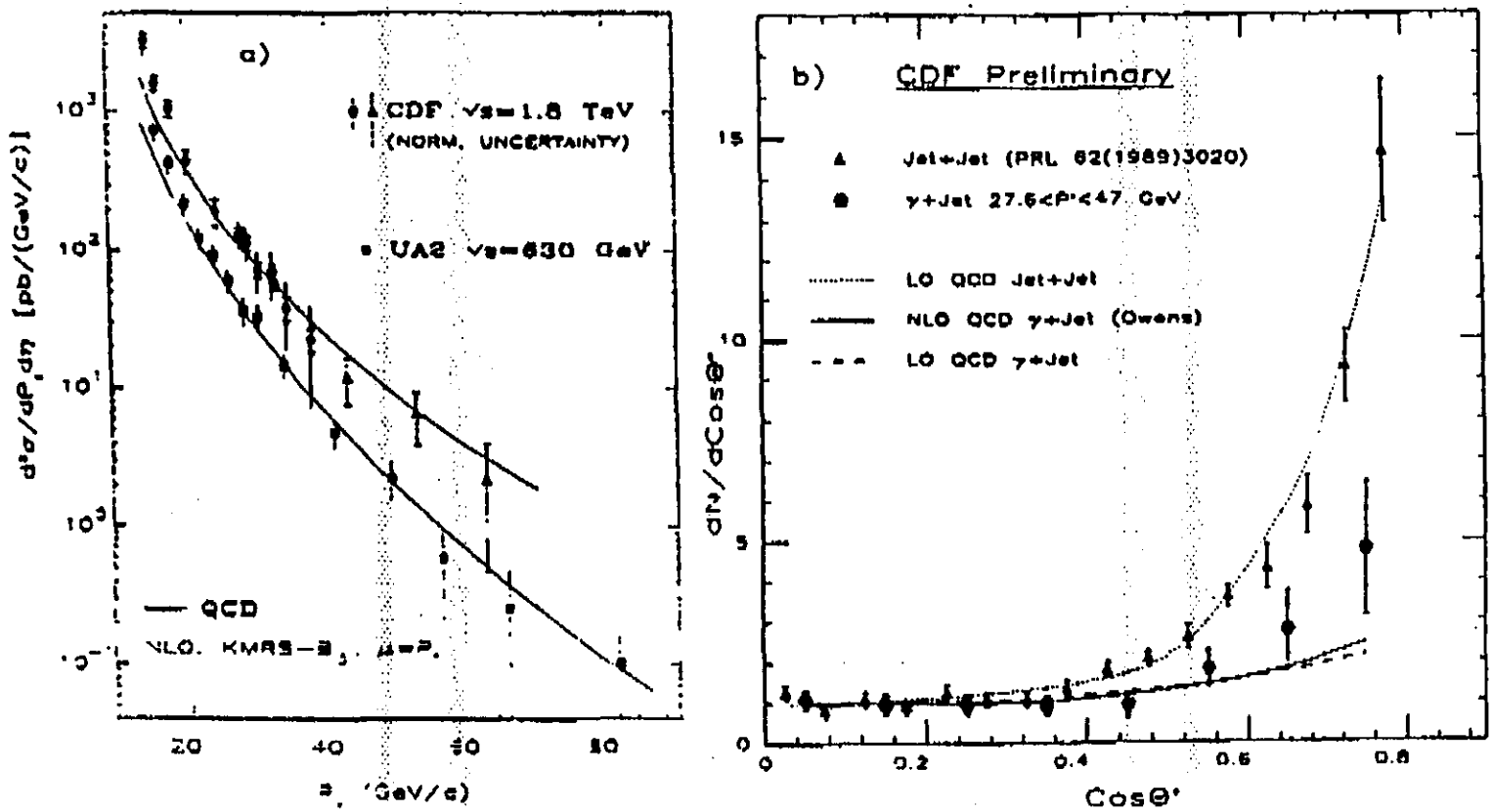

Figure 8: a) The isolated prompt photon cross section is compared to QCD. b) The CMS angular distribution for photon+jet and jet+jet events is compared to QCD.

show the $\cos\theta^*$ distribution for jet+jet events [9] compared to leading order calculations; QCD predicts a Rutherford-like scattering distribution resulting from subprocesses with t-channel gluon exchange (spin 1).

2.3. Isolated Double Photon Cross Section

In addition to probing the gluon distribution and testing QCD, production of two photons is an important background to Higgs $\to \gamma\gamma$ at the SSC. The three types of sub-

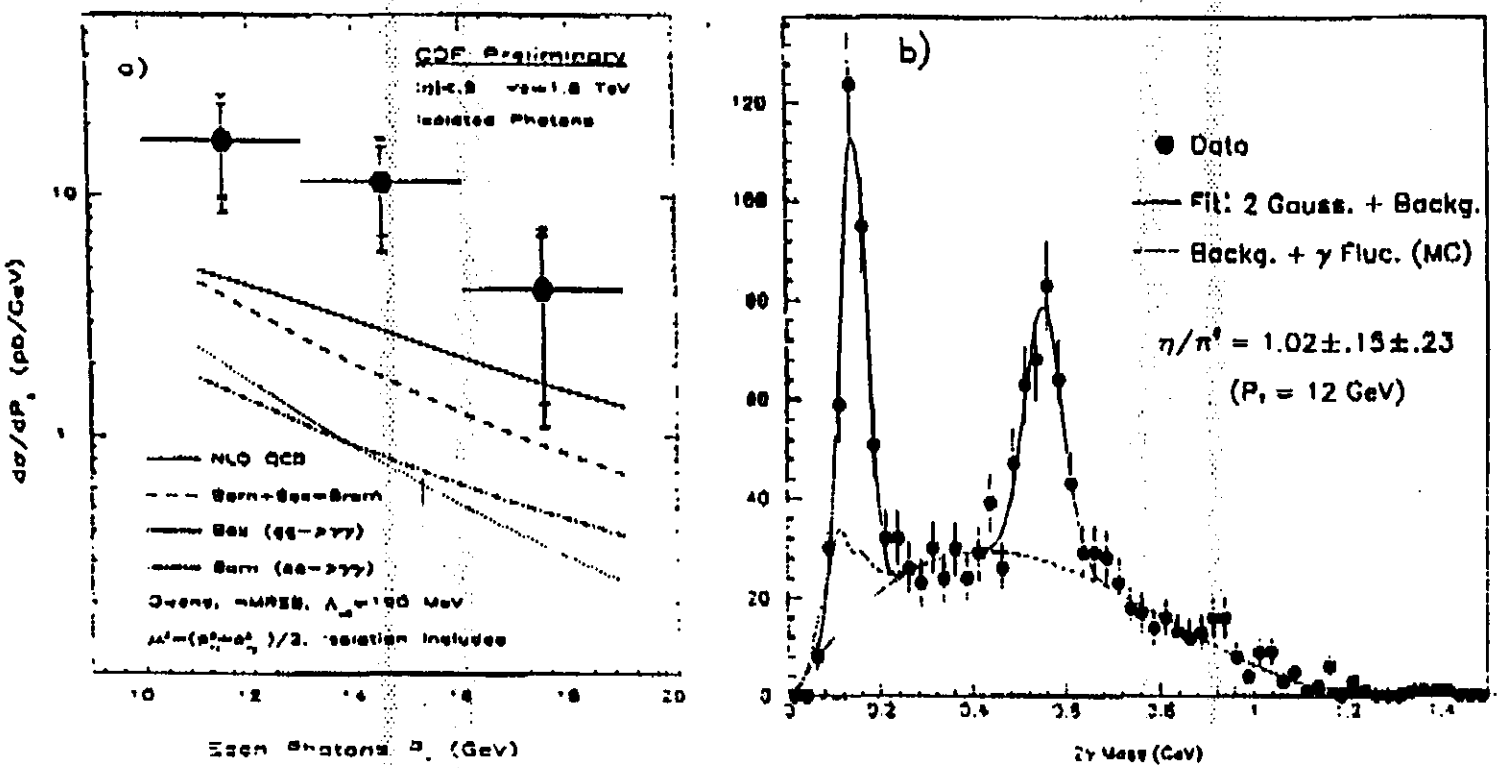

Figure 9: a) The isolated double prompt photon cross section compared to QCD predictions. [20] b) The invariant mass of two non-prompt photons (NOT the di-photon mass) shows peaks from isolated π^0 and η mesons.

2.4. *Isolated Meson Production Ratio η/π^0*

Isolated η and π^0 mesons are the primary background to prompt photons, so their relative production rates is of some interest. Also, the isolation requirement, described in section 2, may enhance the fraction of promptly produced mesons [22] relative to mesons from jet fragmentation. We use small CES clusters (25 mrad), to separate the closely spaced photons from π^0s as well as ηs, and require the two highest energy CES clusters to be in the adjoining CEM towers of a single isolated EM cluster. Multi-π^0 backgrounds are reduced by requiring the energy sum of extra CES clusters in the EM cluster be less than 30% of the sum of the highest two. Misidentification of single photon showers as

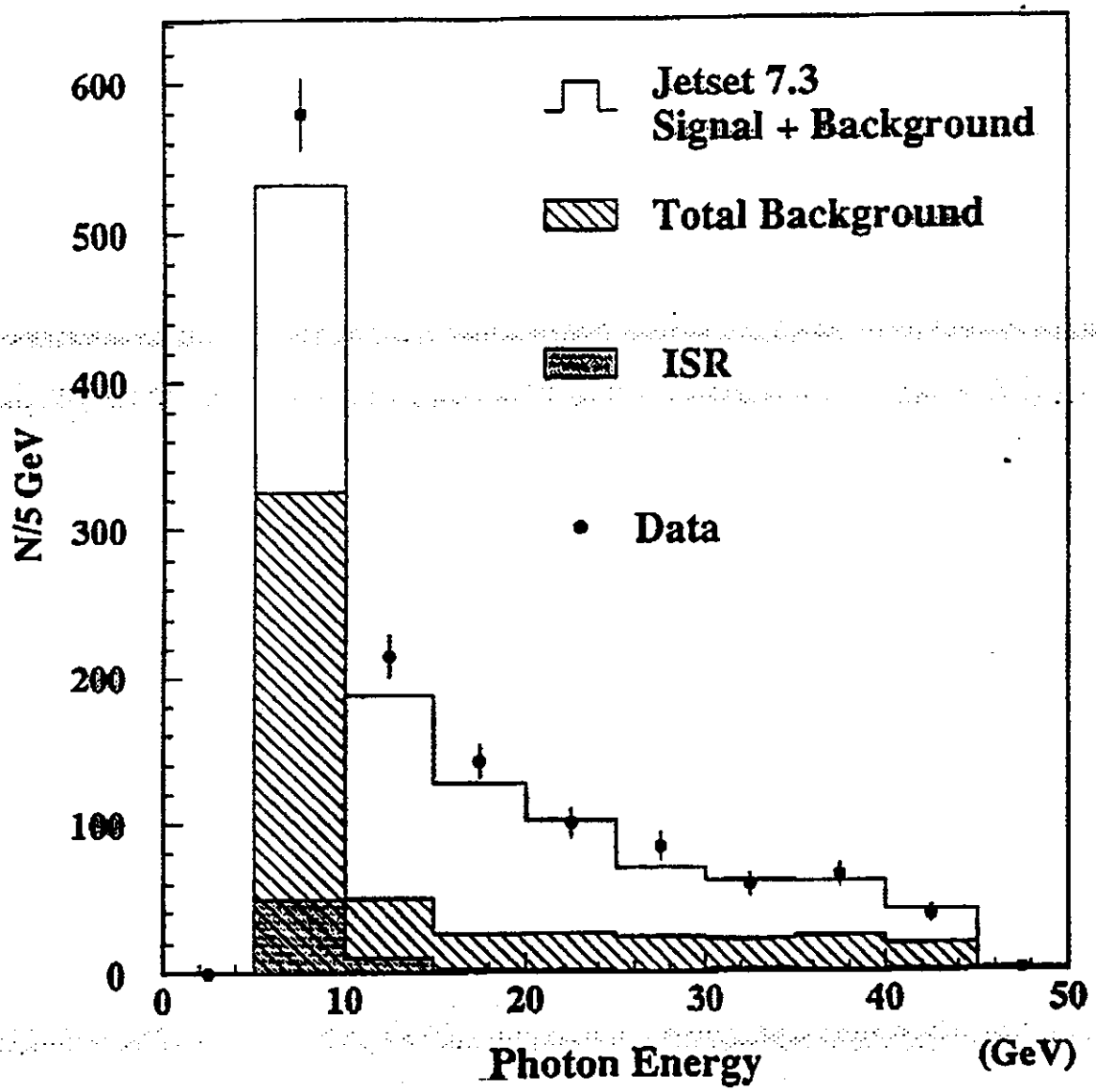
Jetset 7.3
Signal + Background
Total Background
ISR
Data
N/5 GeV
600
500
400
300
200
100
0
0
10
20
30
40
50
Photon Energy
(GeV)

Figure 2

Tomasz Skwarnicki

Tomasz Skwarnicki. SSCL/SMU

ANOTHER SIMULATION OF $H \to \gamma\gamma$ in LAr

purpose: independent check of 2hu & Yamamato results

try to take advantage of EM-HAD segmentation

try to optimize isolation cuts for γ/j rejection

use FAST1 program:

- transverse and longitudinal shower profiles by Bock parametrization
- fluctuations in interaction depth for hadrons
- spreading of charged particles in magnetic field
- parametrization of energy resolution as a function of η (from full simulation) equivalent to $\frac{7.5}{\sqrt{E}} \oplus 0.5$

most of the code written by H. Ma

→ + detailed simulation of pile-up in the calorimeter

(thermal $\sigma_{EC} = 20$ MeV, $\sigma_{HC} = 130$ MeV)

PILE-UP NOISE IN LAr CALORIMETERS ?

→ Important for γ/jet separation

Scintillation calorimeters are faster → lower pile-up noise TN-91-41 $\frac{\sigma_{BaF_2}}{\sigma_{LAr}} \approx \frac{1}{1.7}$

Zhu's analysis was not optimized for optimal γ/jet rejection in LAr

<u>method</u>:
- generate minimum bias events by PYTHIA
- deposit energies in EC, HC by FAST1i with termal and pile-up noise set to zero
- generate number of minimum bias events per bunch crossing from Poisson distribution with mean = 1.67

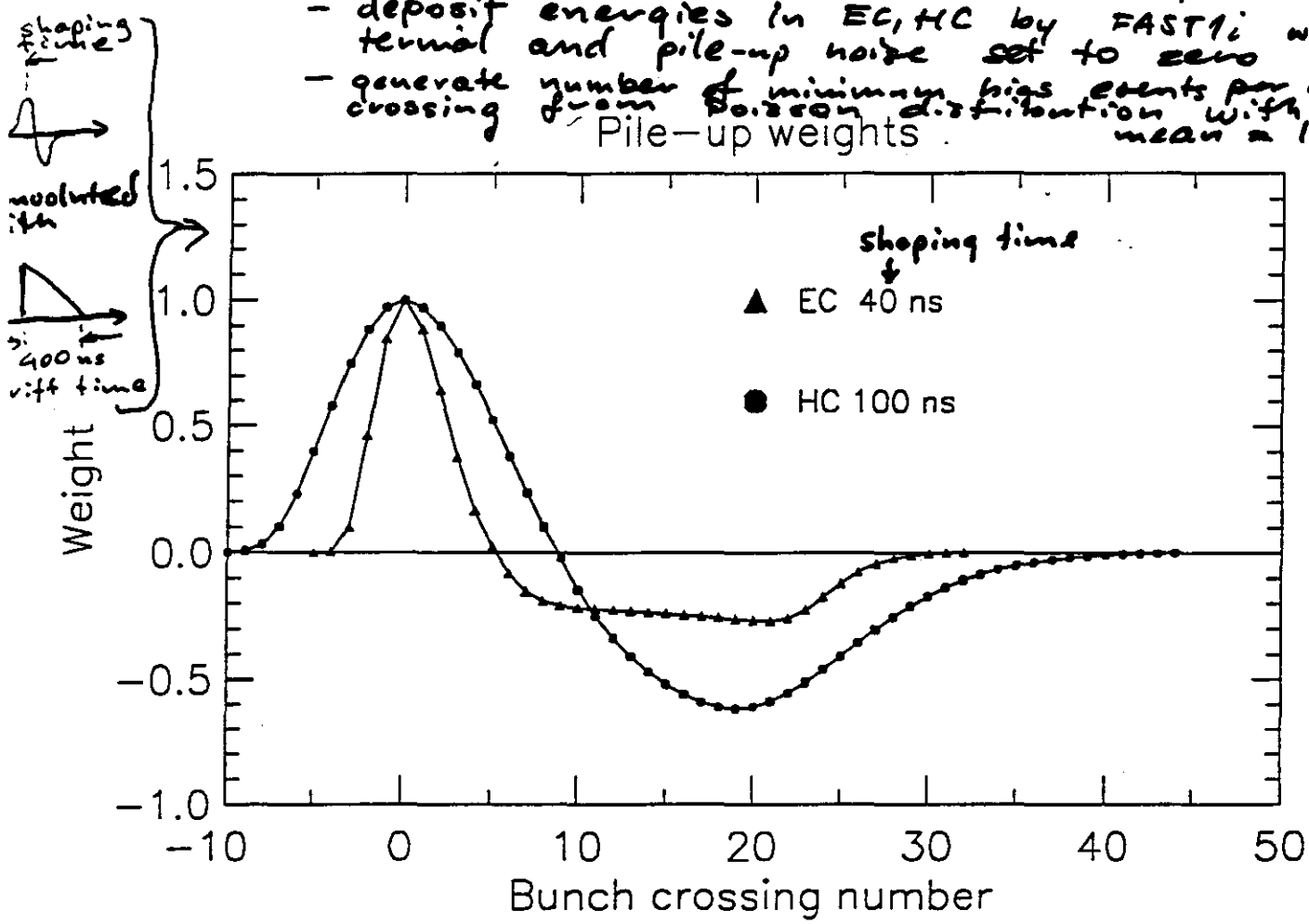

- sum up minimum bias events from past (44) and future (8) bunch crossings (+ present) multiplying cell energies by bunch crossing dependent weight (see above)

Results for RMS $\equiv \sqrt{\langle E_t^2 \rangle - \langle E_t \rangle^2}$
at $\eta = 0$ (in MeV)

EC			HC		
1 cell 0.032×0.032	3×3	5×5	1 cell 0.08×0.08	3×3	5×5
32	163	321	130	568	985
Baseline-I document					
32			118		
TN-91-41	author: "GEM Collaboration"				
30	150		145	1060 (4×4)	

We are used to use RMS numbers as they came from the Gaussian distribution! How Gaussian pile-up E_t distributions are?

MINUIT χ^2 Fit to Plot 101&0
EC Cell
File: H101.DAT 22-JUL-92 22:21:00
Plot Area Total/Fit 33558. / 33558. Fit Status 0
Func Area Total/Fit 33893. / 33893. E.D.M. 1.00
χ^2=144374.6 for 100 − 3 d.o.f., C.L.=0.000E+00%

Errors		Parabolic	Minos	
Function 1: Gaussian Distribution (sigma)				
AREA	33992.	±0.1000	−0.0000E+00	+0.0000E+00
MEAN	−5.30000E−04	±1.0000E−02	−0.0000E+00	+0.0000E+00
SIGMA	3.36000E−02	±1.0000E−02	−0.0000E+00	+0.0000E+00

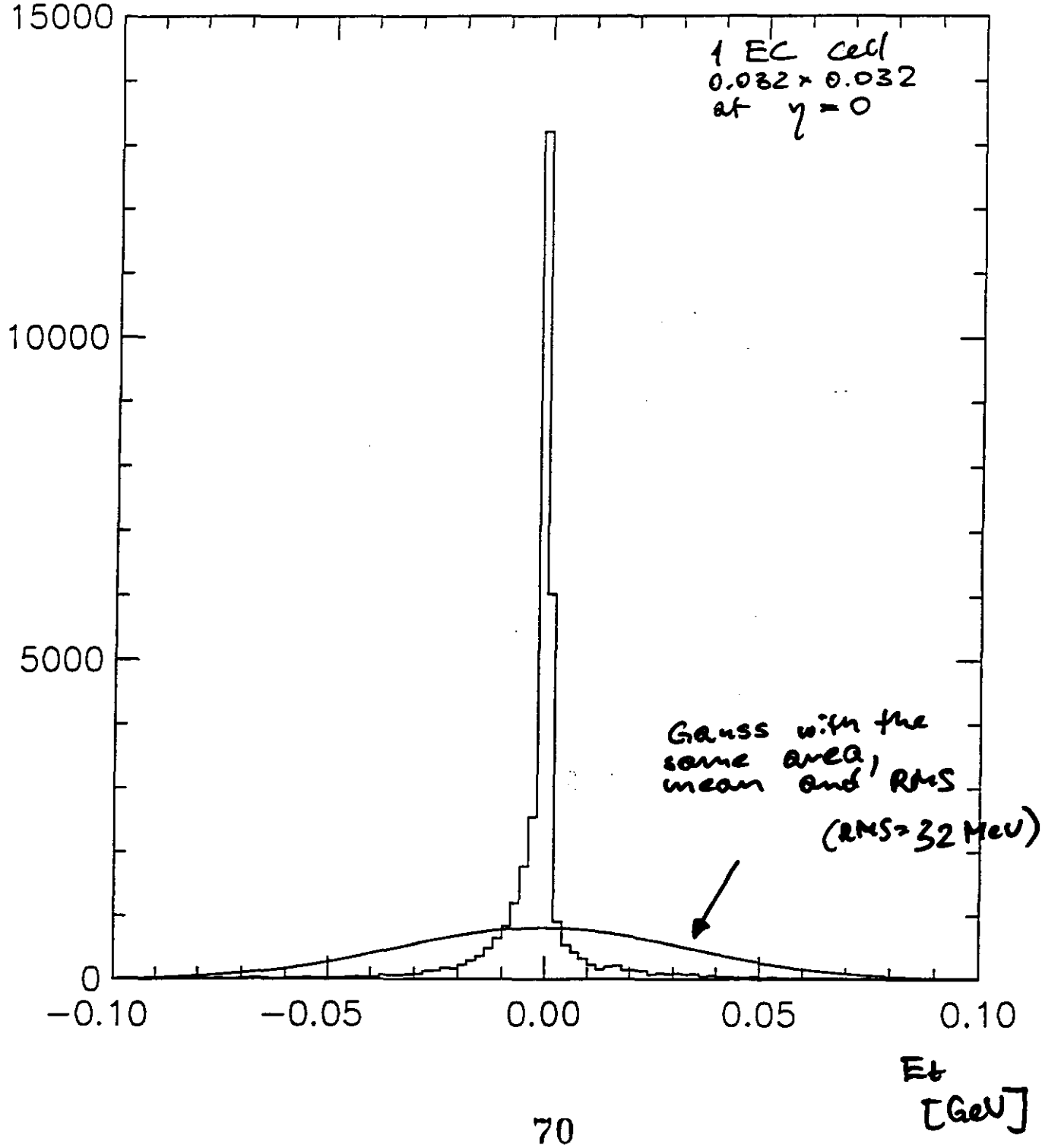

File: Generated internally

ID	IDB	Symb	Date/Time	Area	Mean	R.M.S.
3211	0	1	920723/1127	1.000	−6.9362E−03	0.9847
1	0	−1	920723/1129	1.0000	−6.9359E−03	0.9847

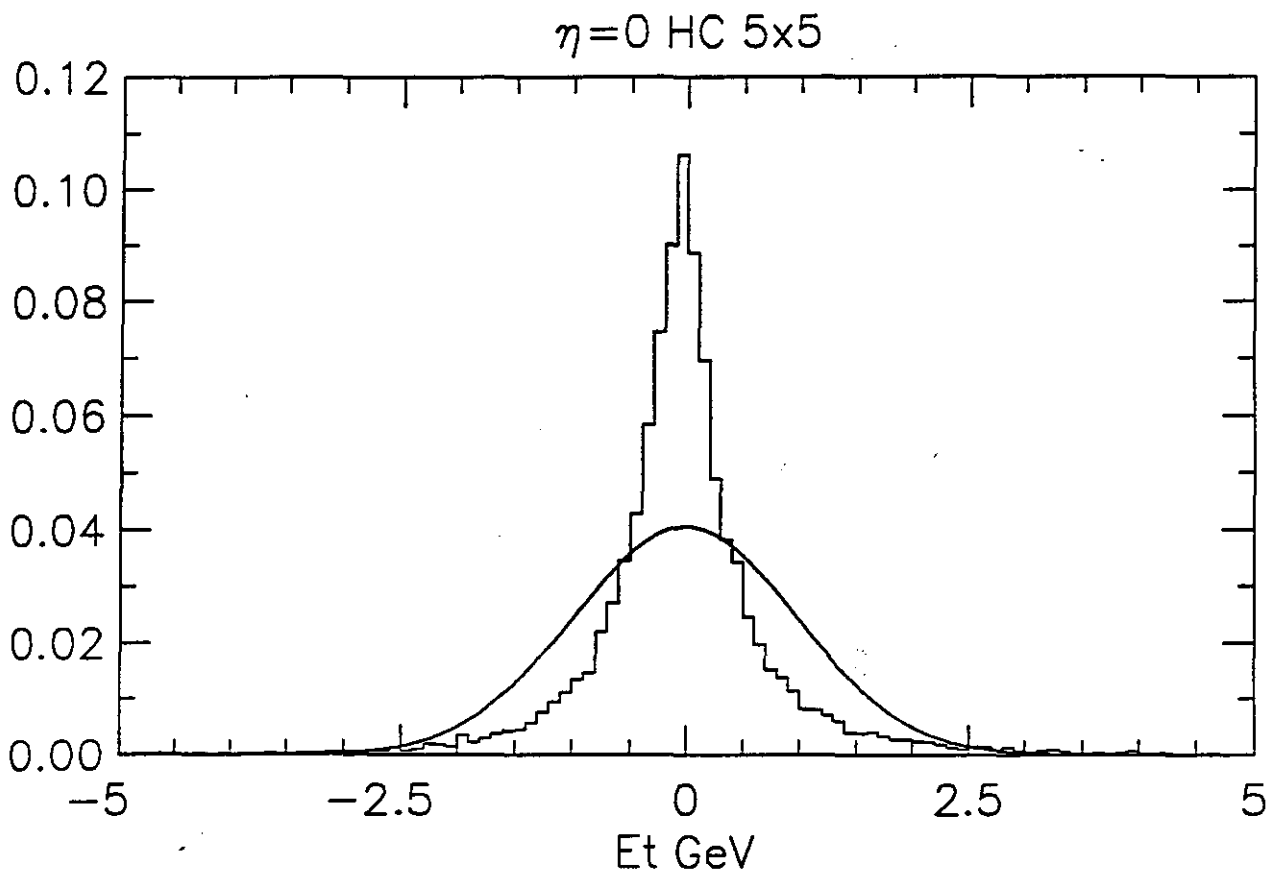

central part of the distribution (relevant for γ/jet cuts) is by a factor of 2 narrower than Gaussian of the same RMS

use ~ 12,000 statistically independent pile-up events

generate 10,000 events per Higgs mass

10,000 direct $\gamma\gamma$ events $\sigma_{generated}$

$\hat{m} > 75$ GeV

$\hat{p}_t > 20$ GeV 55.6 pb

$|\hat{\eta}| < 2.7$

320,000 γj events 42,900 pb

no jj background simulation so far

Initial cuts:

"γ" – local energy maximum in EC (in group 3x3)

E_t^γ – from 5x5 in EC corrected for transverse shower leakage at large η

select two highest E_t "γ"s

$E_t^\gamma > 20$ GeV

$|\eta^\gamma| < 2.5$ $|\eta^\gamma - 1.5| > 0.11$ to exclude barrel-endcap transition region → picture

$|\cos\theta^*| < 0.85$ → picture

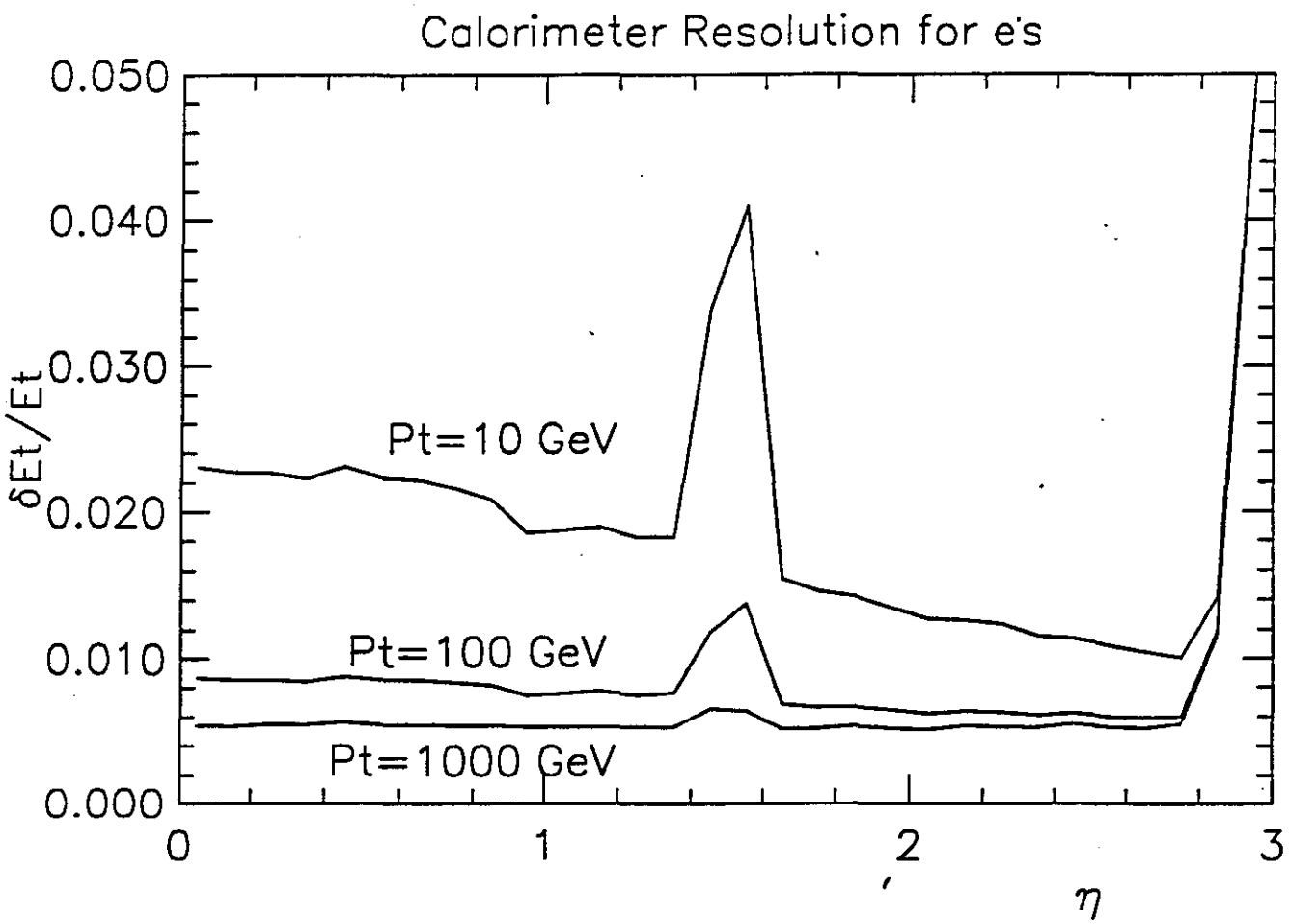
Calorimeter Resolution for e's
0.050
0.040
0.030
0.020
0.010
0.000
δEt/Et
Pt=10 GeV
Pt=100 GeV
Pt=1000 GeV
0
1
2
3
η

File: Generated internally

ID	IDB	Symb	Date/Time	Area	Mean	R.M.S.
1091	0	1	920804/0221	1.000	0.5589	0.2940
1092	0	−31	920804/0221	1.000	0.4268	0.2534
1093	0	−36	920804/0221	1.000	0.5143	0.2755

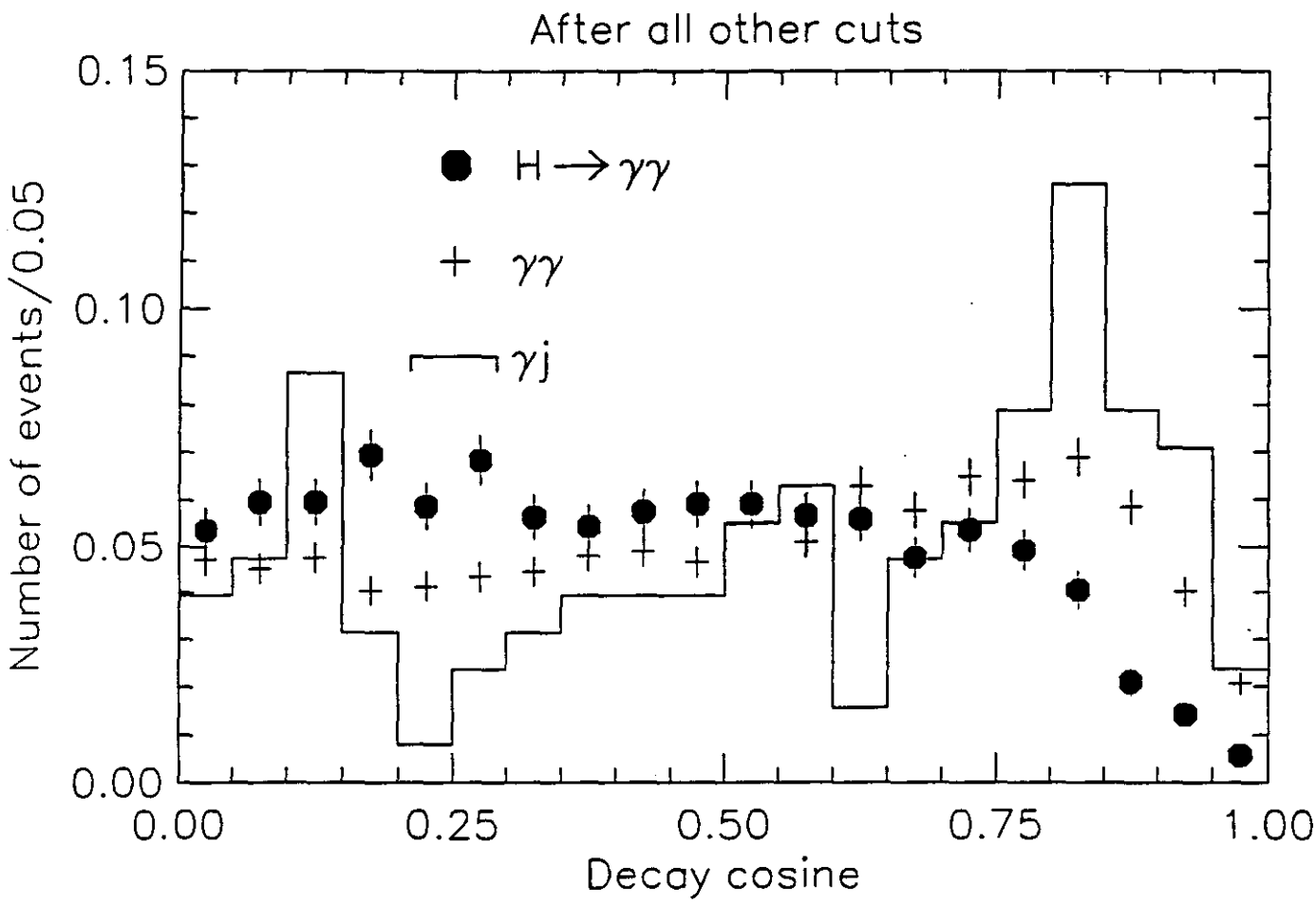

isolation cut in HC:

$\Delta\eta \quad \Delta\phi$
$(.24 \times .24)$

E9HC – 3×3 sum in HC behind EC cluster (ie. in EC direction)

E25EC – 5×5 sum in EC $(.16 \times .16)$

File: Generated internally

ID	IDB	Symb	Date/Time	Area	Mean	R.M.S.
1031	0	−1	920803/2120	640.0	0.0000E+00	0.0000E+00
1032	0	−1	920803/2121	687.2	0.0000E+00	0.0000E+00

$$\frac{E9HC}{E25EC} < 0.035$$

selects photons and jets which fragmented mostly to neutrals

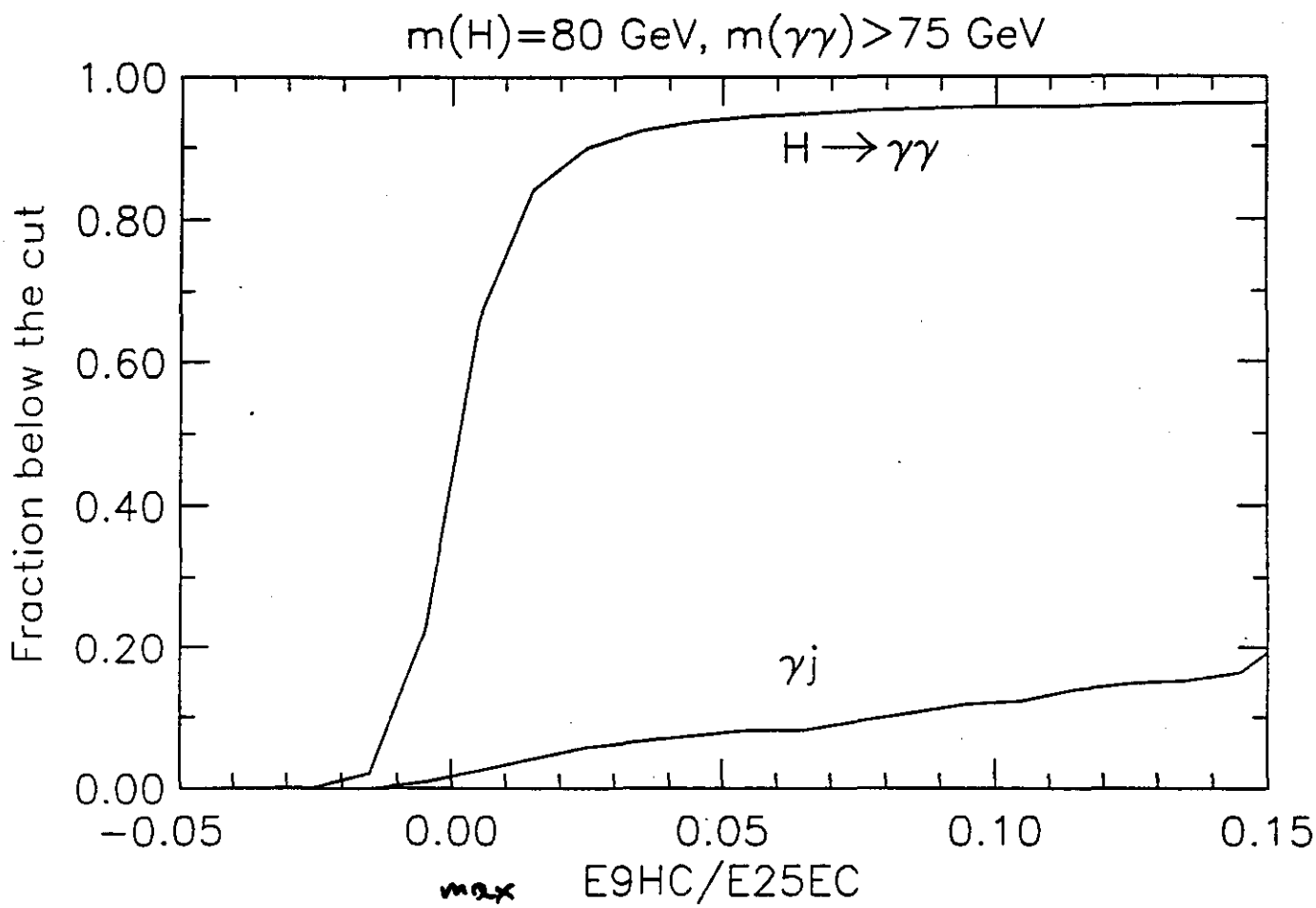

max from two "γ" in the event

isolation cut in EC:

cone of $R = \sqrt{\Delta\eta^2 + \Delta\varphi^2} < 0.4$

sum-up only cells with $E_t > 75$ MeV

$$75 = 2 \times \sqrt{\sigma^2_{thermal} + RMS^2_{pile\text{-}up}}$$

20 32

subtract leakage corrected 5×5 $E_t\gamma$

File: Generated internally

ID	IDB	Symb	Date/Time	Area	Mean	R.M.S.
41	0	1	920803/2200	1.000	9.152	7.820
42	0	1	920803/2200	1.000	2.013	2.725

(after E9HC/E25EC < .035)

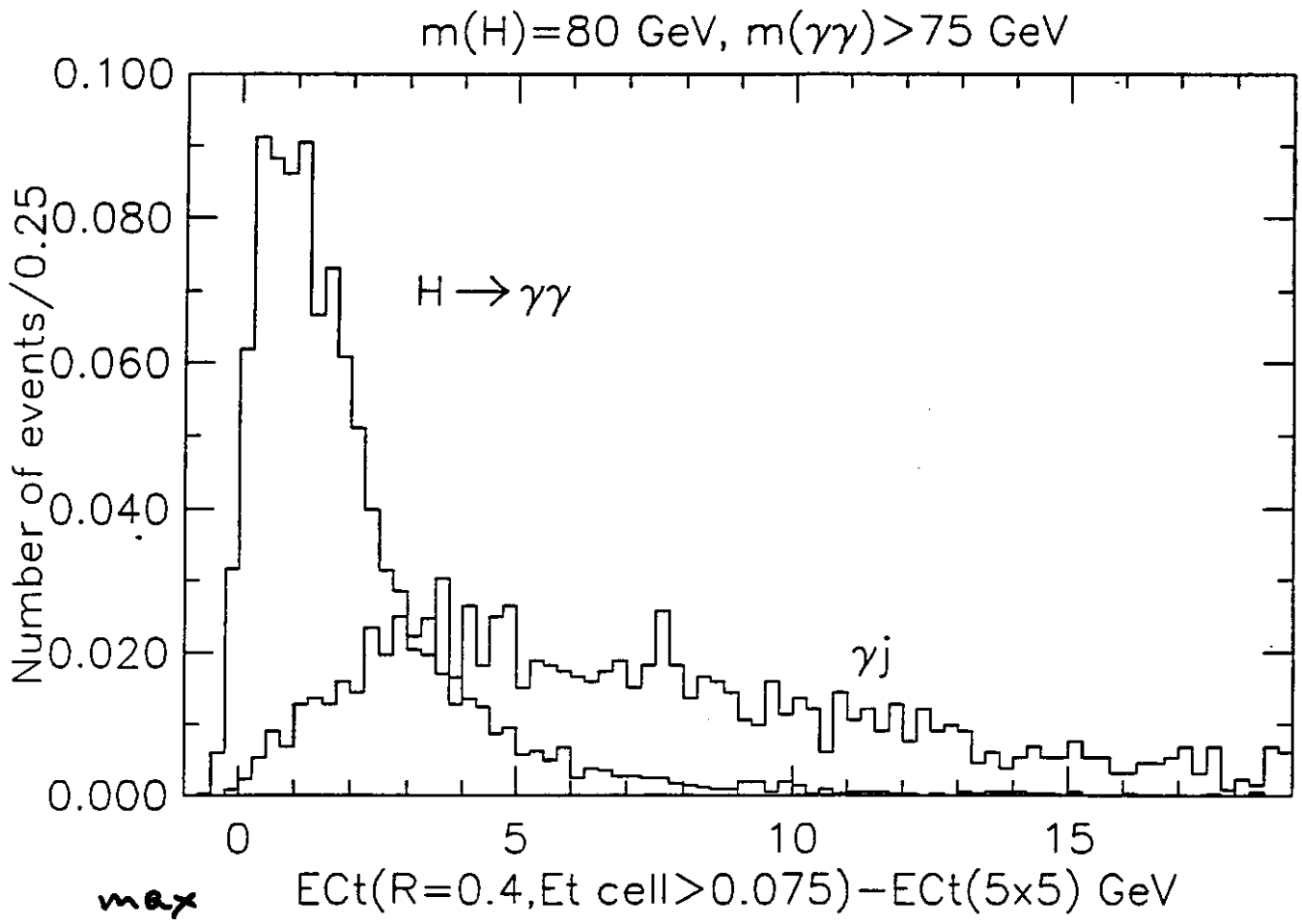

File: Generated internally

ID	IDB	Symb	Date/Time	Area	Mean	R.M.S.
1041	0	−1	920803/2200	343.9	0.0000E+00	0.0000E+00
1042	0	−1	920803/2200	372.4	0.0000E+00	0.0000E+00

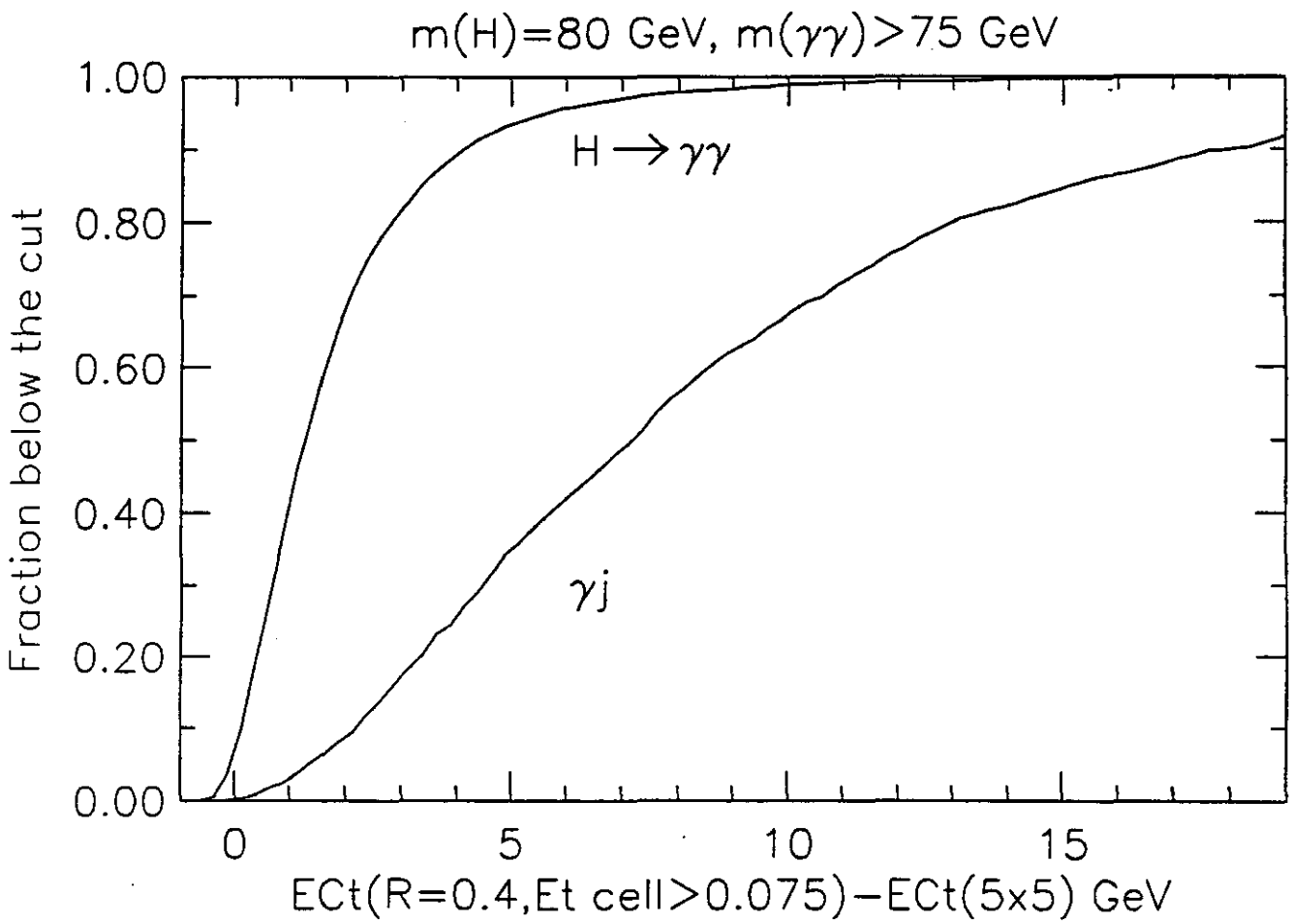

choose cut value to maximize signal <u>significance</u>:

$\Delta BC < 2$ GeV

File: Generated internally

ID	IDB	Symb	Date/Time	Area	Mean	R.M.S.
2041	0	−1	920803/2215	434.0	0.0000E+00	0.0000E+00
99	0	−1	000000/0000	2.000	100.0	100.0

$$\text{Significance gain} = \frac{\epsilon_{signal}}{\sqrt{\epsilon_{background}}}$$

> 1.0 gain significance

< 1.0 loose significance

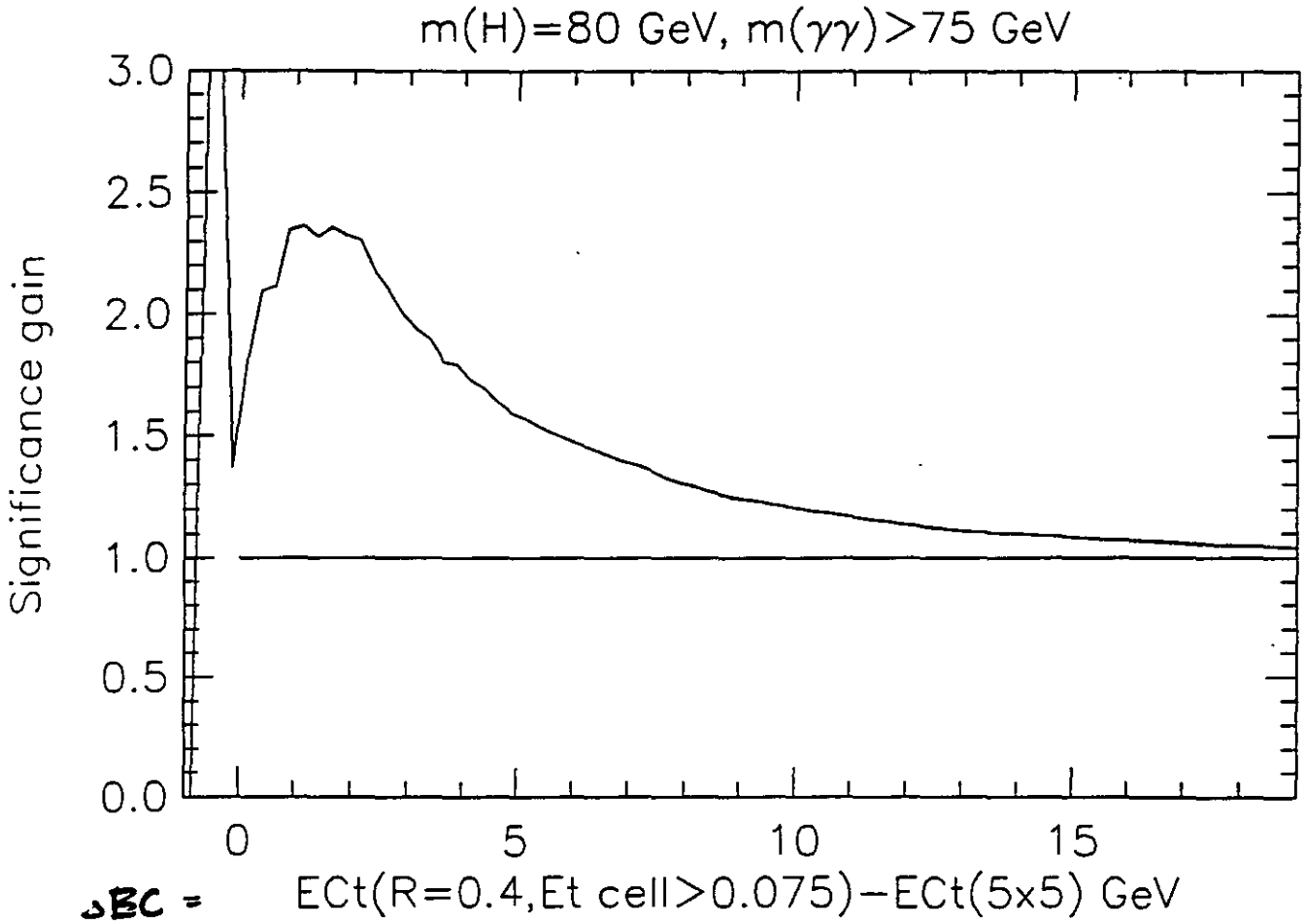

after this cut find that wide cone isolation cut in H.C. brings negligible [illegible] significance

"shower shape"

$E9/E25 > 0.88$

File: Generated internally

ID	IDB	Symb	Date/Time	Area	Mean	R.M.S.
72	0	1	920804/0252	1.000	0.9191	2.4757E−02
71	0	−31	920804/0252	1.000	0.8769	5.6621E−02

$\epsilon_{Back.}$ 0.56

$\epsilon_{sig} = 0.92$

I would not trust fast simulation in this number

but it happens to be exactly the same as the result of Ma's full simulation quoted in GEM-TN-92-126

After all other cuts

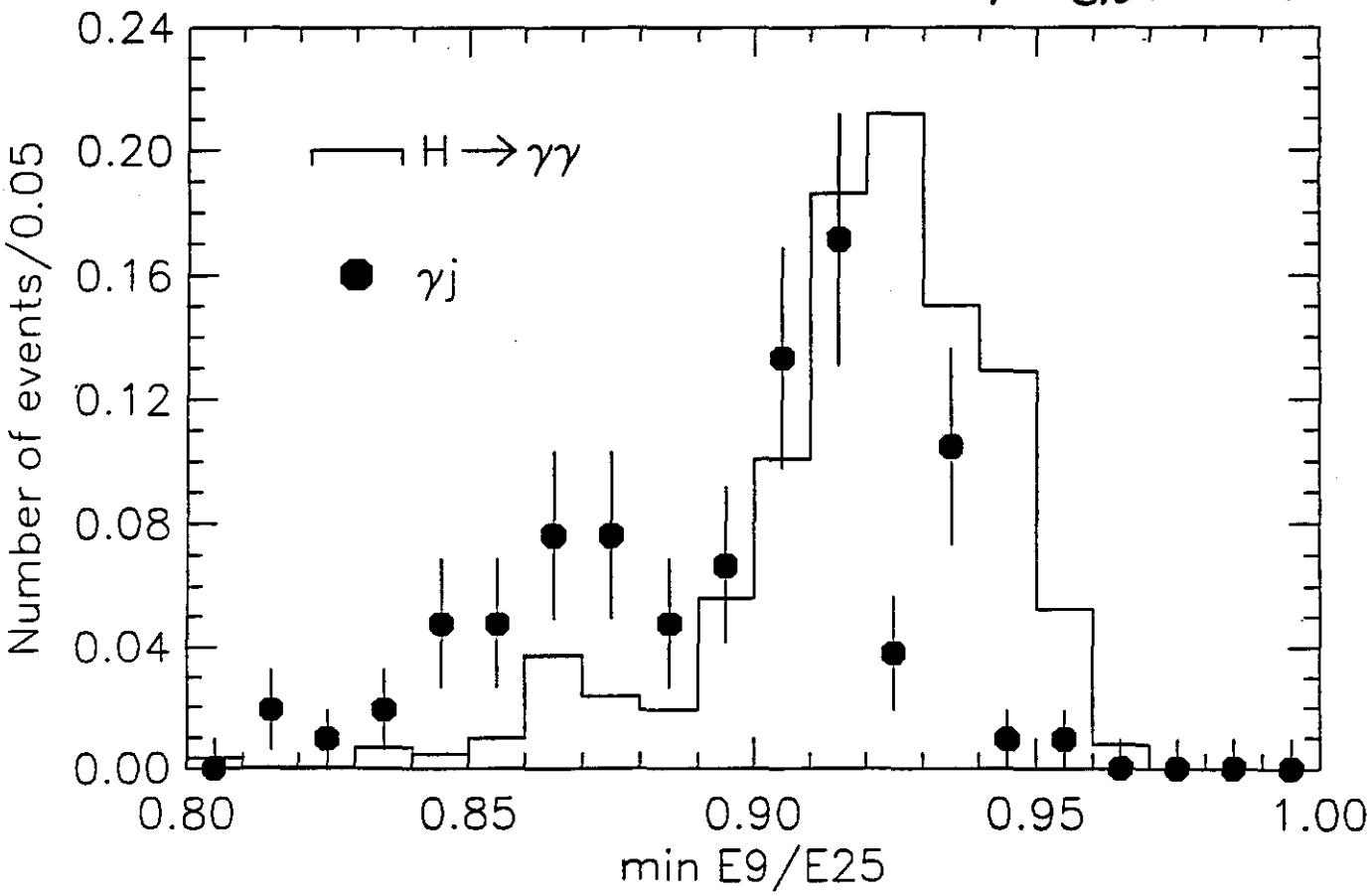

accept is as reasonable estimate

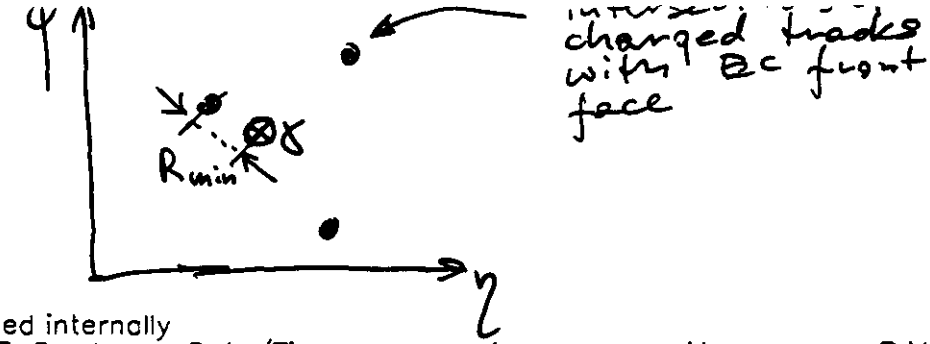

File: Generated internally

ID	IDB	Symb	Date/Time	Area	Mean	R.M.S.
251	0	1	920804/0303	1.037	0.1434	9.5782E−02
252	0	−31	920804/0304	0.8092	0.2081	9.5783E−02
253	0	−36	920804/0305	0.9420	0.2083	9.6097E−02

so far have not used CT at all since this is not realistic — e background! —

require: $\min R(\gamma - CT) < 0.07$

Brings only 9% improvement in $\epsilon_\gamma/\sqrt{\epsilon_j}$

This assumes that every track is detected in IPC for example γ (as hit, not necessarily reconstructed as track)

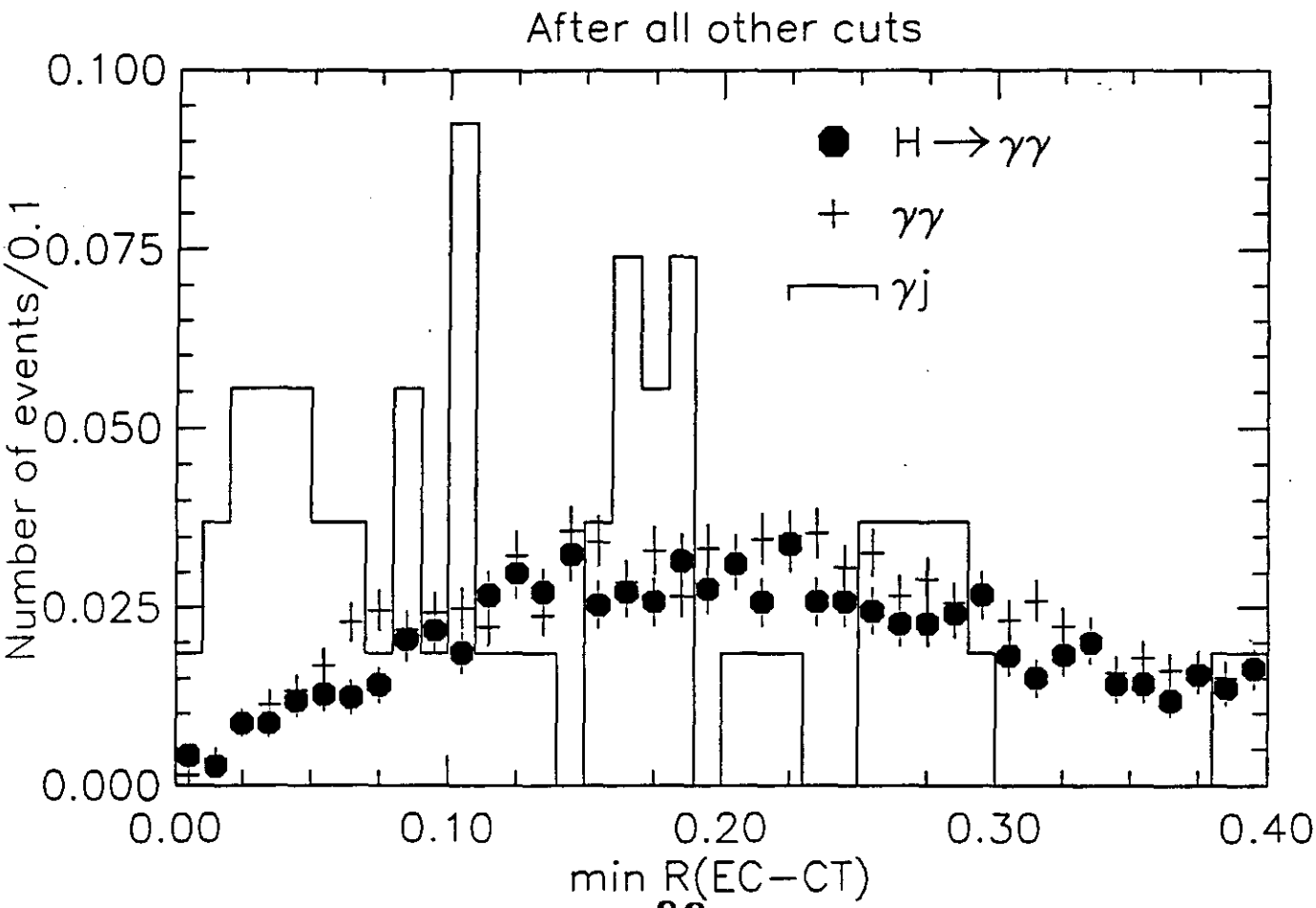

The above is not correct since the fast simulation does not convert γs yet. Converted γs should help in γ/j rejection even more!

visible background in $M_{\gamma\gamma}$ 75 – 165 GeV
[pb]

process	THIS ANALYSIS			GEM-TN-92-126	
	after isolation	after shower shape	after neutral by CT	after isolation & neutral by CT	after shower shape & neutral by CT
$\gamma\gamma$	18	16	15.2 *	31	31
γj	13	7	5.4	55	31
jj	?	?	2 **	140	73

* $H \to \gamma\gamma$ also has lower efficiency in this analysis

γ/j rejection in γj process improved by a factor of ~5.7 with loss of efficiency by a factor of ~2

** $\frac{73}{5.7^2} = 2.2$ pb ?

assume conservatively $\sigma_{jj} = \sigma_{\gamma j}$

MINUIT Likelihood Fit to Plot 201&0
Proj. onto MGG axis
File: hgg09_hgg_a.rz 3-AUG-92 23:15:00
Plot Area Total/Fit 2074.0 / 2037.0 Fit Status 3
Func Area Total/Fit 2054.0 / 2036.3 E.D.M. 3.961E-06

Likelihood = 17.4
χ^2= 17.5 for 16 - 3 d.o.f., C.L.= 17.8%

Errors		Parabolic	Minos	
Function 1: Gaussian Distribution (sigma)				
AREA	2054.0	±45.28	-0.0000E+00	+0.0000E+00
MEAN	79.967	±1.7382E-02	-0.0000E+00	+0.0000E+00
SIGMA	0.76059	±1.3858E-02	-0.0000E+00	+0.0000E+00

vs. 0.66 MeV in GEM-TN-92-126

likely to be caused in this analysis by exact non-gaussian pile-up simulation and 5×5 → E

$M_H = 80$ GeV 10,000 generated

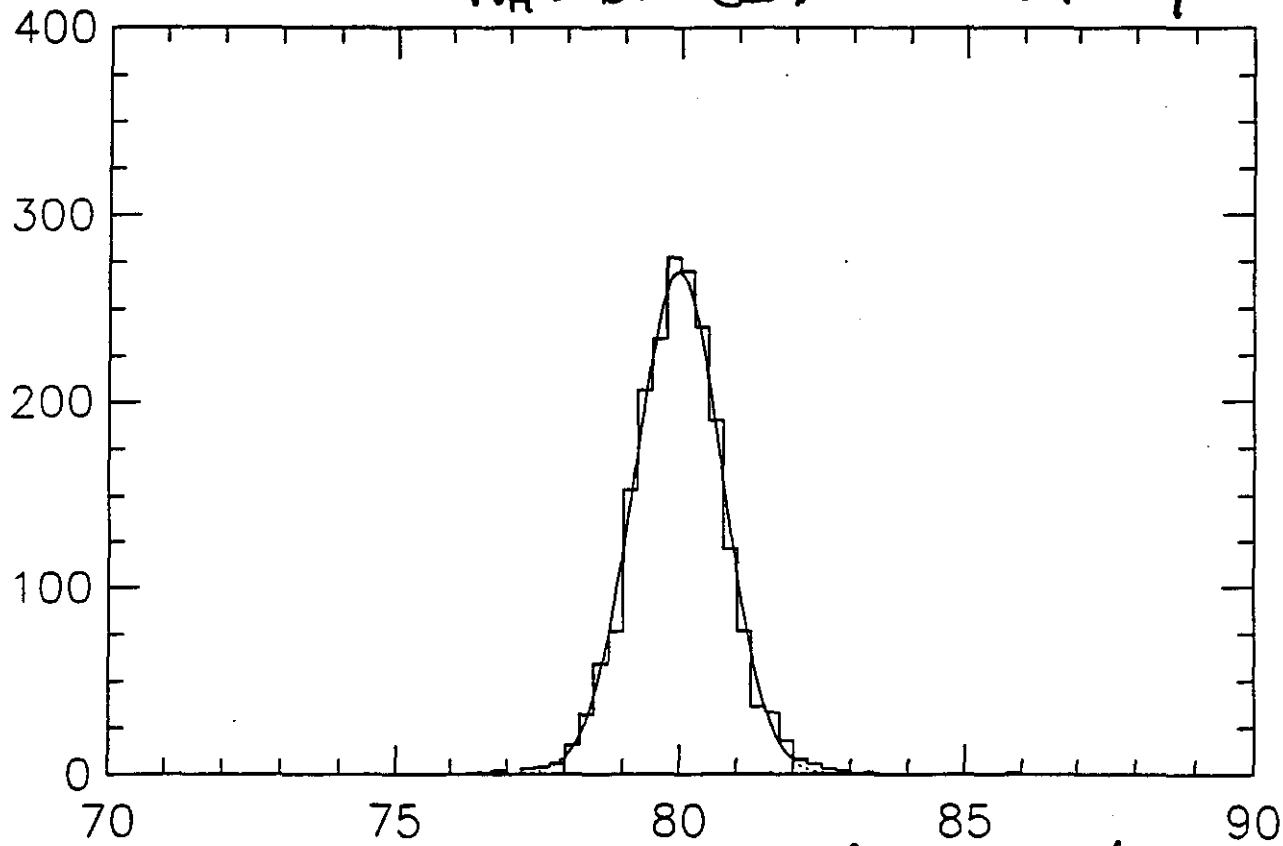

assumes vertex identified correctly!

File: Generated internally

ID	IDB	Symb	Date/Time	Area	Mean	R.M.S.
1051	0	−31	920803/2233	1.000	92.92	17.44
1053	0	1	920803/2233	1.000	101.6	22.68

assume $M_{\gamma\gamma}$ for γj, jj background the same as for $\gamma\gamma$ background

this may be wrong!
have not enough γj statistics to verify
(same assumption in GEM-TN-92-126 analysis)

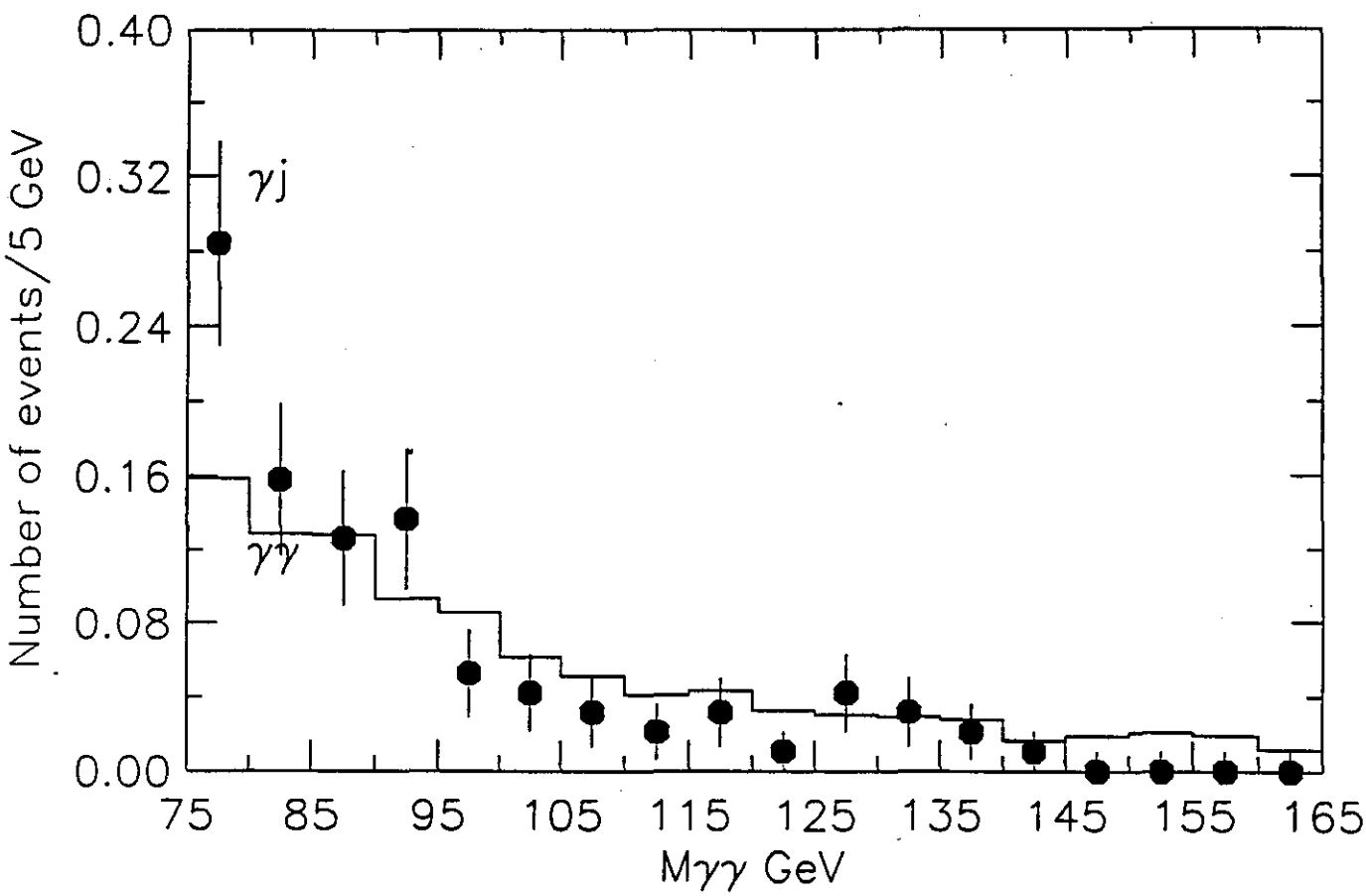

M_H	RMS ($M_{\gamma\gamma}$) this analysis	RMS ($M_{\gamma\gamma}$) GEM-TN-92-126	total cross-section generated by PYTHIA $\epsilon_{H\to\gamma\gamma}$	within $\pm 1\sigma$ $\sigma_{H\to\gamma\gamma}$ [pb]
80 GeV	.76	.66	.21	.026
100 GeV	.84	.73	.23	.039
120 GeV	.89	.77	.24	.049
140 GeV	1.05	.89	.24	.043
160 GeV	1.12	1.10	.25	.012

DOES NOT INCLUDE K-factor

significance of the signal using formula from GEM-TN-92-126 (back. integrated in $\pm 1\sigma$) and assuming $\sigma_{ii} = \sigma_{j\gamma}$

	Significance in 1 SSCY		GEM-TN-92-126 (no pre-radiator)
80	2.5	1.7	1.5
100	4.9	3.3	3.0
120	8.3	5.5	5.2
140	9.1	6.1	5.7
160	3.3	2.2	2.2

no K-factor

DOES INCLUDE K-factor of 1.5

$1\ \text{SSCY} = 10^4\ \text{pb}^{-1}$

<u>conclusion</u>: can search for $H \to \gamma\gamma$ in 1 SSCY with LAr and <u>no pre-radiator</u> for $m_H \sim 100-140$ GeV

80, 160 significance is marginal

```
PLAY OF EC

  2.0 R   .40 RR   .39 HETA,HPHI          12          12

------- tracks ---------
Pt            .273 ID   211 A JY JP          7          -7
Pt            .462 ID  -211 B JY JP          7          -3
r of CT tracks          2
------- bumps ---------
Et          30.374 # JY JP          0          0
r of EC bumps          1
------- particles ---------
Pt            4.438 ID    22 a JY JP         -1           0
Pt           26.054 ID    22 b JY JP          0           0
Pt             .582 ID    22 c JY JP          3          -7
Pt             .273 ID   211 d JY JP          7          -9
Pt             .462 ID  -211 e JY JP          7          -2
Pt             .194 ID   211 f JY JP         -6           9
   -12  -11  -10   -9   -8   -7   -6   -5   -4   -3   -2   -1    0    1    2    3    4    5    6    7    8    9   10   11   12
```

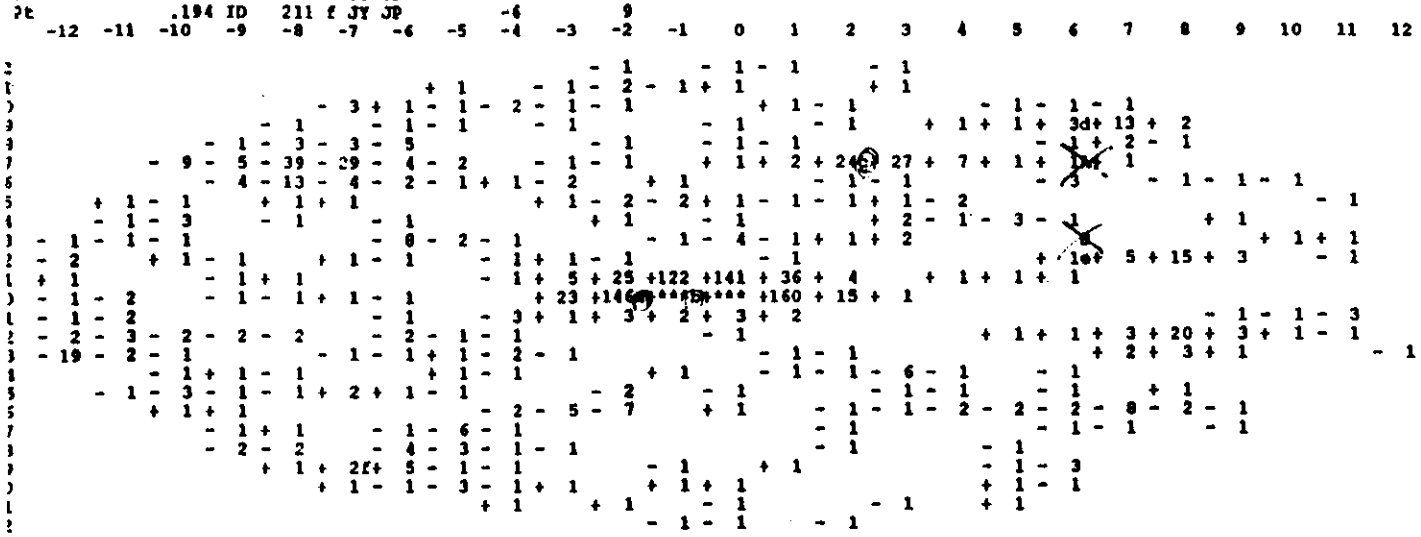

```
   -12  -11  -10   -9   -8   -7   -6   -5   -4   -3   -2   -1    0    1    2    3    4    5    6    7    8    9   10   11   12
 energy  31.28099
```

π^0 $P_t = 30$ GeV from u-jet with $p_t = 31.4$ GeV

X – charged tracks both from minimum bias event in the same bunch crossing

$I = 10$ MeV

γ from $\pi^0 \to \gamma e^+ e^-$
.6 GeV
from the same jet

$M_H = 80$

Can tighter E_t cuts help?

File: Generated internally

ID	IDB	Symb	Date/Time	Area	Mean	R.M.S.
1011	0	−1	920803/1654	15.02	0.0000E+00	0.0000E+00
1012	0	−1	920803/1654	17.10	0.0000E+00	0.0000E+00
1013	0	−1	920803/1655	15.97	0.0000E+00	0.0000E+00

$M_H = 80$ GeV

$|M_{\gamma\gamma} - 80| < 5$ for $\gamma j, \gamma\gamma$ IMPORTANT!

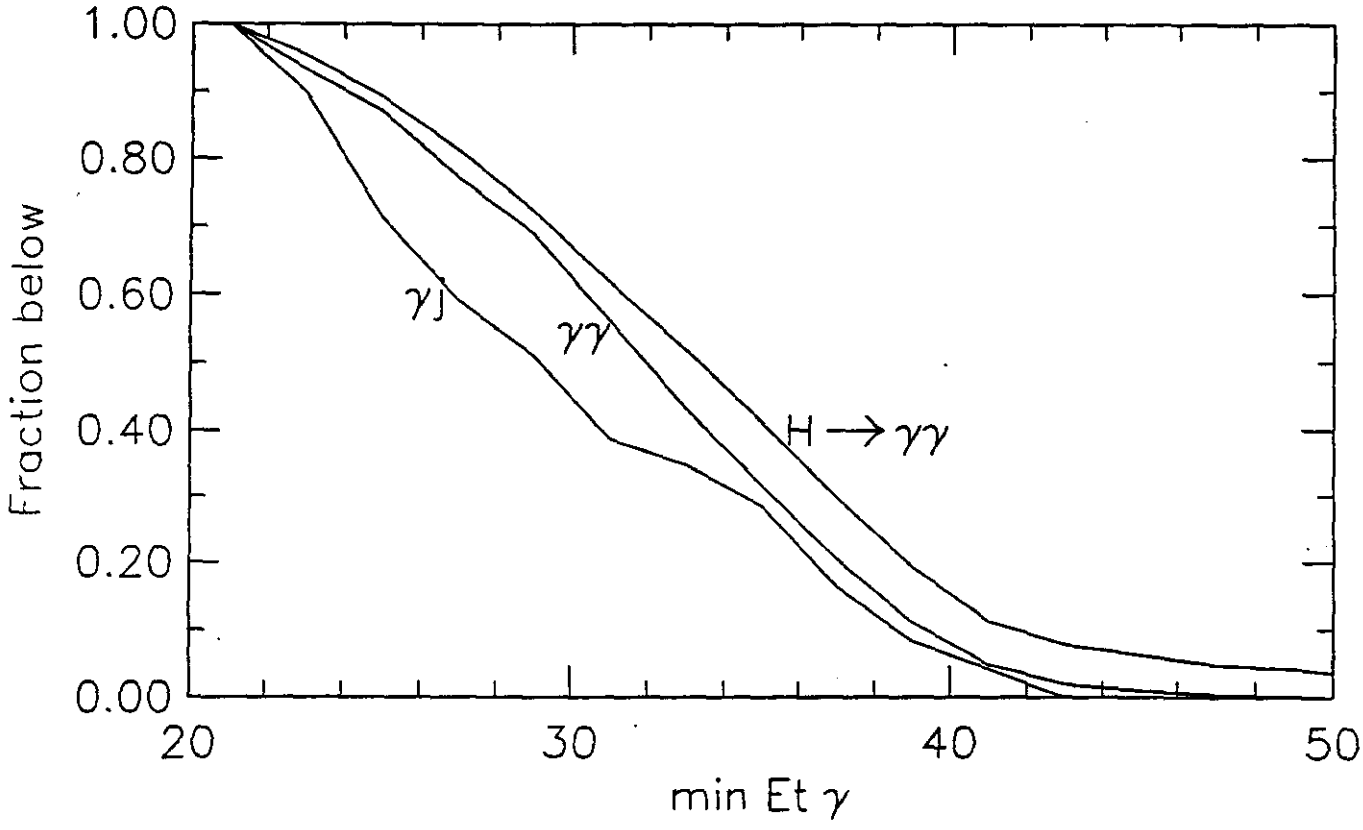

$m_H = 130$

File: Generated internally

iD	IDB	Symb	Date/Time	Area	Mean	R.M.S.
1021	0	−1	920803/1706	42.02	0.0000E+00	0.0000E+00
1022	0	−1	920803/1706	51.31	0.0000E+00	0.0000E+00
1023	0	−1	920803/1707	42.56	0.0000E+00	0.0000E+00

the difference is too small to make $\frac{\epsilon_S}{\sqrt{\epsilon_B}} > 1$

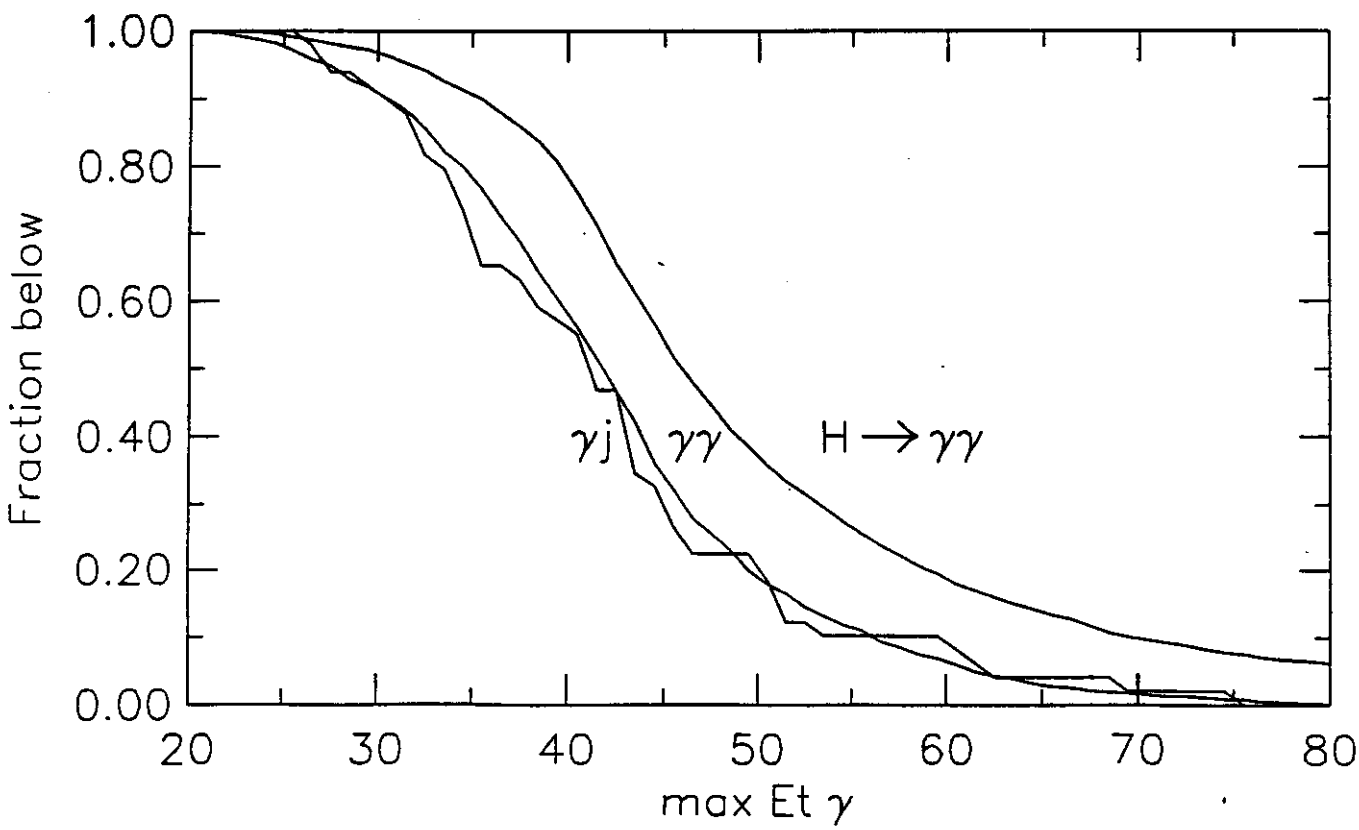

$m_H = 62$ GeV

File: Generated internally

ID	IDB	Symb	Date/Time	Area	Mean	R.M.S.
1031	0	−1	920803/1717	21.12	0.0000E+00	0.0000E+00
1032	0	−1	920803/1718	35.06	0.0000E+00	0.0000E+00
1033	0	−1	920803/1718	20.65	0.0000E+00	0.0000E+00

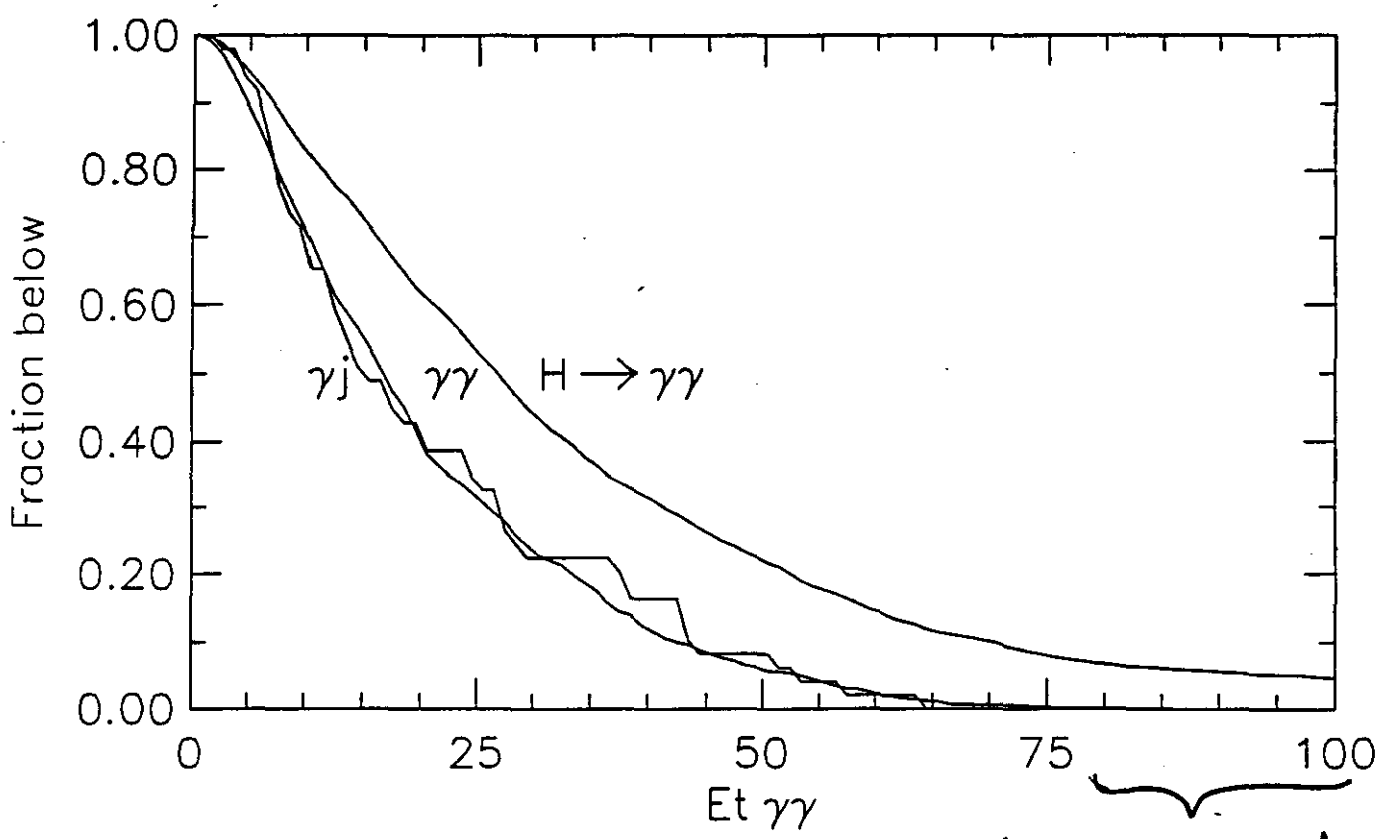

if this was true could detect ~10% of signal with no background

$m_H = 80$

File: Generated internally

ID	IDB	Symb	Date/Time	Area	Mean	R.M.S.
1131	0	−1	920803/1723	1414.	0.0000E+00	0.0000E+00
1133	0	−1	920803/1724	1.0740E+05	0.0000E+00	0.0000E+00
99	0	−1	000000/0000	2.000	100.0	100.0

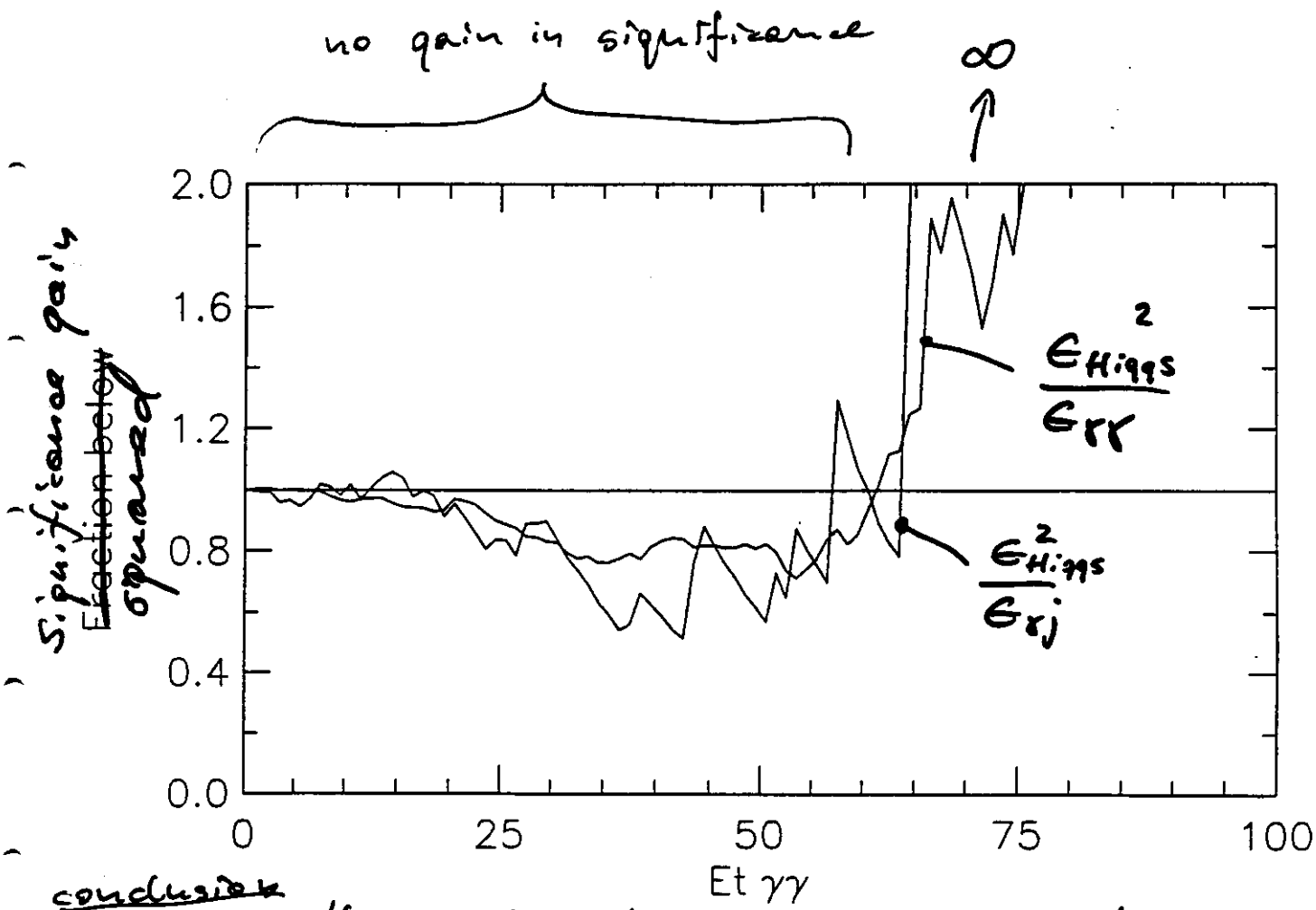

conclusion

after the cuts done in this analysis tighter E_t^γ, $E_t^{\gamma\gamma}$ cuts don't help

Sasha Vanyashin

A. Vanyashin
Aug. 4, 92

on correlation between

$M_{\gamma''\gamma''} > 80$ GeV cut

and

$P_T^H > 40$ GeV cut

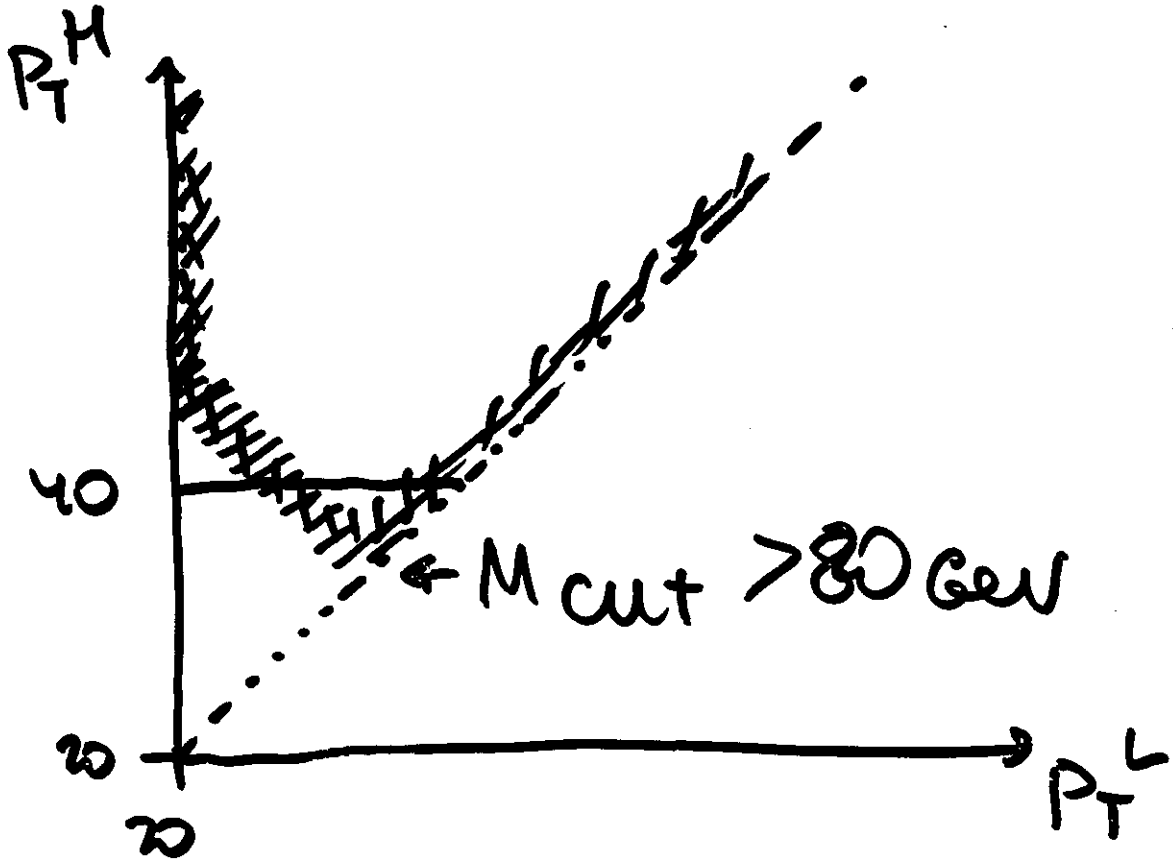

no improvement from $P_T^H > 40$ GeV cut in γ-jet Background

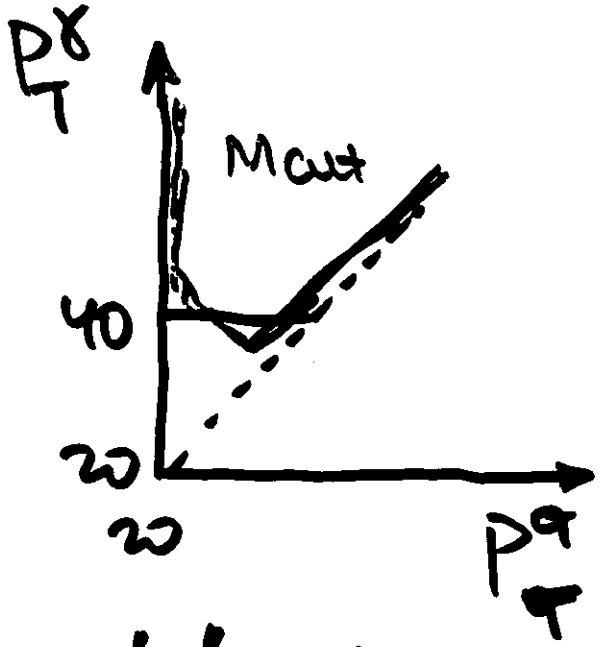

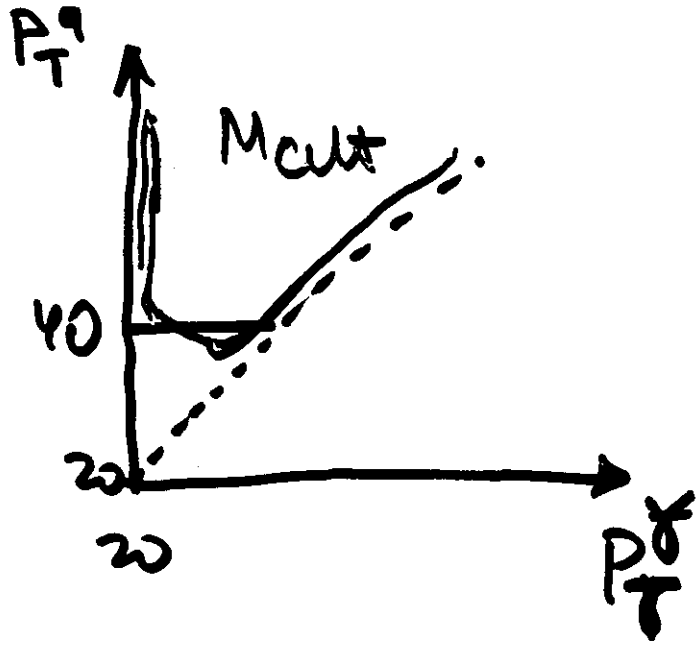

$$\sigma^{\text{"}\gamma\gamma\text{"}}_{\gamma\cdot\text{jet}}(P_T^H > 40) =$$

$$= \sigma^{q\gamma}_{QCD}(M_{q\gamma} > 20) \cdot \left\{ \frac{1}{2} \underbrace{R\left(\frac{\gamma_{40}}{\gamma_{max}}\right)}_{=0.84} \cdot R\left(\frac{\text{"}\gamma\text{"}_{20}}{q_{min}}\right) \right.$$

$$\sim 10^{-3}$$

$$+ \frac{1}{2} \underbrace{R\left(\frac{\gamma_{20}}{\gamma_{min}}\right)}_{=1} \cdot R\left(\frac{\text{"}\gamma\text{"}_{40}}{q_{max}}\right)$$

20 GeV in 0.45 cone:

$$R\left(\frac{\text{"}\gamma\text{"}_{20}}{q_{min}}\right) = 1.35\, R\left(\frac{\text{"}\gamma\text{"}_{20}}{q_{all}}\right)$$

$33 \cdot 10^{-4}$

$\boxed{\text{RY: } 54 \cdot 10^{-4}}$

$$R\left(\frac{\text{"}\gamma\text{"}_{40}}{q_{max}}\right) = \frac{1}{(4 \pm 1)}\, R\left(\frac{\text{"}\gamma\text{"}_{20}}{q_{all}}\right)$$

improvement after $P_T^M > 40$ GeV

(isol. : 20 GeV in 0.45 cone)

$$\sigma_{\gamma jet}^{\gamma \text{"}\gamma\text{"}} (P_T^H > 40) = 0.7\, \sigma_{\gamma jet}^{\gamma \text{"}\gamma\text{"}}$$

mostly quark jets

$$\sigma_{qq}^{\text{"}\gamma\text{"}\text{"}\gamma\text{"}} (P_T^H > 40) = \frac{R(\text{"}\gamma\text{"}40/jet)}{R(\text{"}\gamma\text{"}20/jet)} \cdot \sigma_{qq}^{\text{"}\gamma\text{"}\text{"}\gamma\text{"}} =$$

$$= \frac{1}{(4 \pm 1)}\, \sigma_{qq}^{\text{"}\gamma\text{"}\text{"}\gamma\text{"}} \text{ (no cut)}$$

---

would be better for tighter isolation cut

Kostya Shmakov

Pointing and Light Higgs Mass Reconstruction With LKr/LAr EM calorimeter

- Light Higgs mass reconstruction at different luminosities.
- Energy resolution of LKr/LAr EM calorimeter

  Paramerization of resolution vs Θ

- Angular resolution and pointing - experimental data ($RD3$) vs Monte Carlo
- Stable method for position and angular reconstruction
- Pointing to the vertex and angular resolution with LKr/LAr EM calorimeter
- Impact on $H_0 \rightarrow 2\gamma$ width

K.Shmakov

$H_0 \rightarrow \gamma\gamma$ decay:

$$\frac{\delta M_{H_0}}{M_{H_0}} = \frac{1}{2}\sqrt{\left(\frac{\delta E_1}{E_1}\right)^2 + \left(\frac{\delta E_2}{E_2}\right)^2 + \left(\frac{\delta\Theta}{\tan(\frac{\Theta}{2})}\right)^2}$$

EM calorimeter should pick up:

(1) *Energy resolution* $\sigma(E)/E$

(2) *Position resolution*

(3) *Angular resolution*

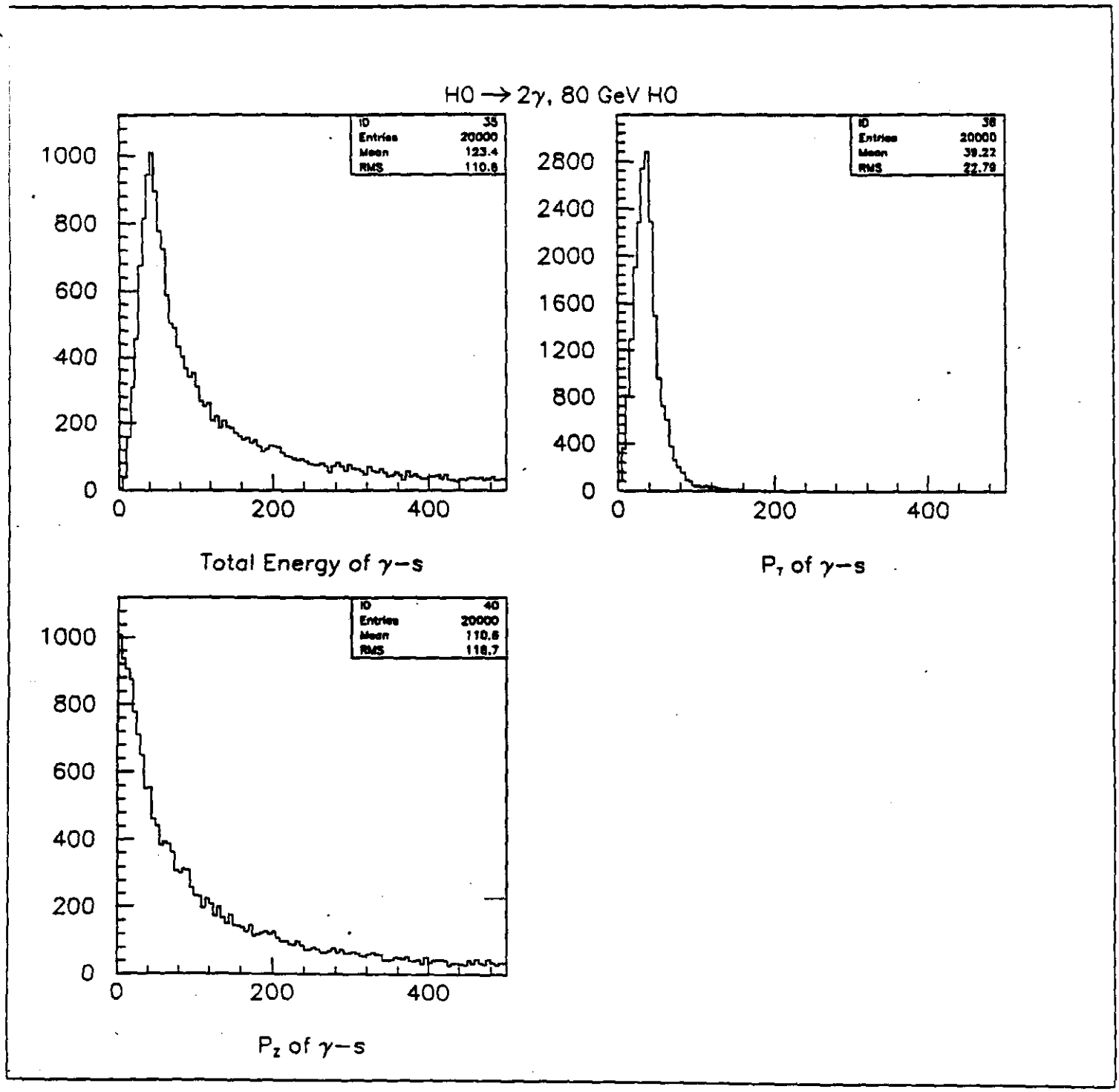
H0 → 2γ, 80 GeV H0
ID 35
Entries 20000
Mean 123.4
RMS 110.6
Total Energy of γ−s
ID 38
Entries 20000
Mean 39.22
RMS 22.79
P_T of γ−s
ID 40
Entries 20000
Mean 110.6
RMS 118.7
P_z of γ−s

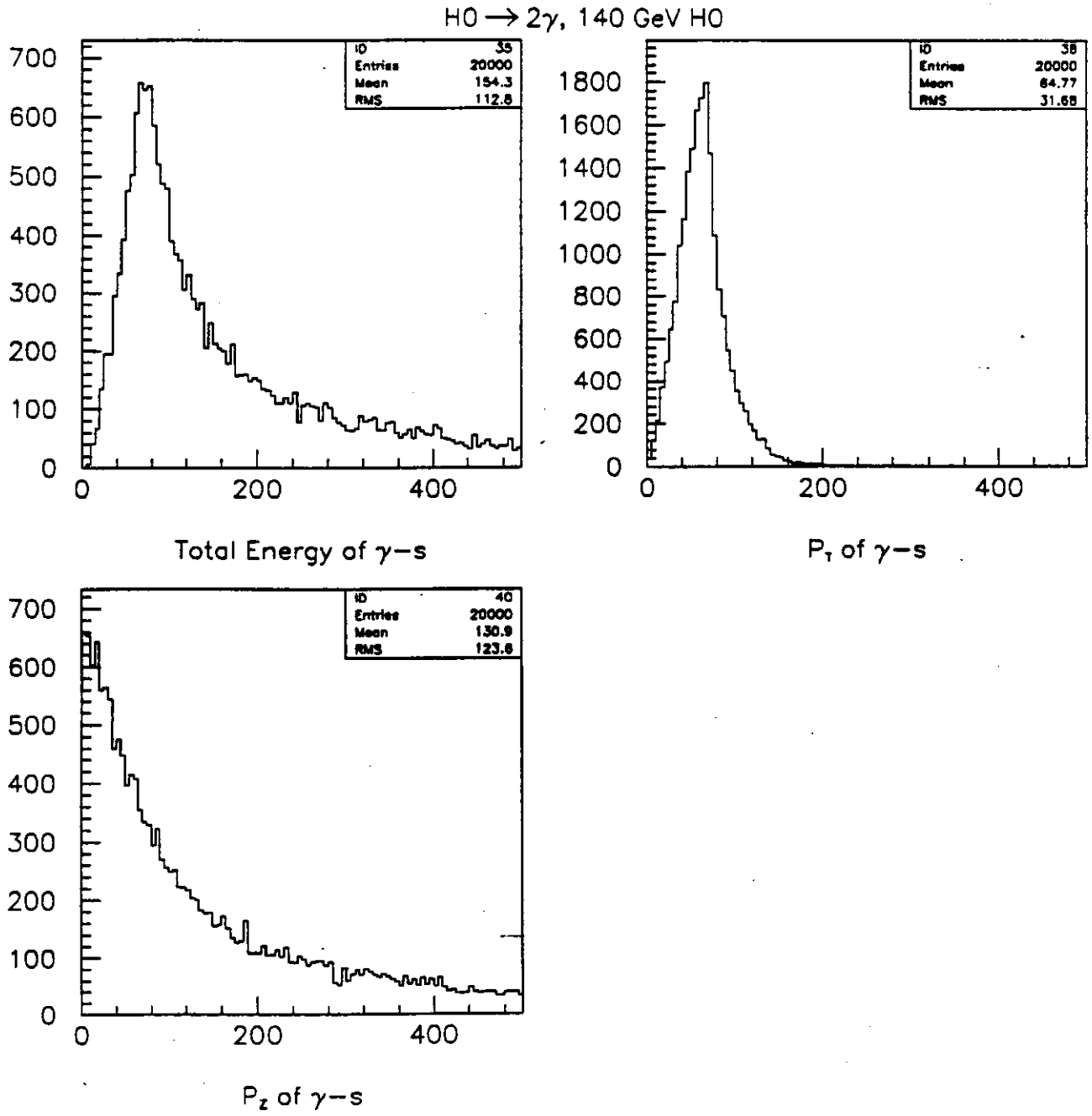
H0 → 2γ, 140 GeV H0
ID 35
Entries 20000
Mean 154.3
RMS 112.8
Total Energy of γ−s
ID 38
Entries 20000
Mean 64.77
RMS 31.68
P_T of γ−s
ID 40
Entries 20000
Mean 130.9
RMS 123.6
P_z of γ−s

$\delta\theta_{12}$ contribution to H_0 width.

1)

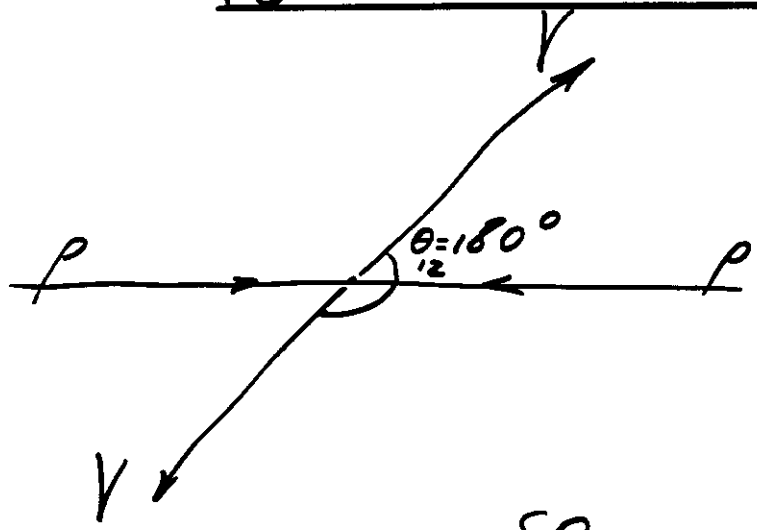

$$\delta m/m \simeq \frac{\delta\theta_{12}}{\infty} = 0.$$

2)

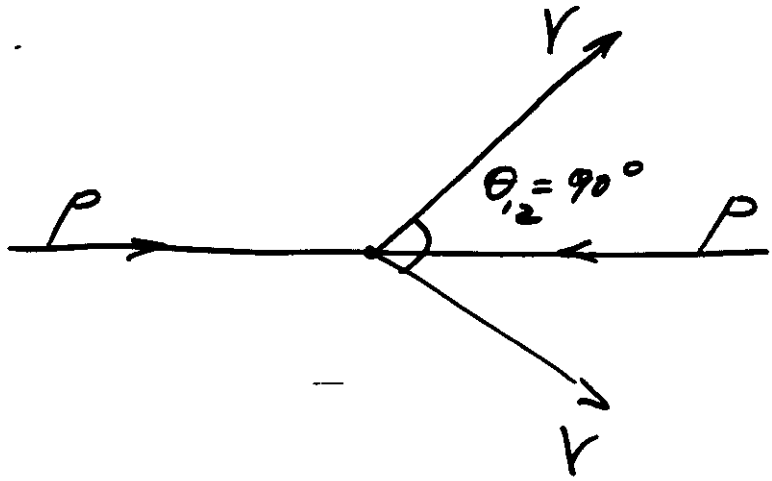

$$\delta m/m \sim \delta\theta_{12}$$

Example:

if $\delta\theta_1 = \delta\theta_2 = 10$ mrad $\Rightarrow$

$\delta m/m = \sqrt{2}\,\delta\theta_1 = 14$ mrad $= 1.4\%$

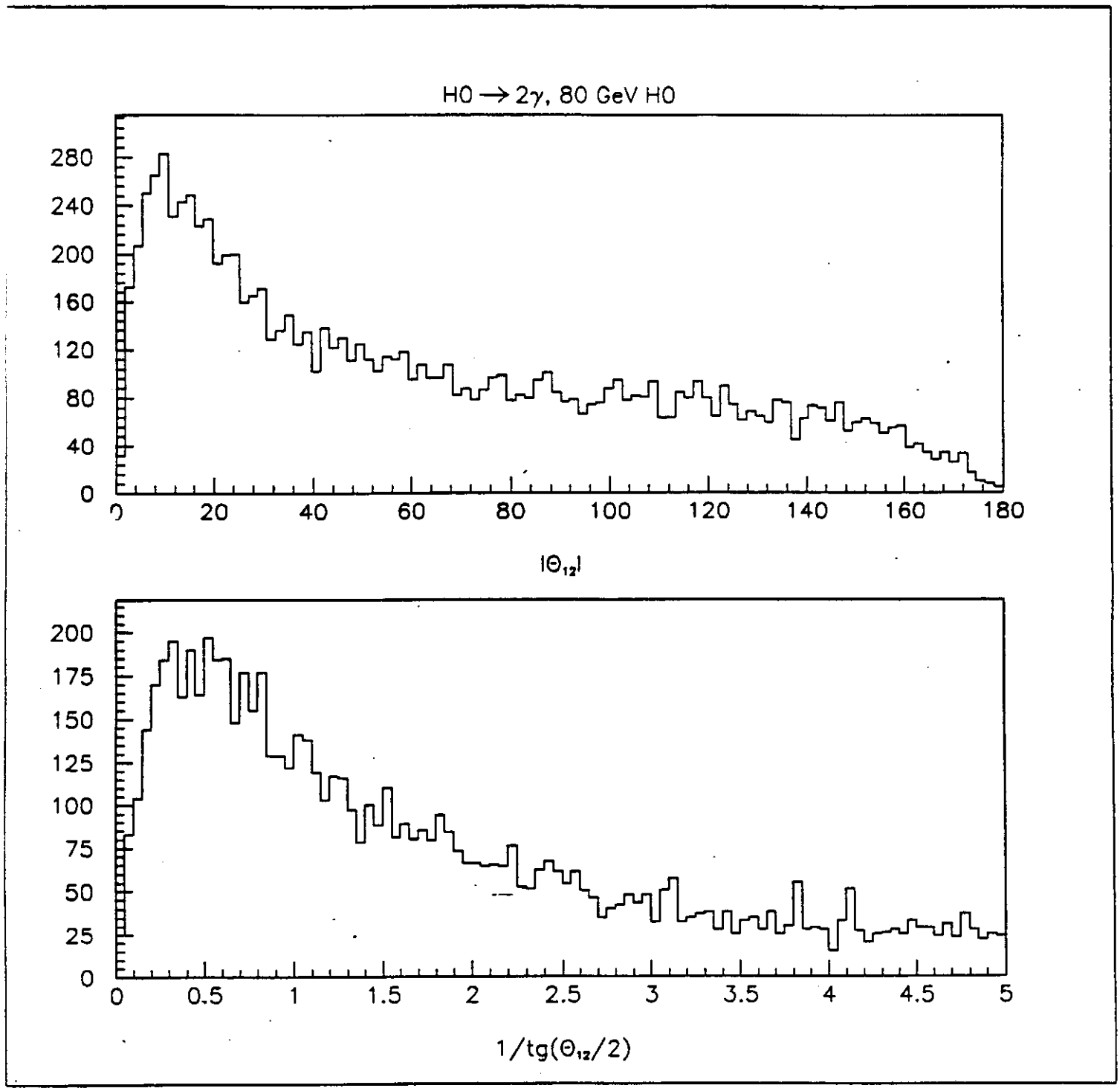
H0 → 2γ, 80 GeV H0
280
240
200
160
120
80
40
0
0
20
40
60
80
100
120
140
160
180
|Θ12|
200
175
150
125
100
75
50
25
0
0
0.5
1
1.5
2
2.5
3
3.5
4
4.5
5
1/tg(Θ12/2)

All events

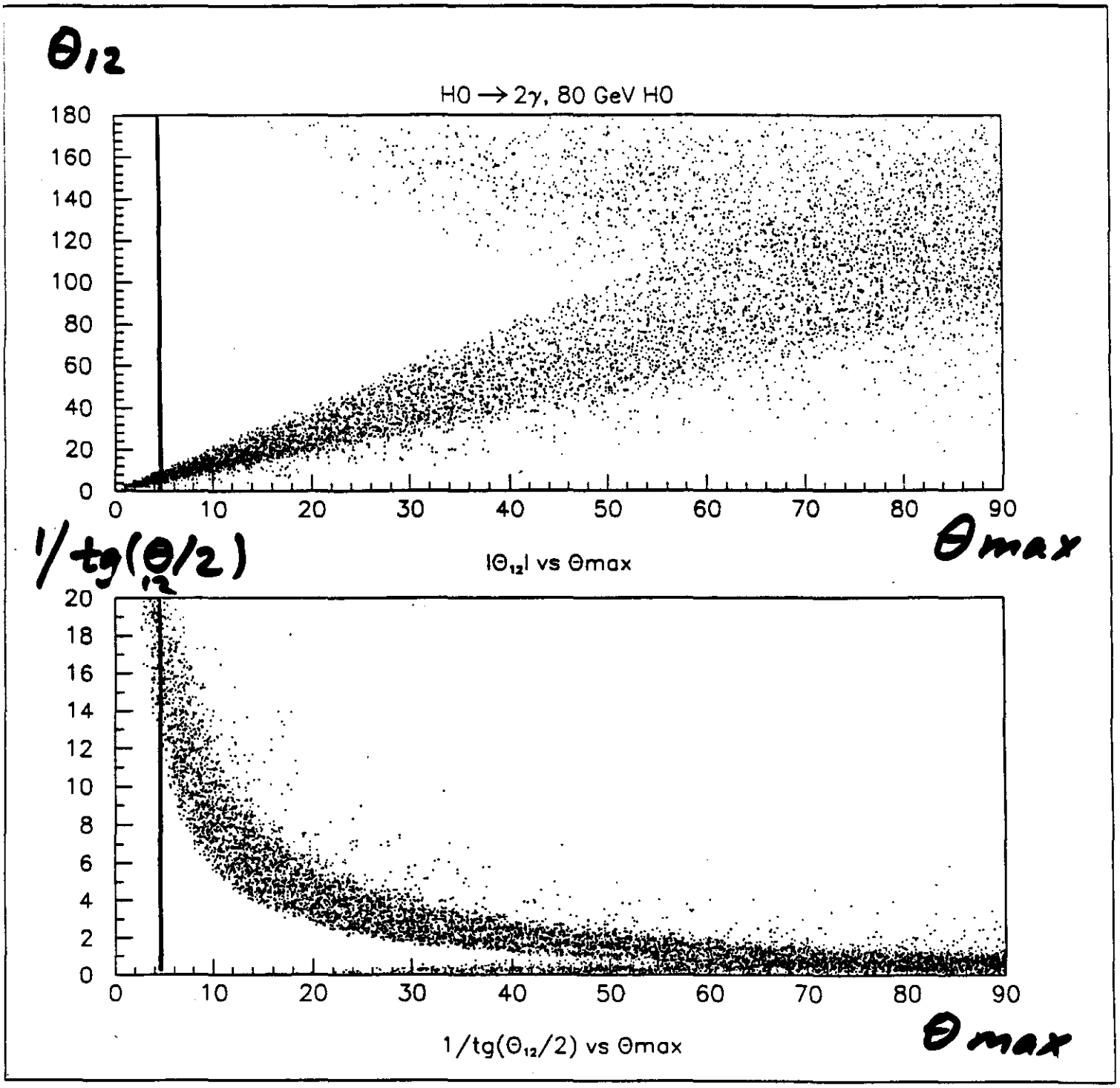
θ12
H0 → 2γ, 80 GeV H0
180
160
140
120
100
80
60
40
20
0
0
10
20
30
40
50
60
70
80
90
θmax
1/tg(θ12/2)
|Θ12| vs Θmax
20
18
16
14
12
10
8
6
4
2
0
0
10
20
30
40
50
60
70
80
90
θmax
1/tg(Θ12/2) vs Θmax

Barrel and Endcap Liquid Argon EM

- with Scintillating Tile Plug

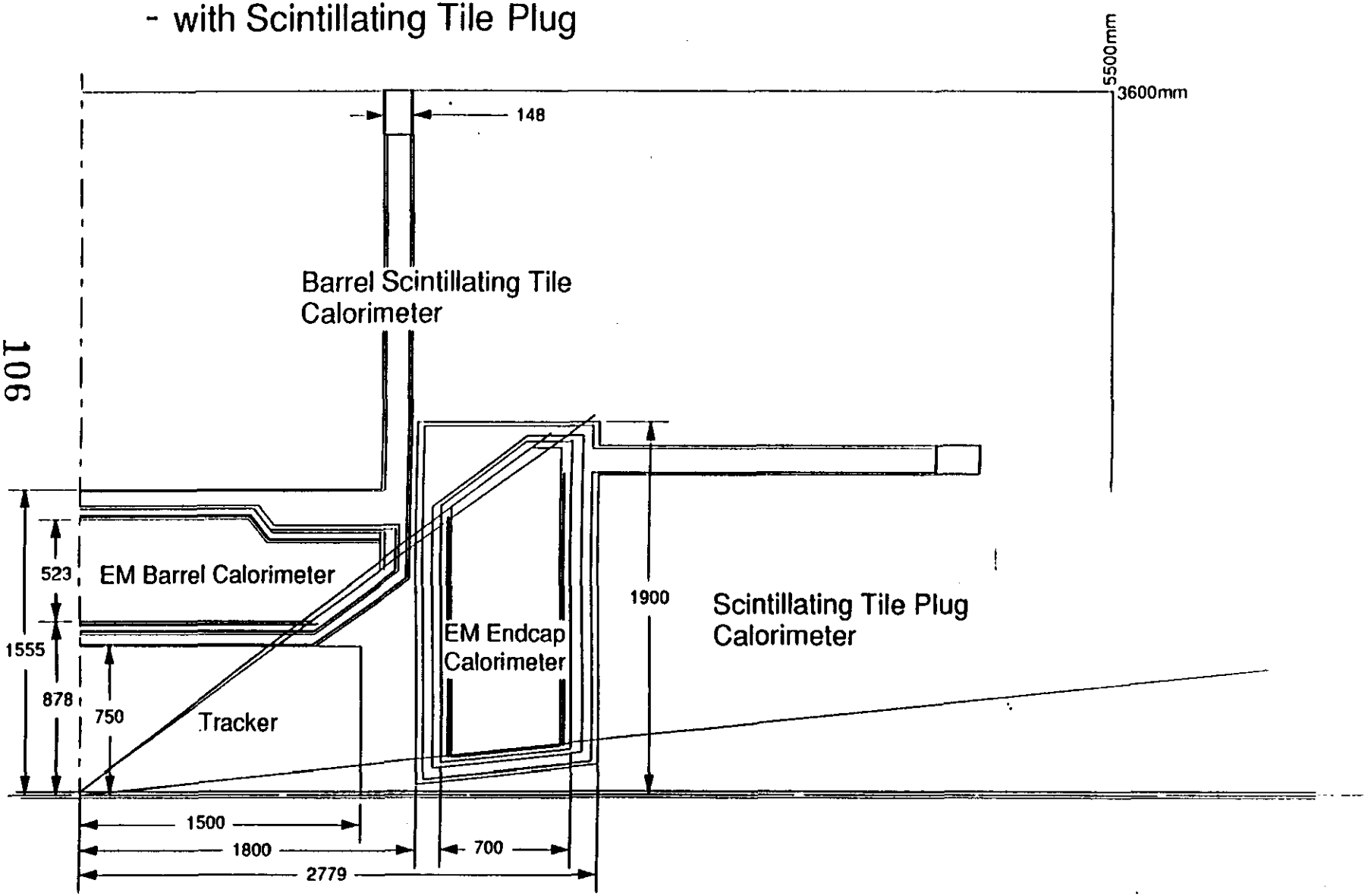

LLMasonn 5/12/92 EM Barrel and Endcap

Layout I

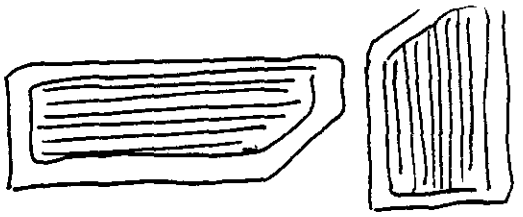

cryostat wall (+1.5 Δη) for 1950 mm option (z_{max})

Pb/LKr Barrel Accordion, comparison of GEANT simulations

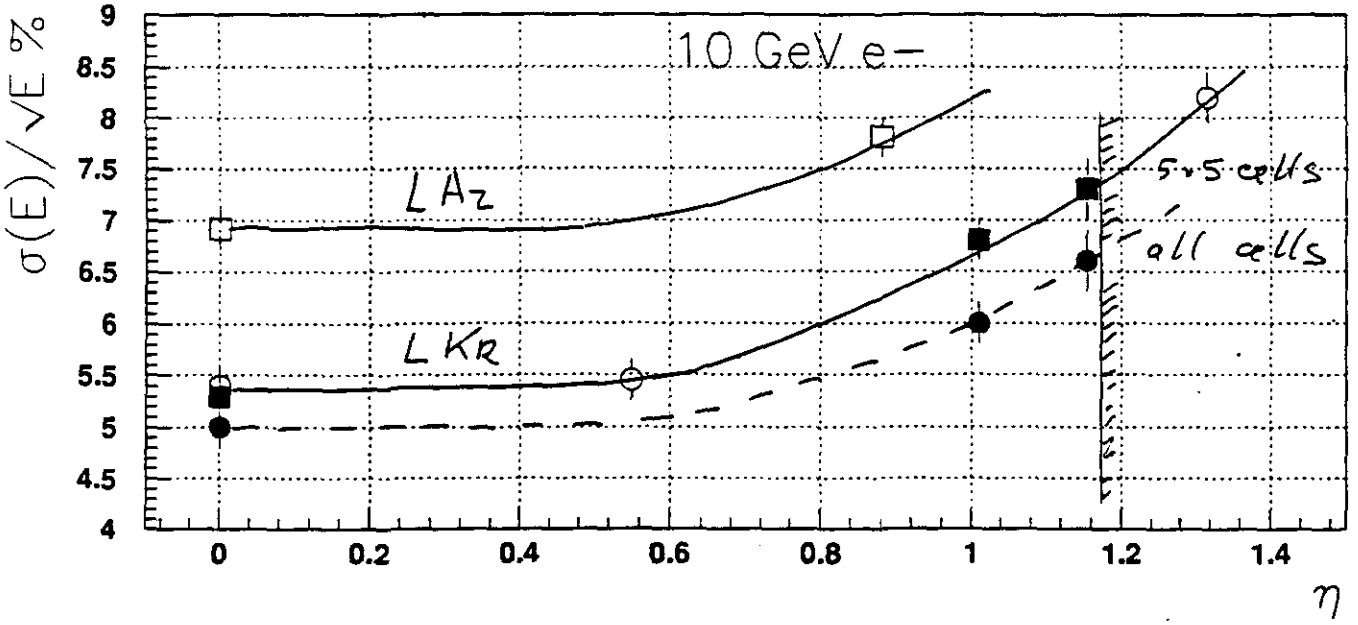

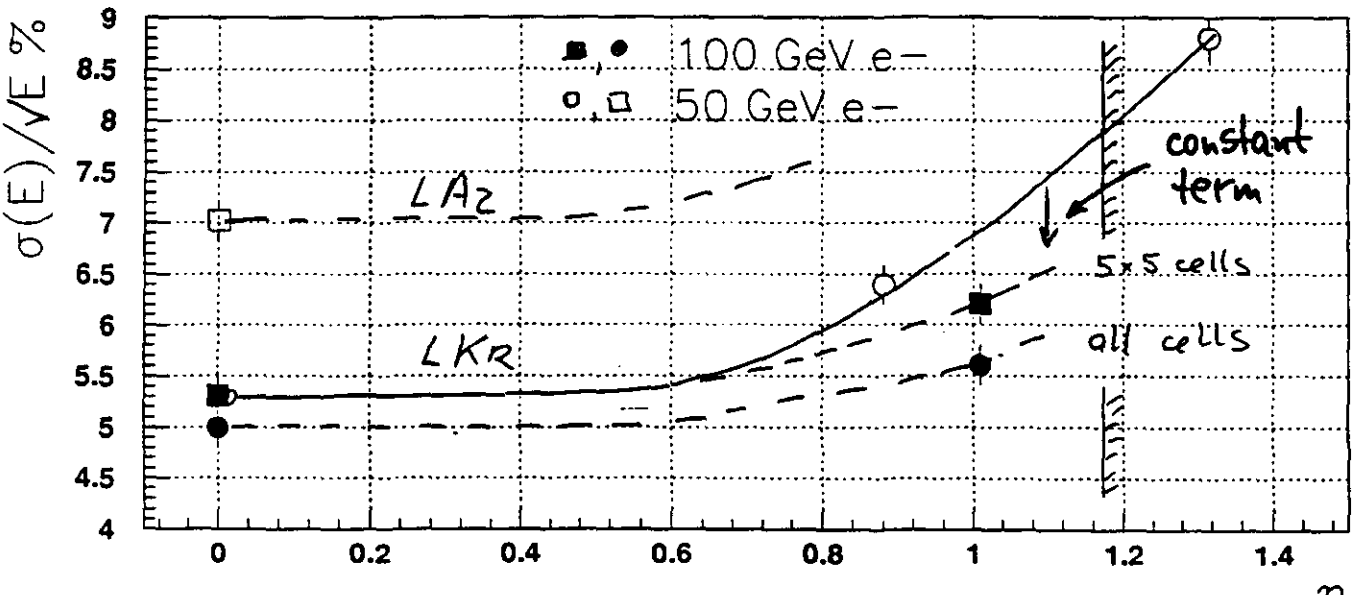

□, ○ – Projective accordion simulations by Michael Seman (report at SSCL June 92)

■, ● – Plate analog of Accordion simulations (×√2) by Konstantin Shmakov

Cryostat walls, B = 8 KG.

Angular Resolution and Vertex Identification

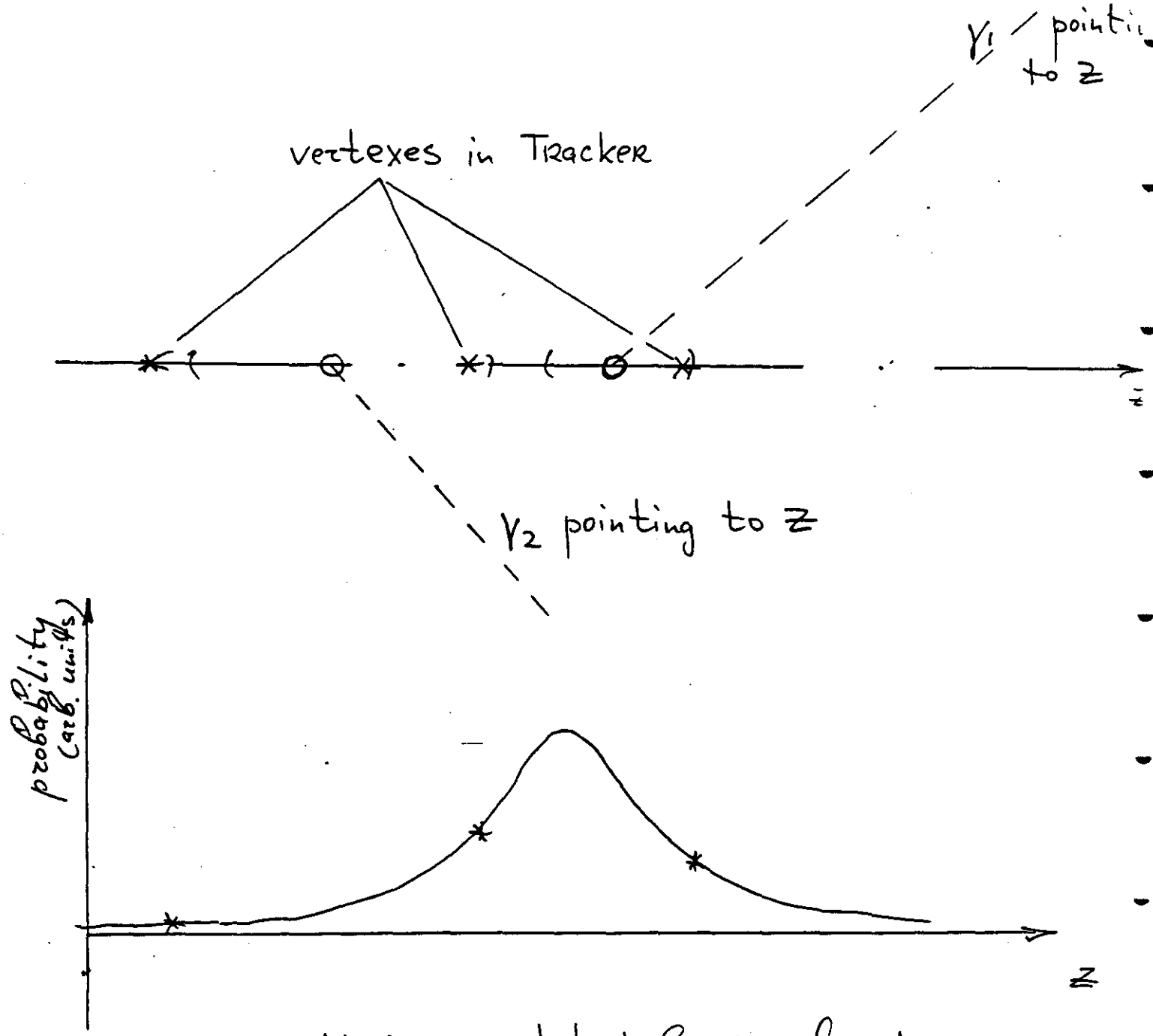

Maximum likelehood function

LKr (barrel) / LAr (endcap)

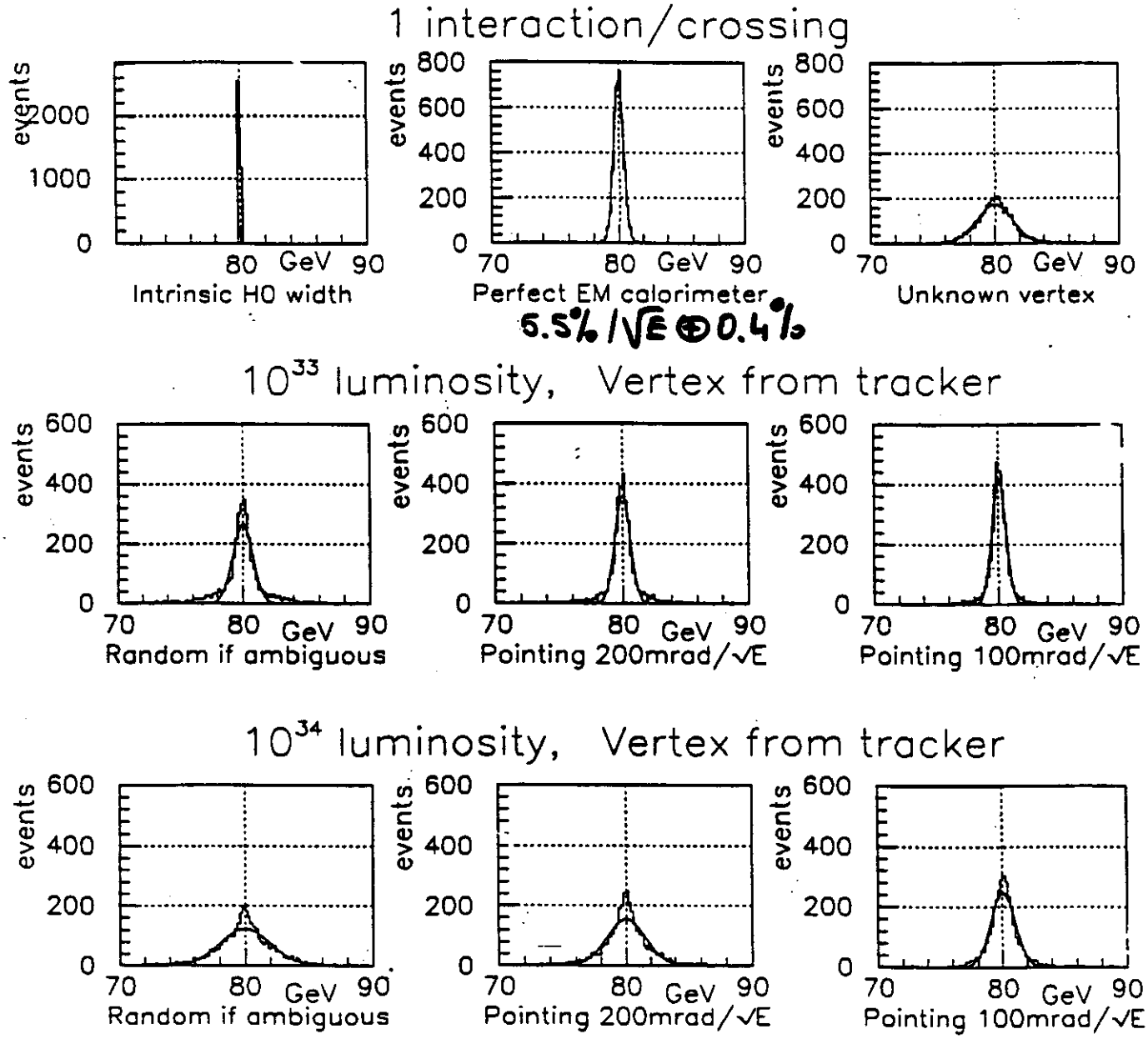

PYTHIA v.5.6 10^4 H0 $\rightarrow 2\gamma$

Energy resolution: LKr $5\%/\sqrt{E} \oplus 0.4\%$

LAr $7.5\%/\sqrt{E} \oplus 0.4\%$

slight angular dependence of resolution and barrel–endcap crack are included

2γ Invariant Mass

LKr (Barrel)/LAr (Endcap), 1 event/Crossing

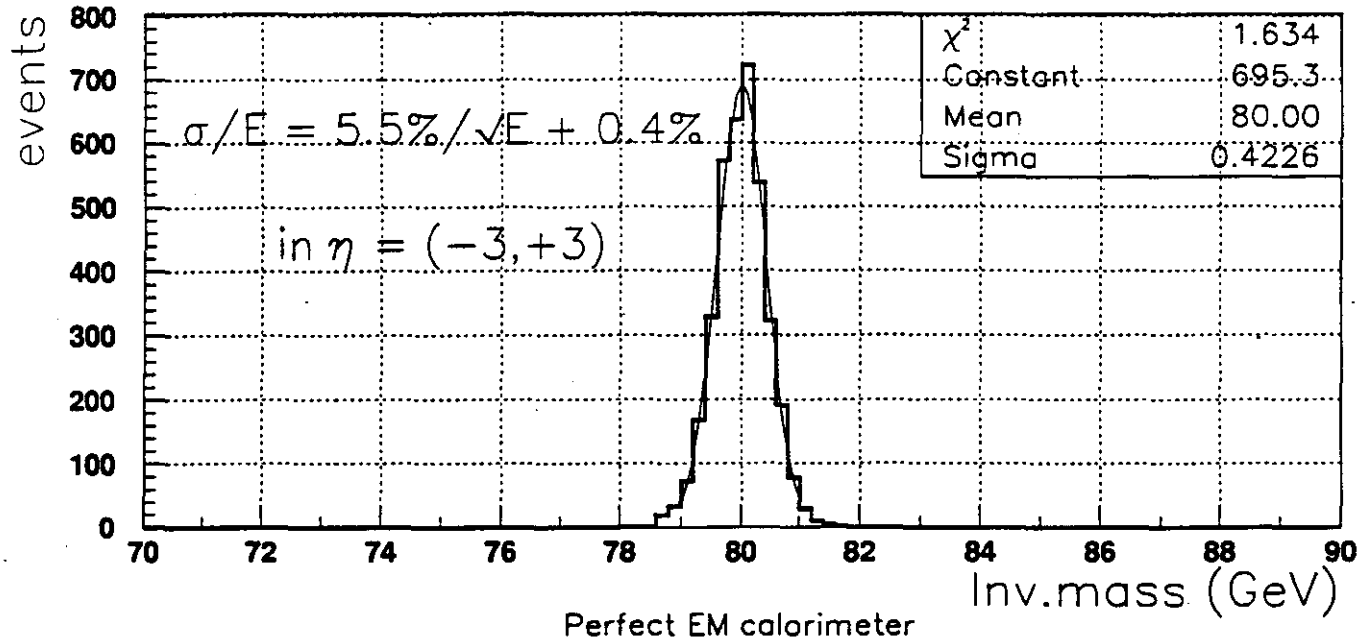

Perfect EM calorimeter

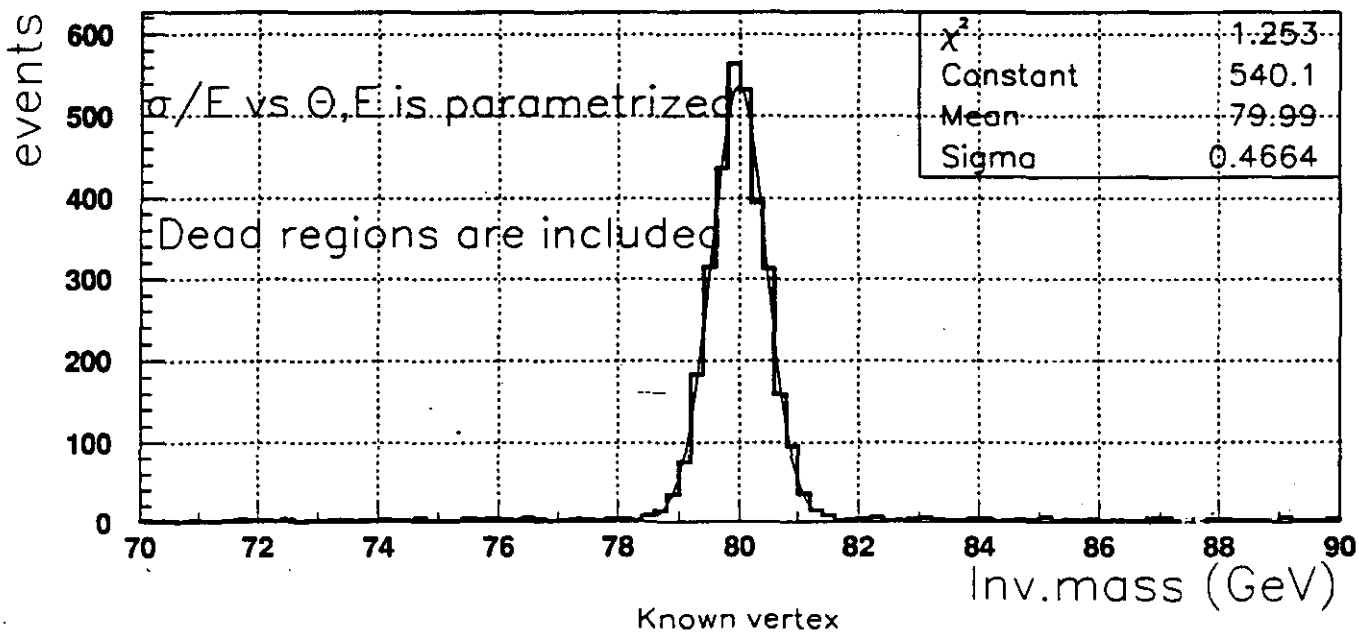

Known vertex

$M_H = 80$ GeV

RD3 SETUP (NIM A309 (1991))

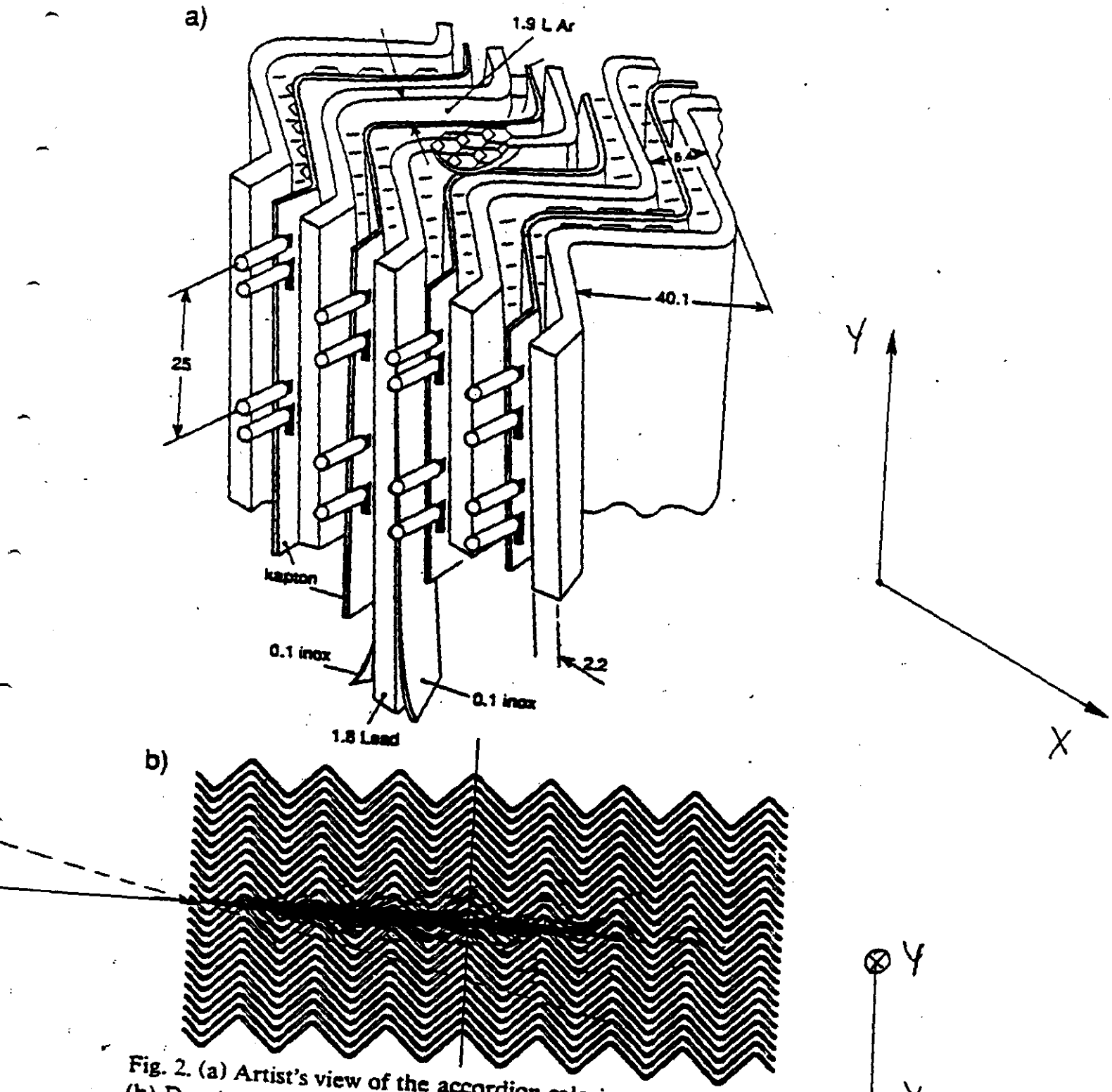

Fig. 2. (a) Artist's view of the accordion calorimeter geometry. (b) Development of a 40 GeV electron shower (Monte Carlo simulation). Only charged tracks above 10 MeV are shown.

From Liquid Argon R & D
RD3 coll. 10-12-91

RD3 - 10 OCT 91

Angular Resolution Studies

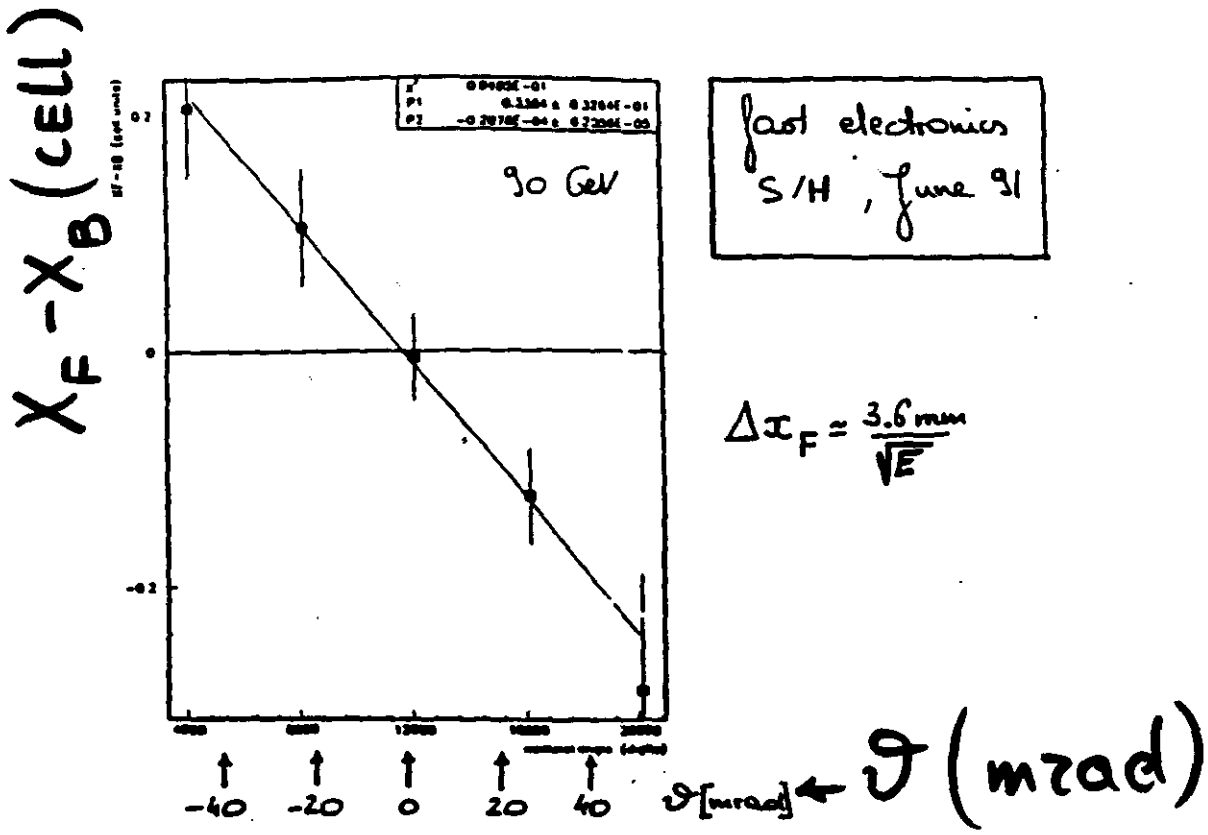

fast electronics
S/H, June 91

$\Delta x_F \simeq \frac{3.6\,mm}{\sqrt{E}}$

fit: $X_F - X_B = R \times \vartheta \Rightarrow R = 125 \pm 8$ mm

Angular resolution:
at $\vartheta = 0°$, $\Delta(X_F - X_B) = 1.00$ mm

$\Rightarrow \boxed{\Delta\vartheta = 8.0 \pm 0.5 \text{ mrad}}$
at 90 GeV, $\vartheta = 0°$

$\sim$ scales as $1/\sqrt{E}$

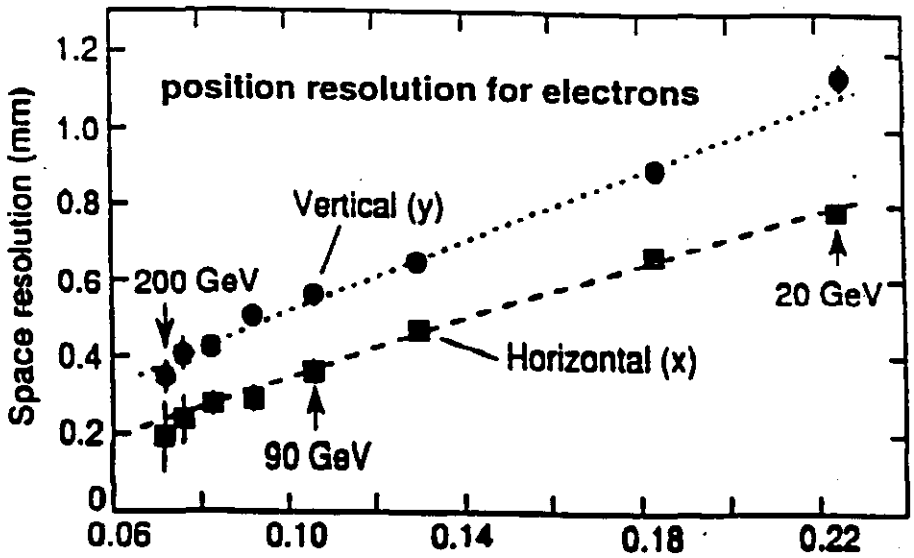

$\frac{4.4\ \text{mm}}{\sqrt{E}}$

$\frac{3.5\ \text{mm}}{\sqrt{E}}$

$1/\sqrt{E}$

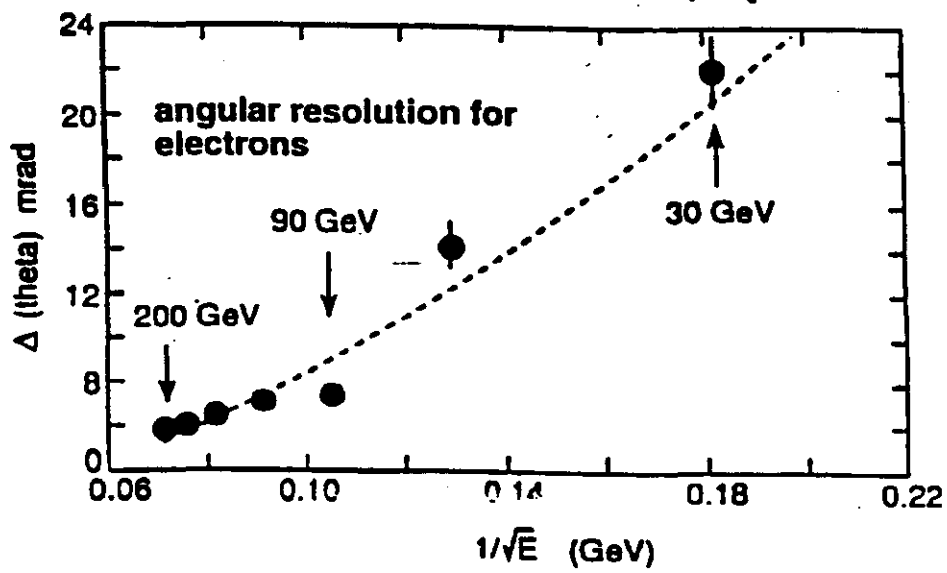

$\frac{80\ \text{mrad}}{\sqrt{E}}$

EAGLE presentation Evian 6/3/1992

Angular Resolution Study, 90 GeV electrons

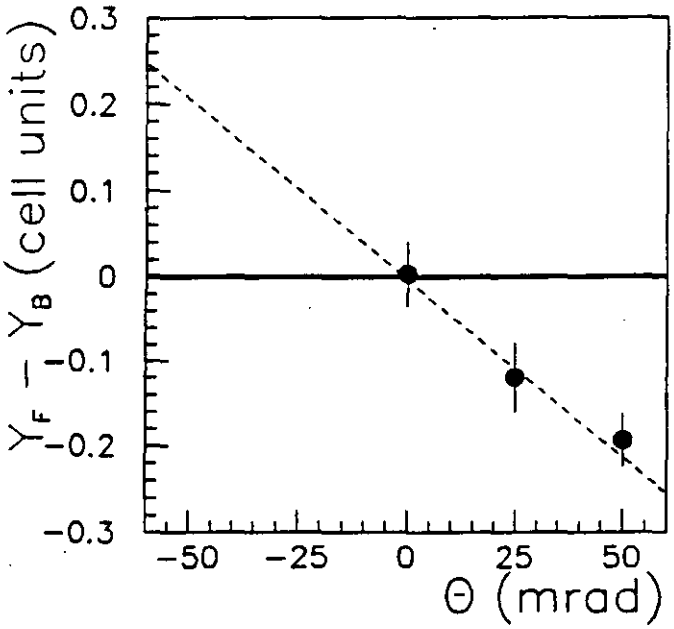

at $\Theta = 0°$, $\Delta(Y_F - Y_B) = 1.002$ mm

$$\Rightarrow \boxed{\Delta\Theta = \frac{1.002\,\text{mm}}{117\,\text{mm}} = 8.6\,\text{mrad}}$$

(RD3 : $\Delta\Theta = 8.0 \pm 0.5$)

$$Y_F - Y_B = R \times \Theta \Rightarrow R = 117 \pm 2\ \text{mm}$$

(RD3 : $R = 125 \pm 8$ mm)

Monte Carlo Simulation for RD3

Segmentation 2.7cm (Y) x 2.5cm (X)

Nonprojective plate calorimeter

Position resolution an Pointing for RD3 prototipe

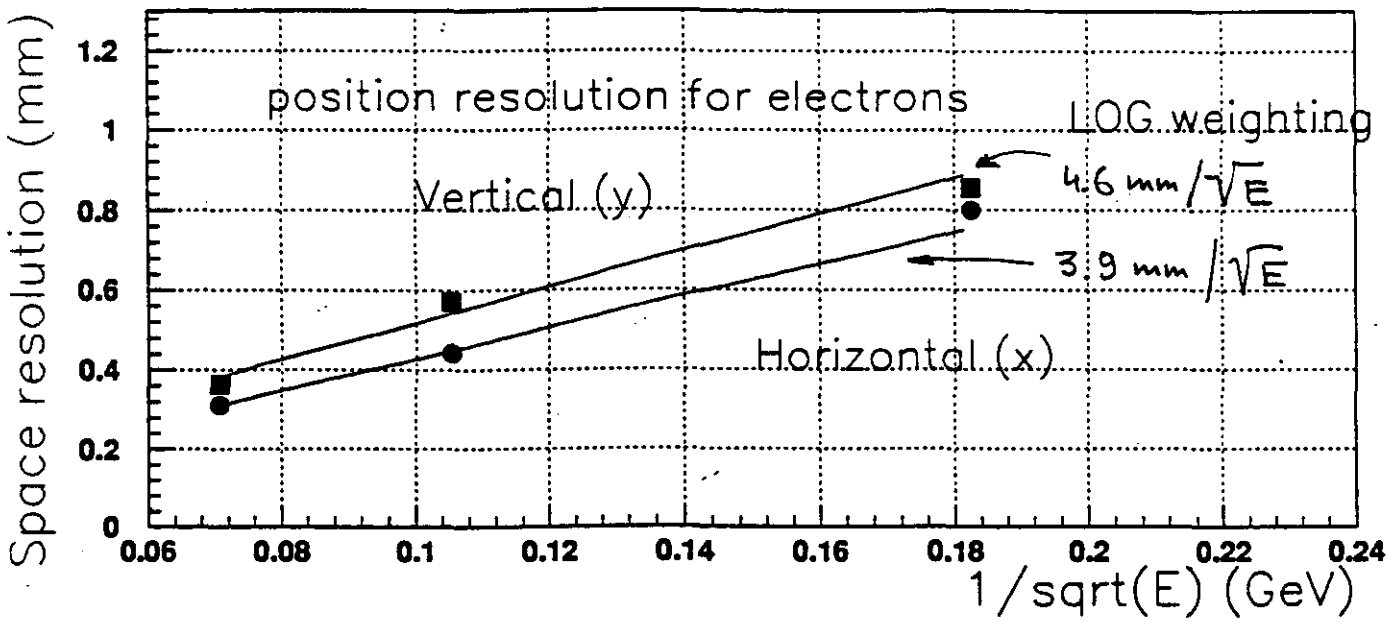

RD3:
$\frac{4.4\ mm}{\sqrt{E}}$
$\frac{3.5\ mm}{\sqrt{E}}$

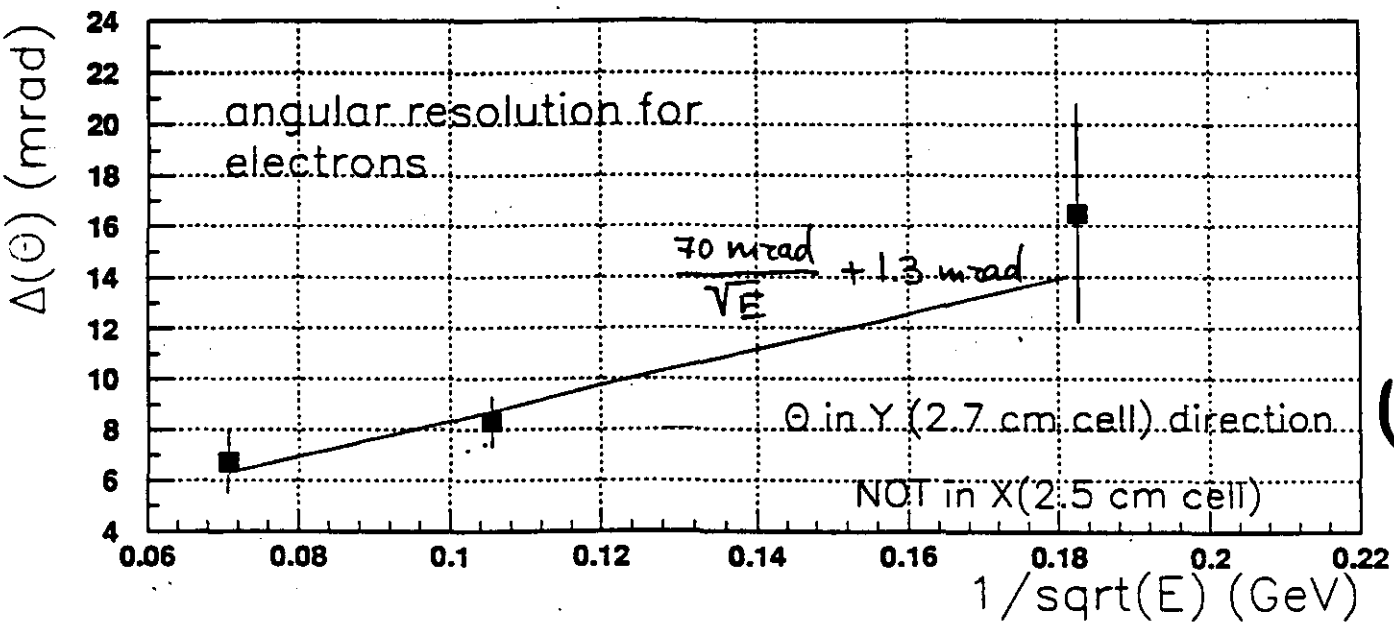

$\frac{80\ mrad}{\sqrt{E}}$
(φ dir)

Monte Carlo simulation of RD3 prototype.

RD3

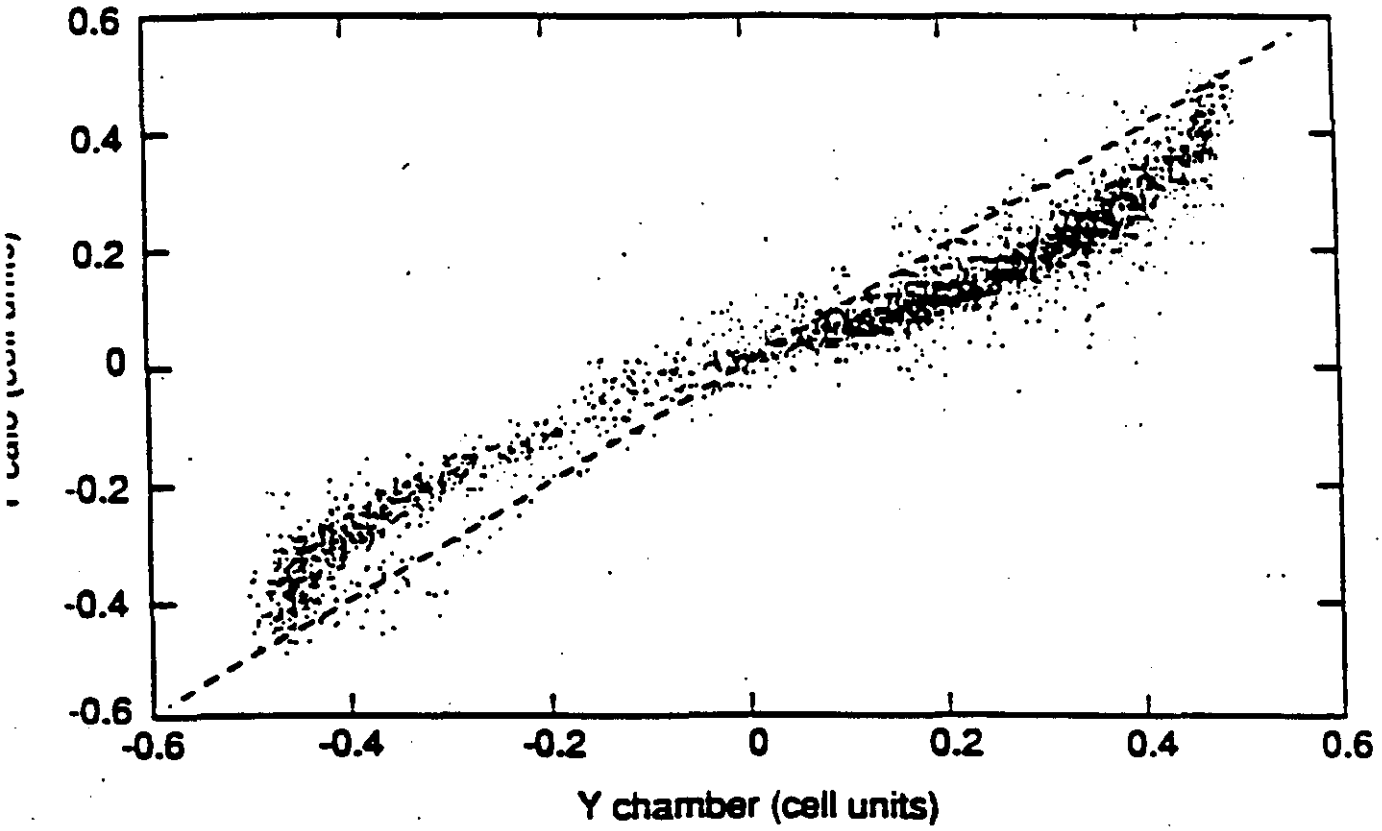

122 GeV/c electron impact point as reconstructed by he calorimeter vs the position determined by the beam chamber system in the x (a) and y (b) view.

EM-shower Position Reconstruction in 2 long. Sections (stable method for Angular measurements)

$$X_{calc} = SUM(W_i \times X_i)/SUM(W_i)$$

$$W_i = E_i$$

$$W_i = \max\{0, W_0 + \ln(E_i/E_{tot})\}$$

(T.C.Awes et al, NIM A311(1992))

S curve:

Corrections depends on energy and long. segmentation

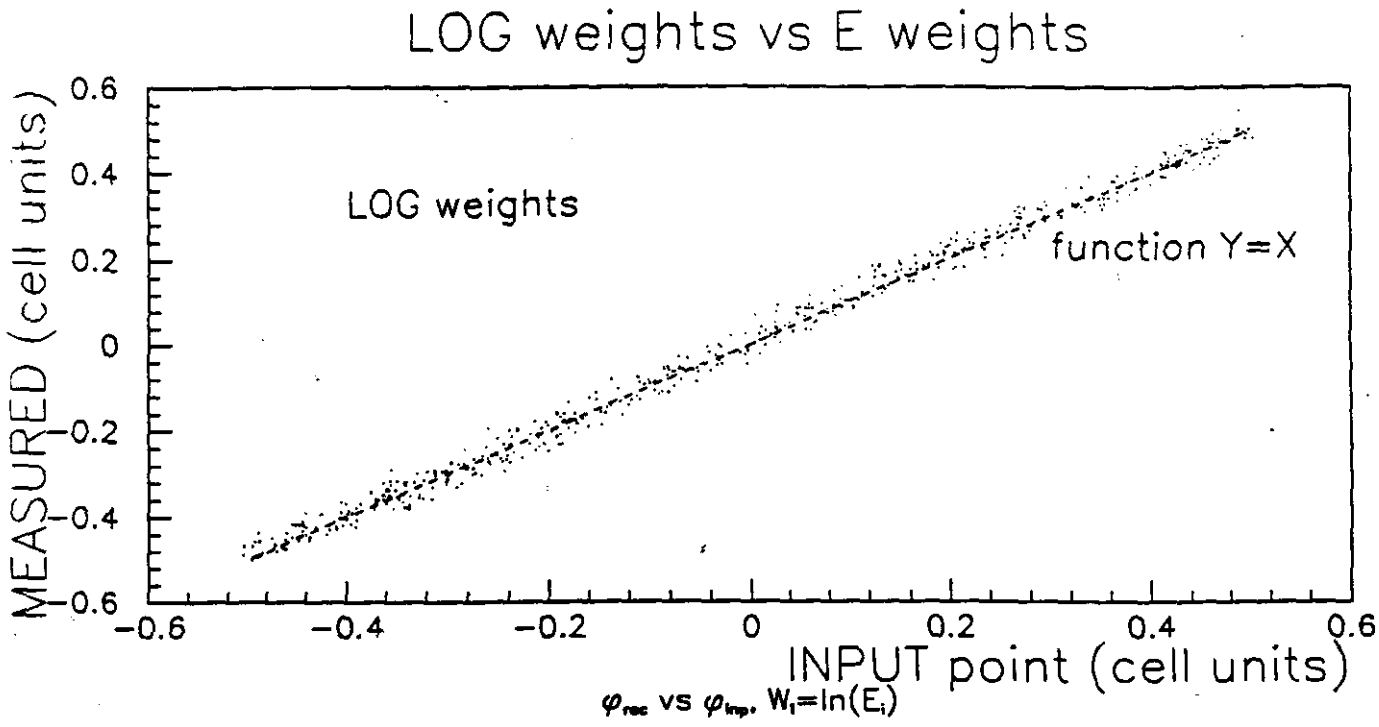

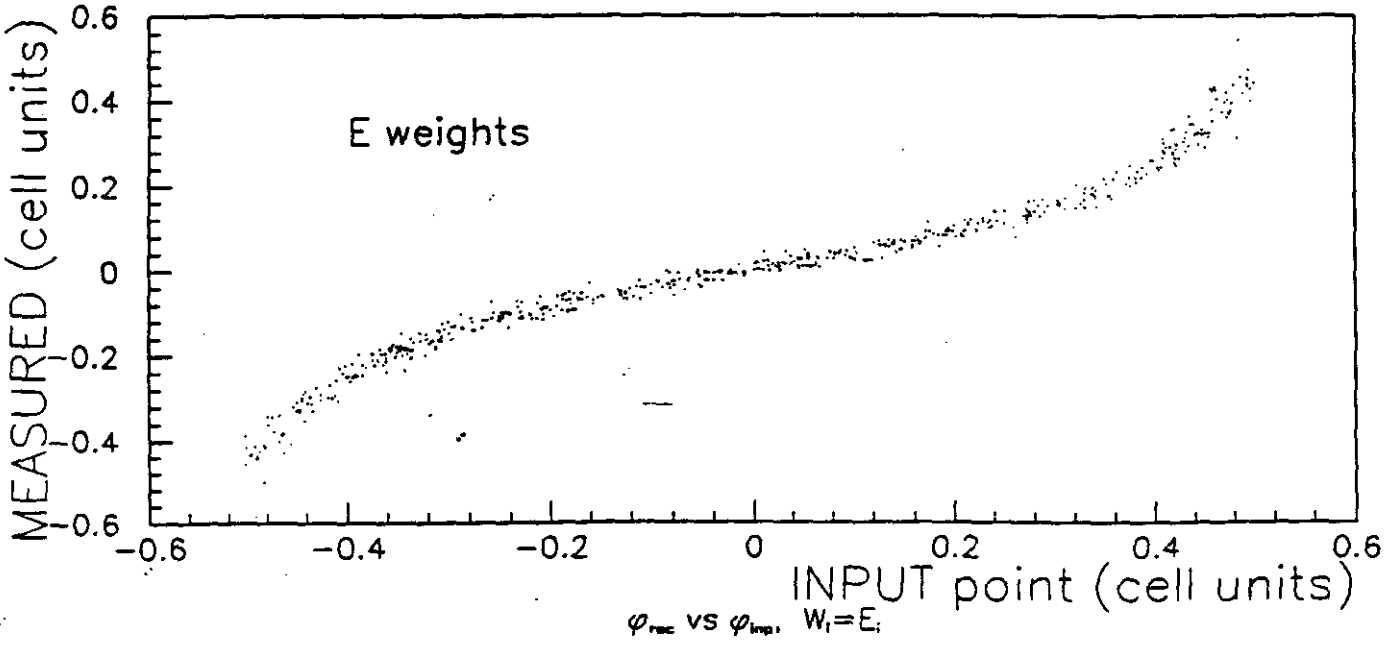

100 GeV γ,
Pb/LKr EM calorimeter with 0.032 × 0.032 segmentation

Position resolution of the test module (RD3 prototype)

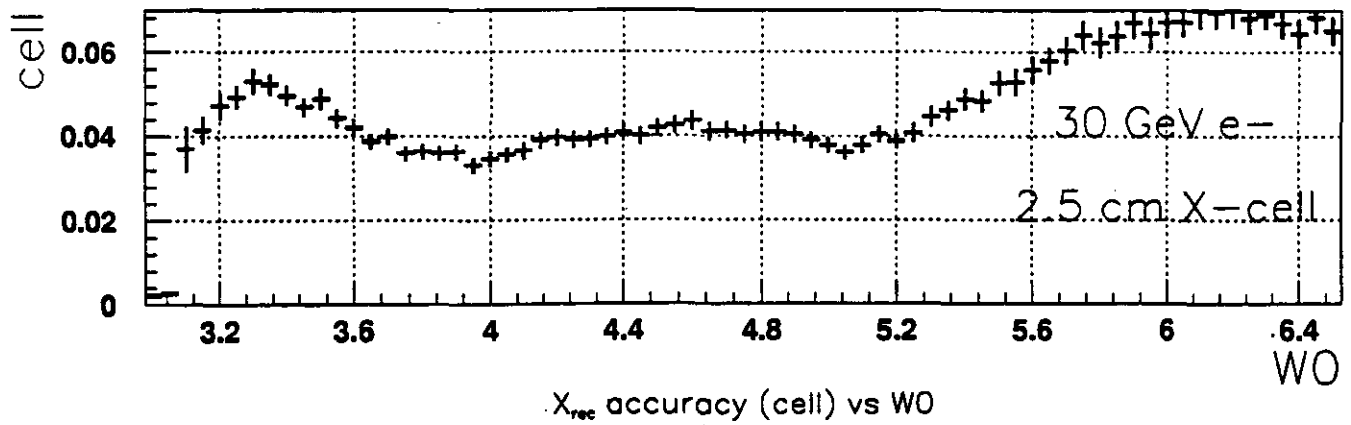

X_{rec} accuracy (cell) vs WO

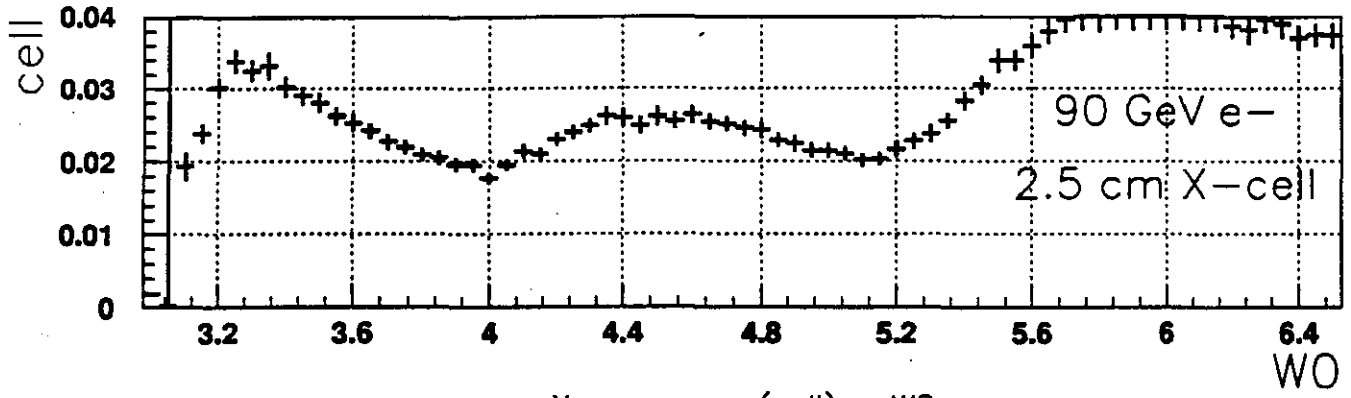

X_{rec} accuracy (cell) vs WO

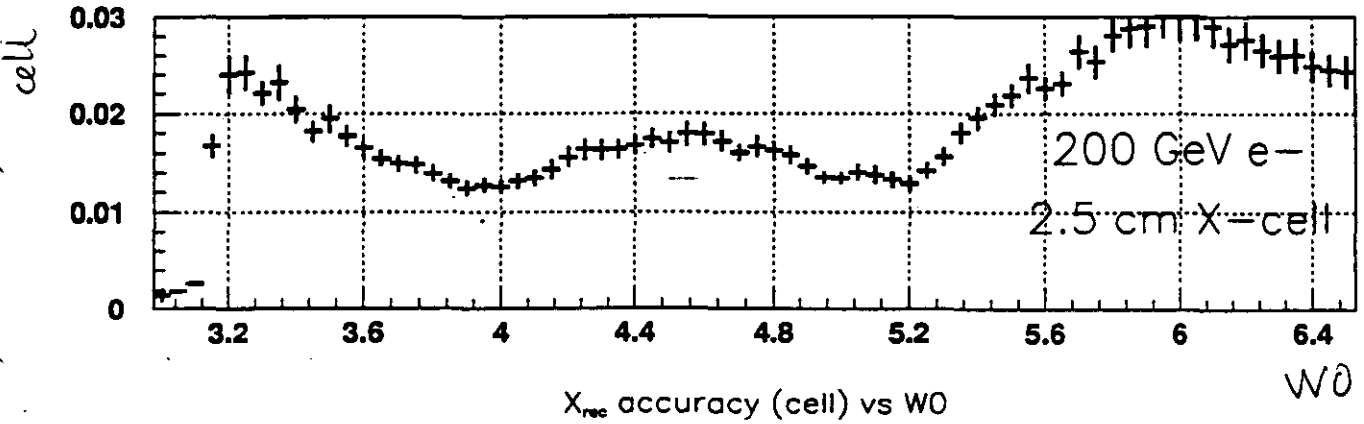

X_{rec} accuracy (cell) vs WO

Position Angular resolution at 90 deg., LKr EM calorimeter

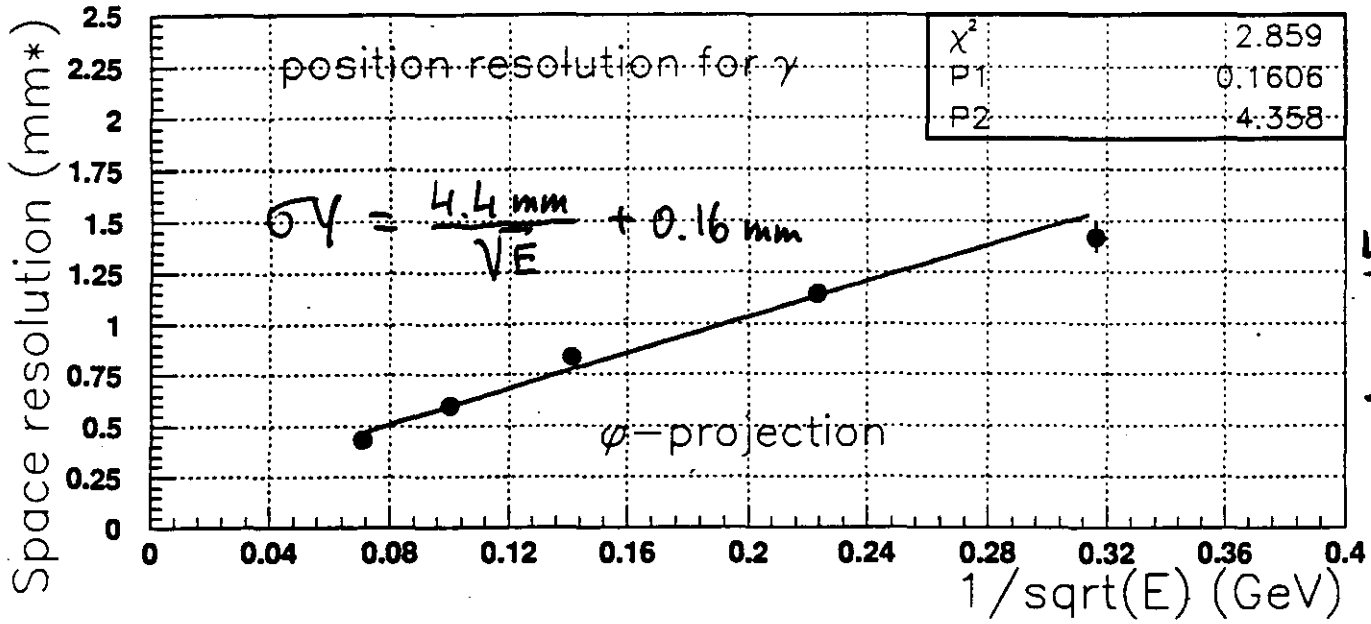

RD3: $\frac{4.38 \pm 0.06}{\sqrt{E}} + 0.07 \pm 0.$

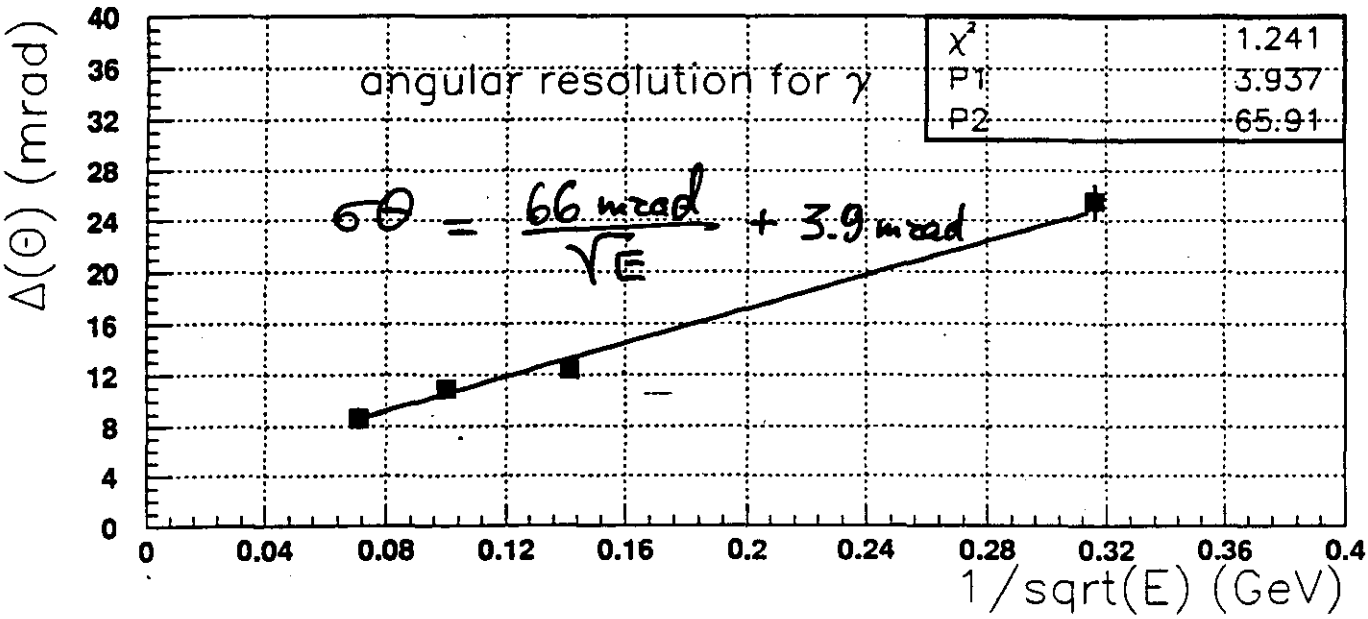

RD3: $\frac{80\,mrad}{\sqrt{E}}$

(φ dir) ↓ +30% θ dir

90 GeV : ~ 7 mrad RD3

~ 10.9 mrad present study

Longitudinal shower position in 2 long sections

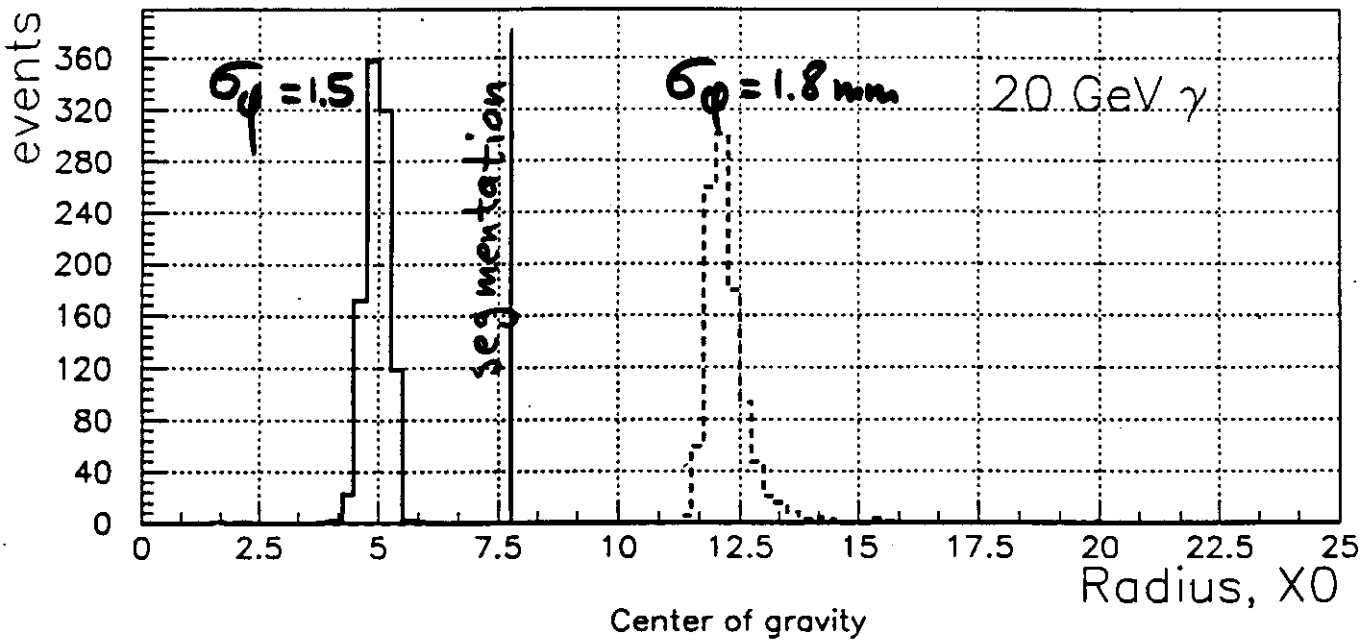

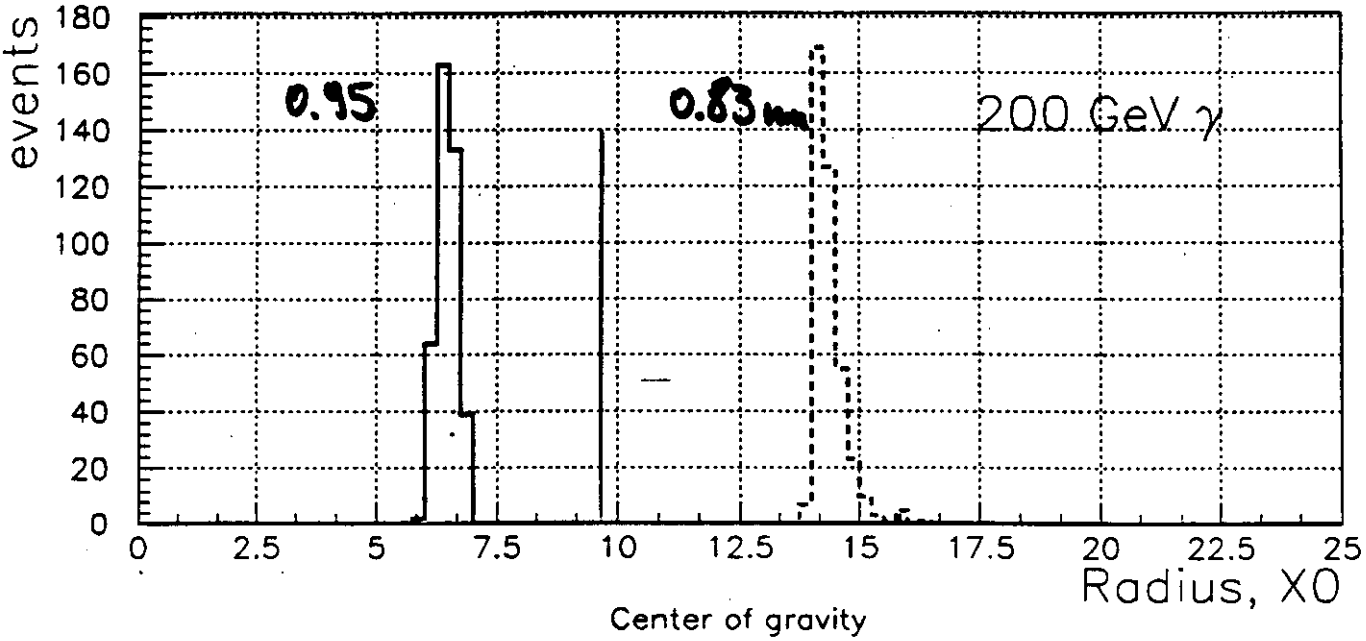

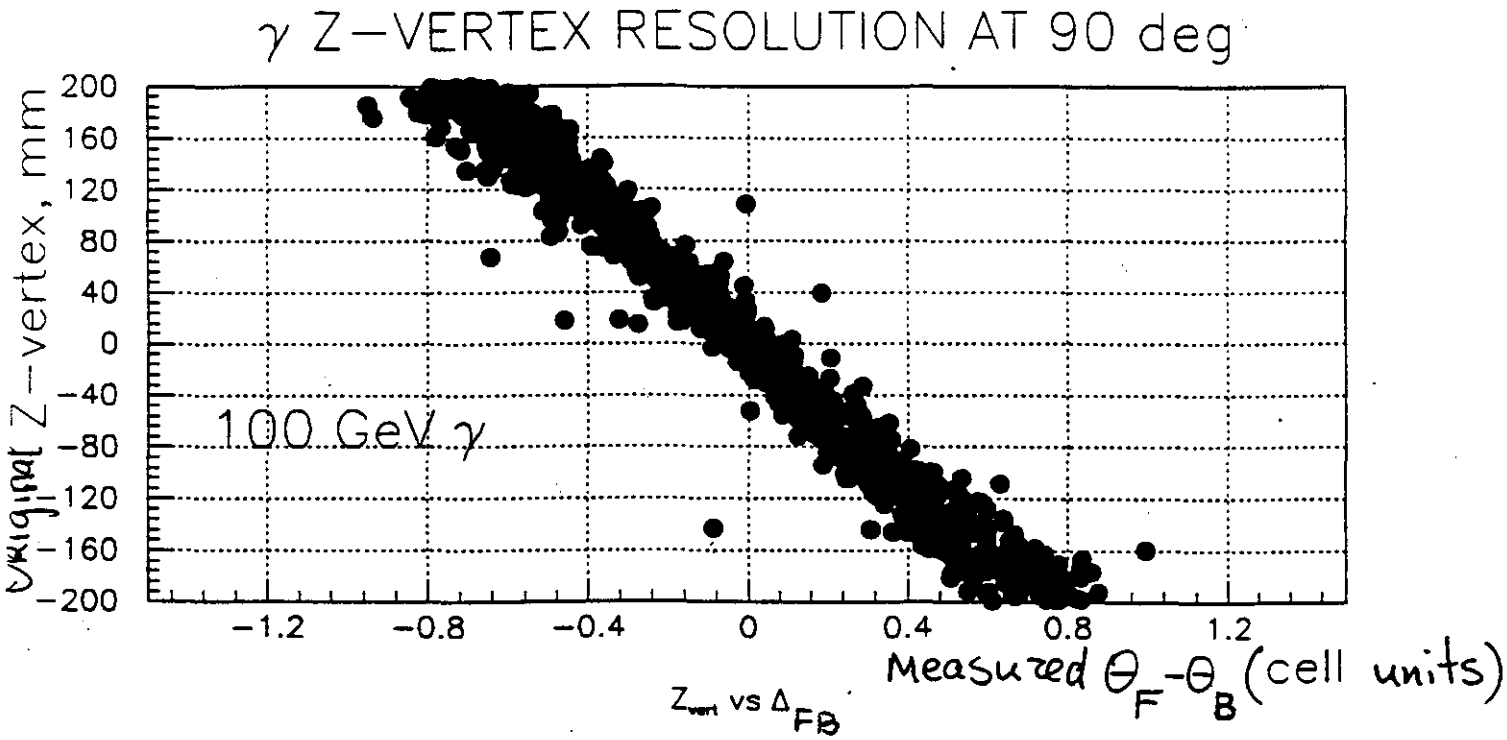

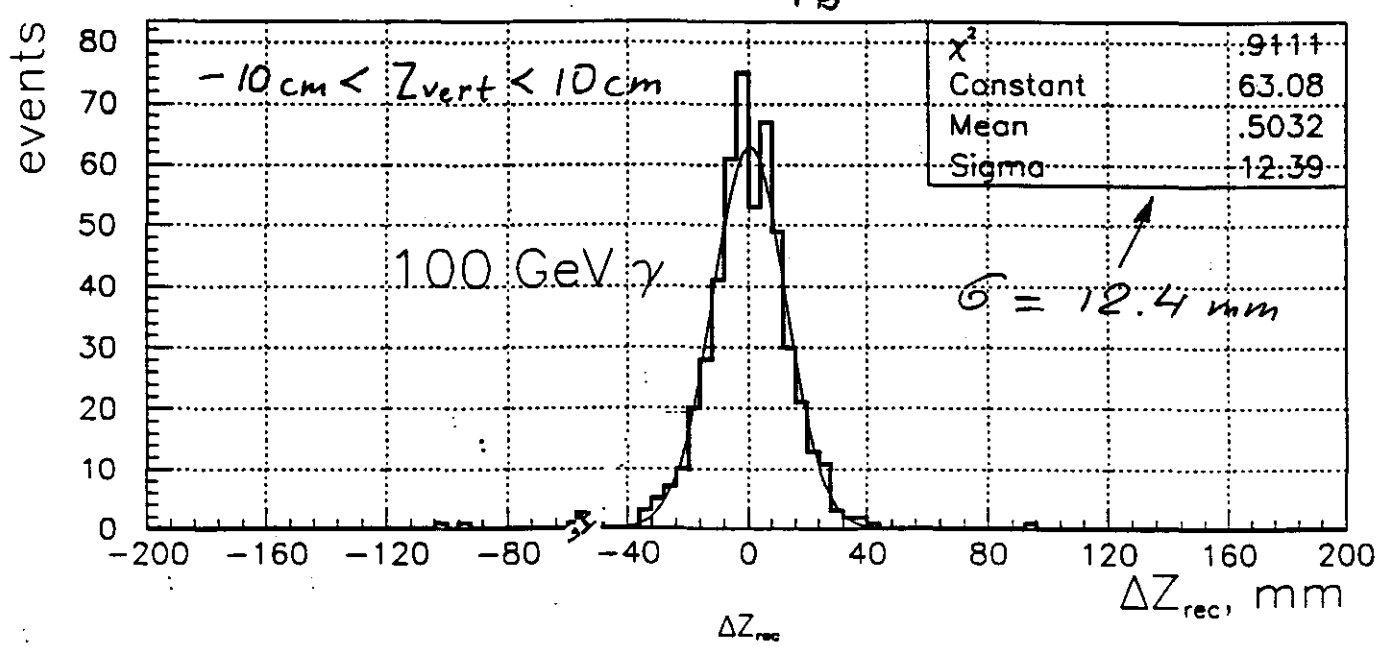

Z - Reconstructed error

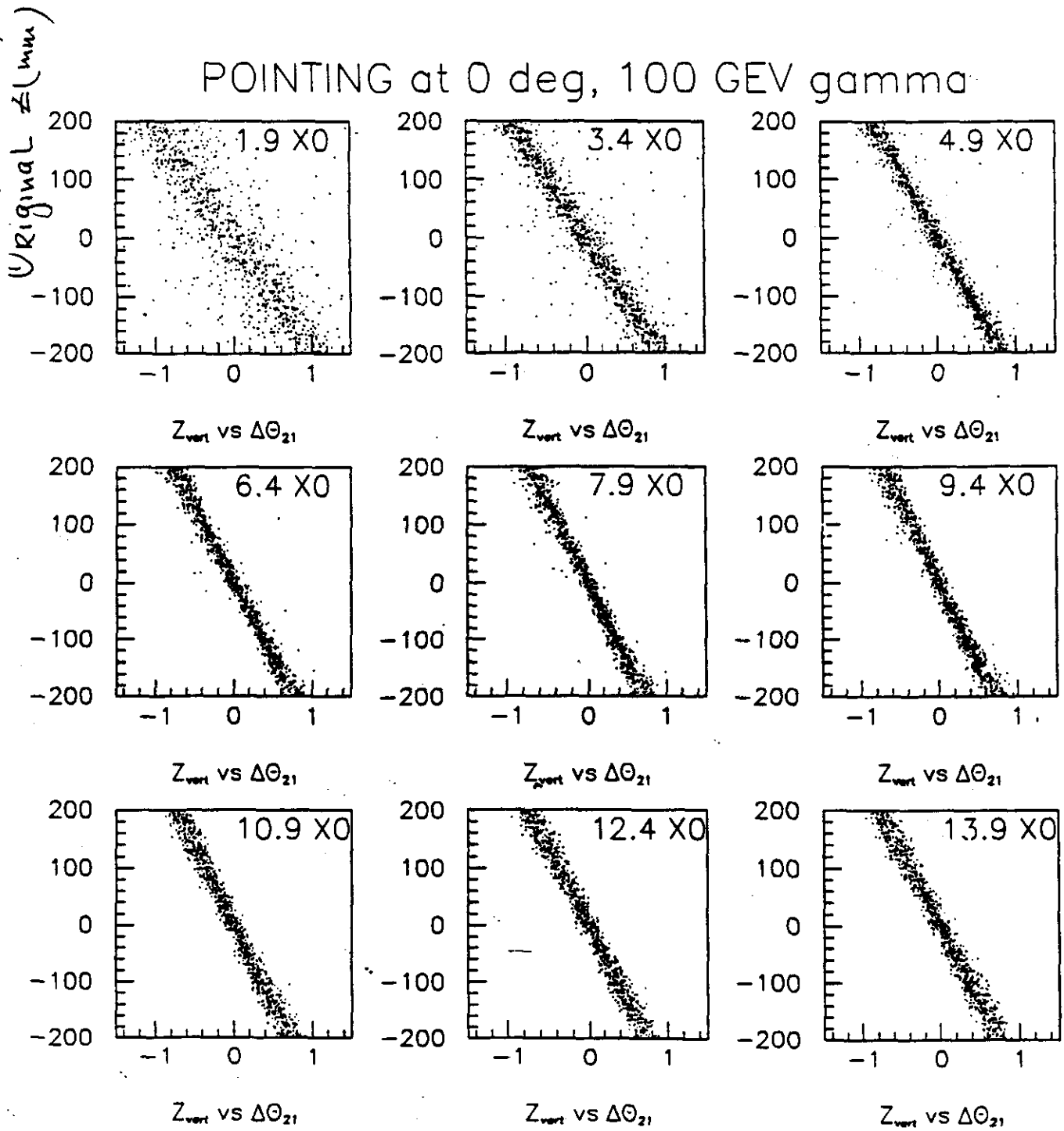

LK_2 EM – 0.032 × 0.032 segmentation

$\Delta\Theta_{21} \equiv \Theta_2(\text{cell}) - \Theta_1(\text{cell})$ [back.-forw. position]

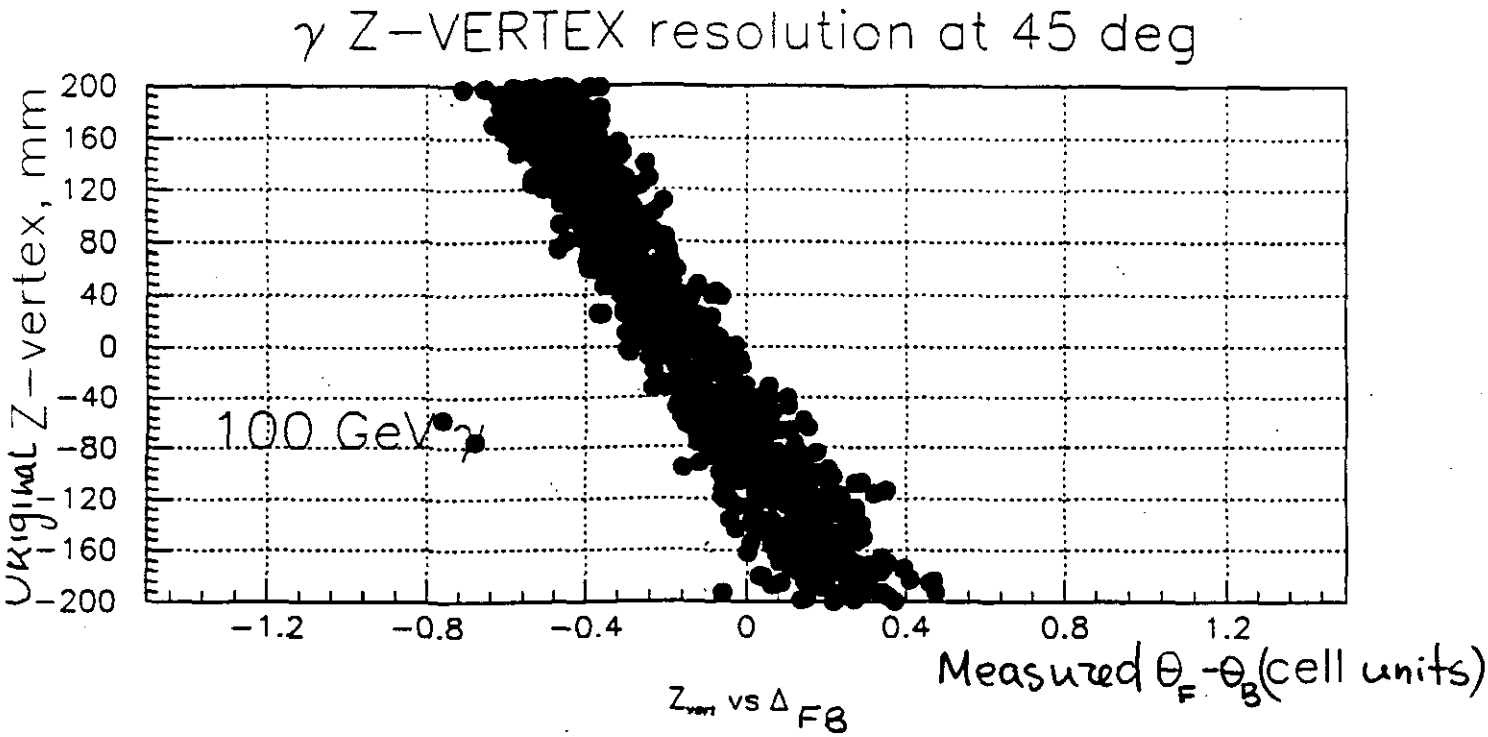

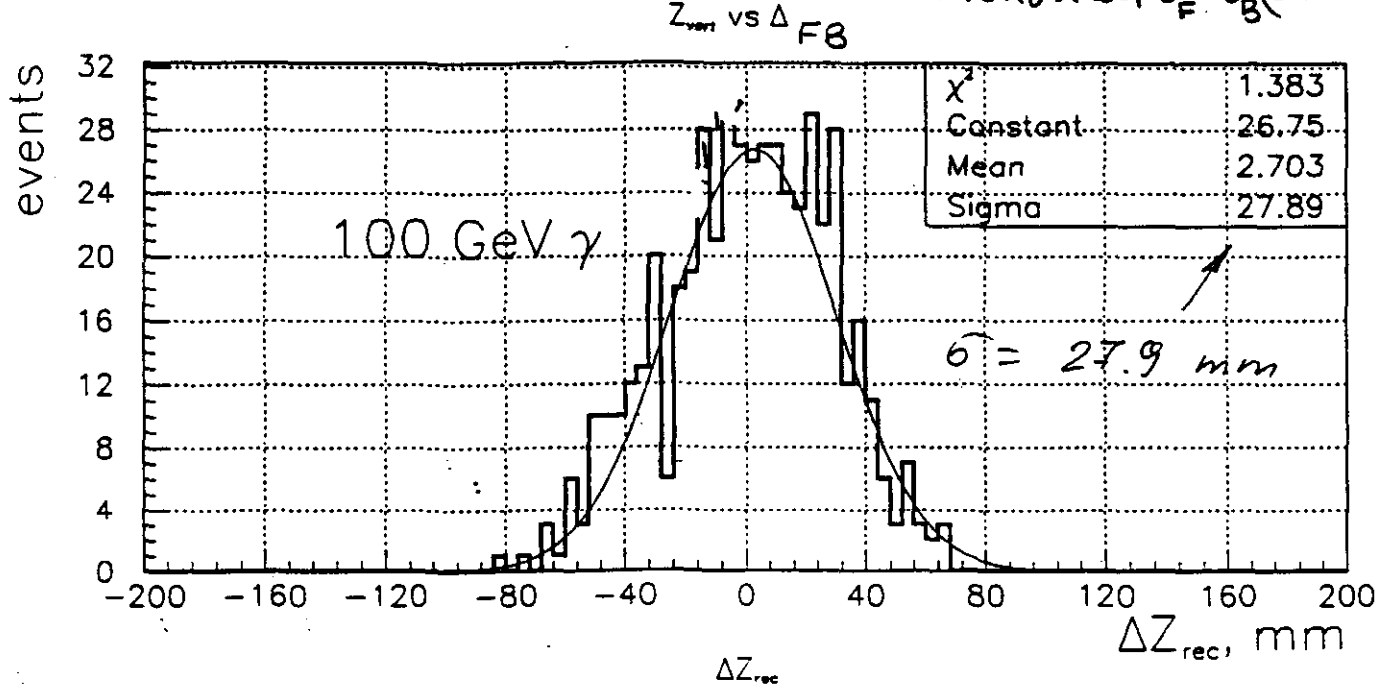

Z - reconstructed error

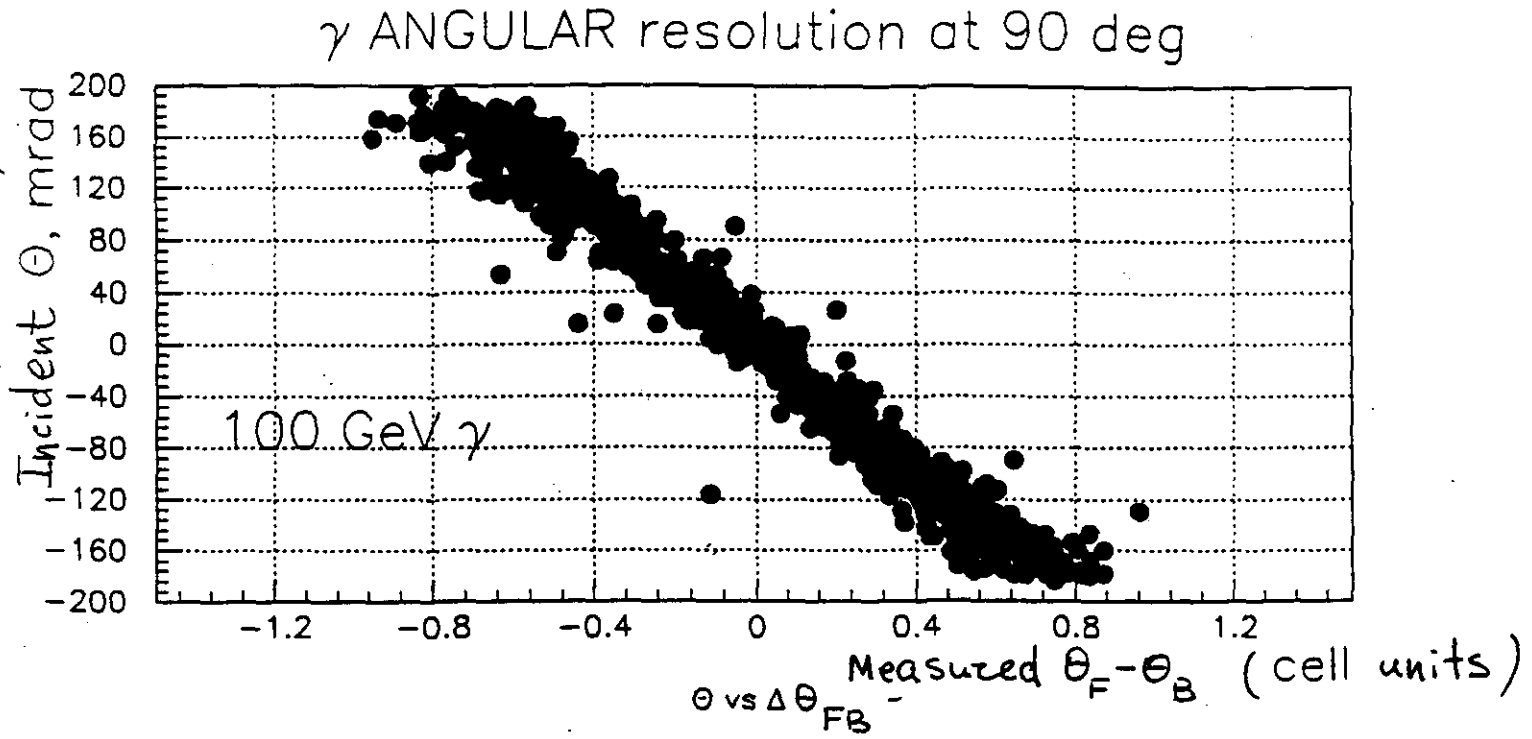

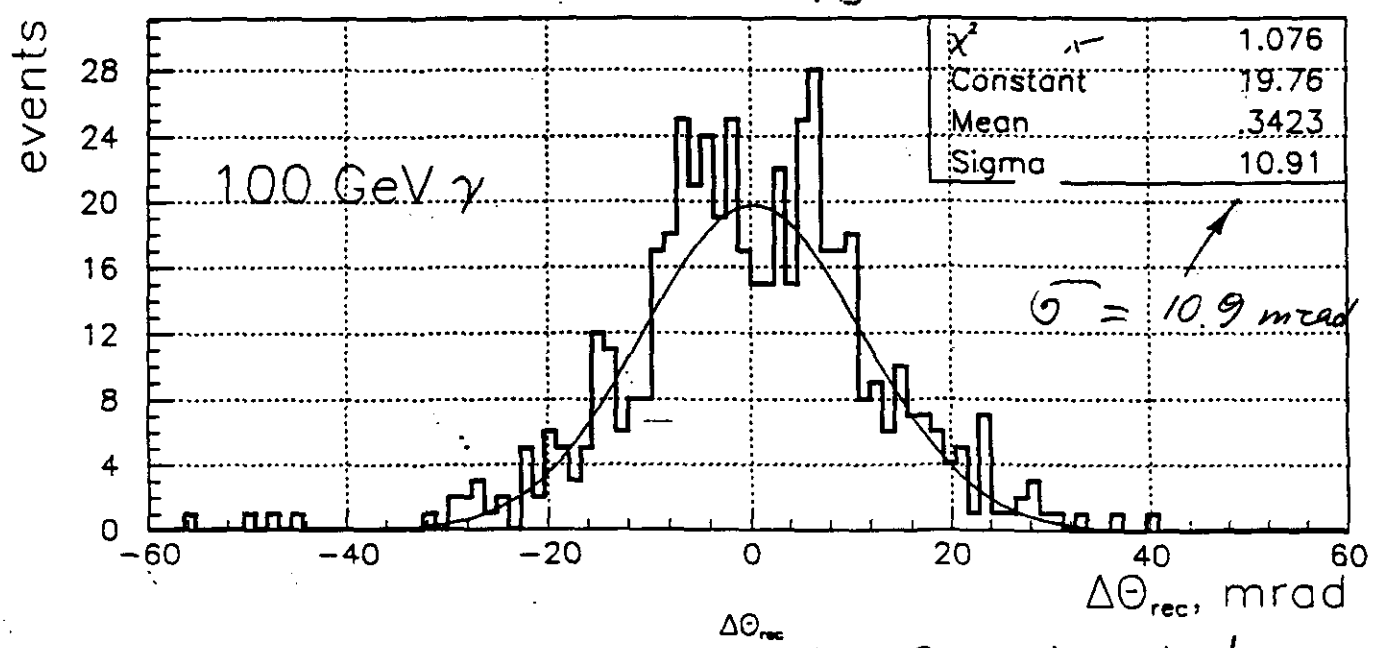

Θ – Reconstructed error

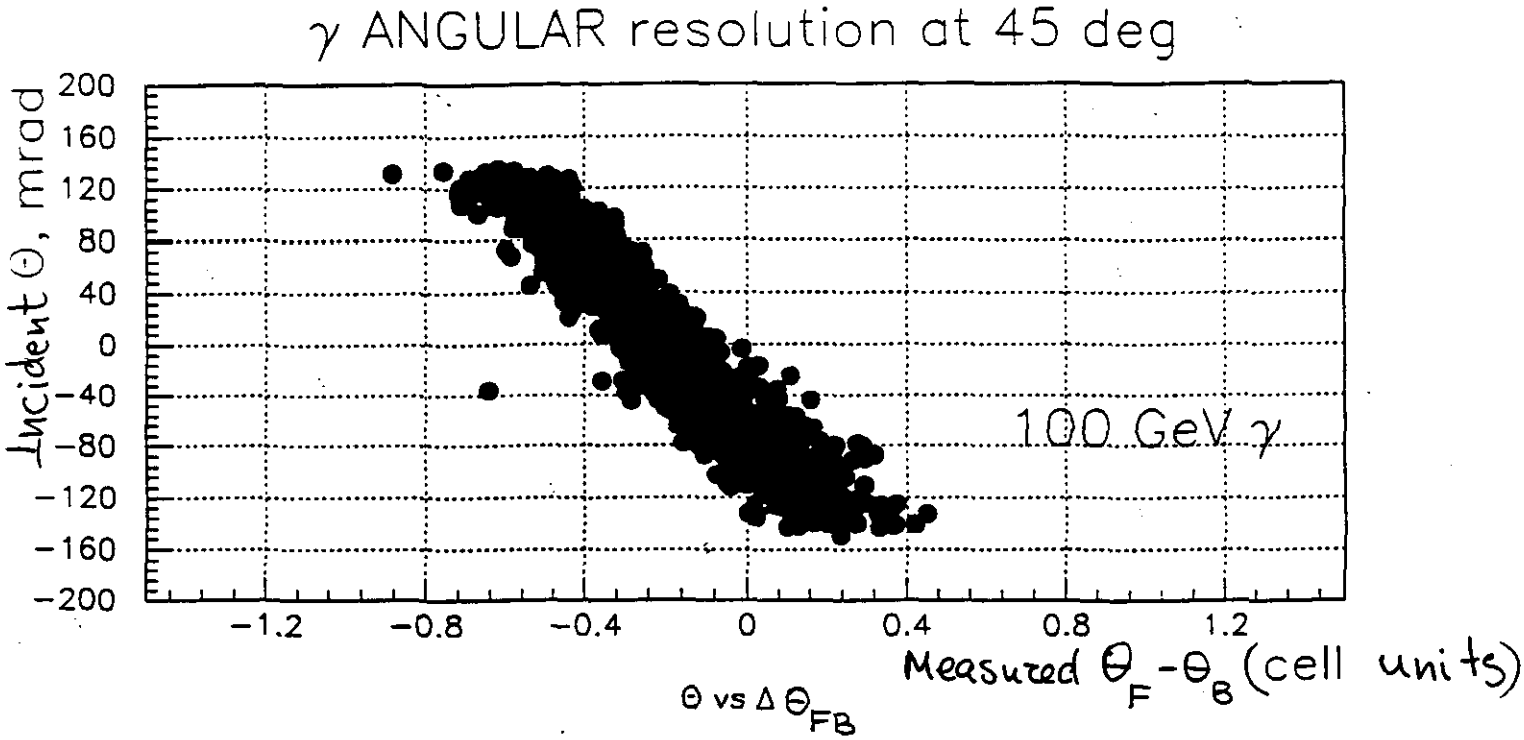

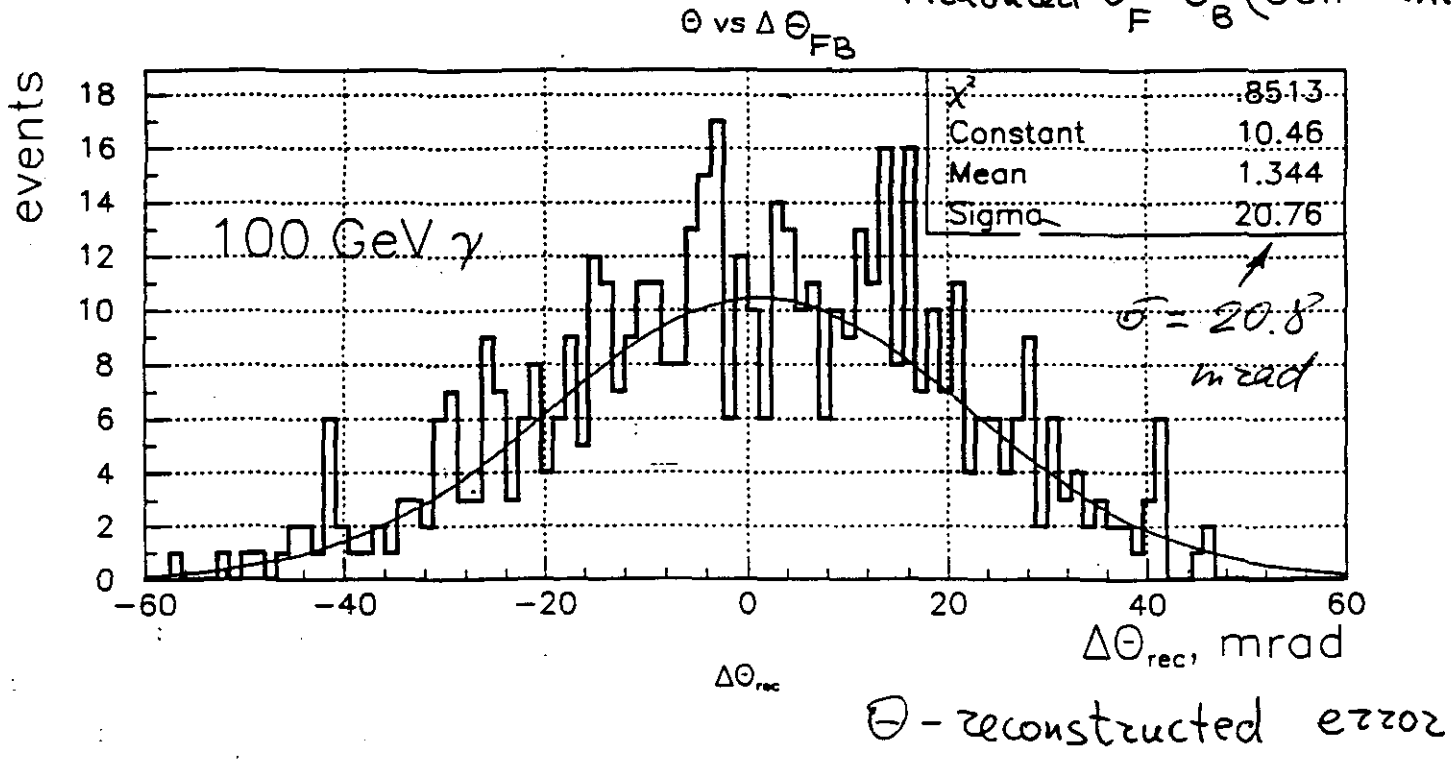

Θ - reconstructed error

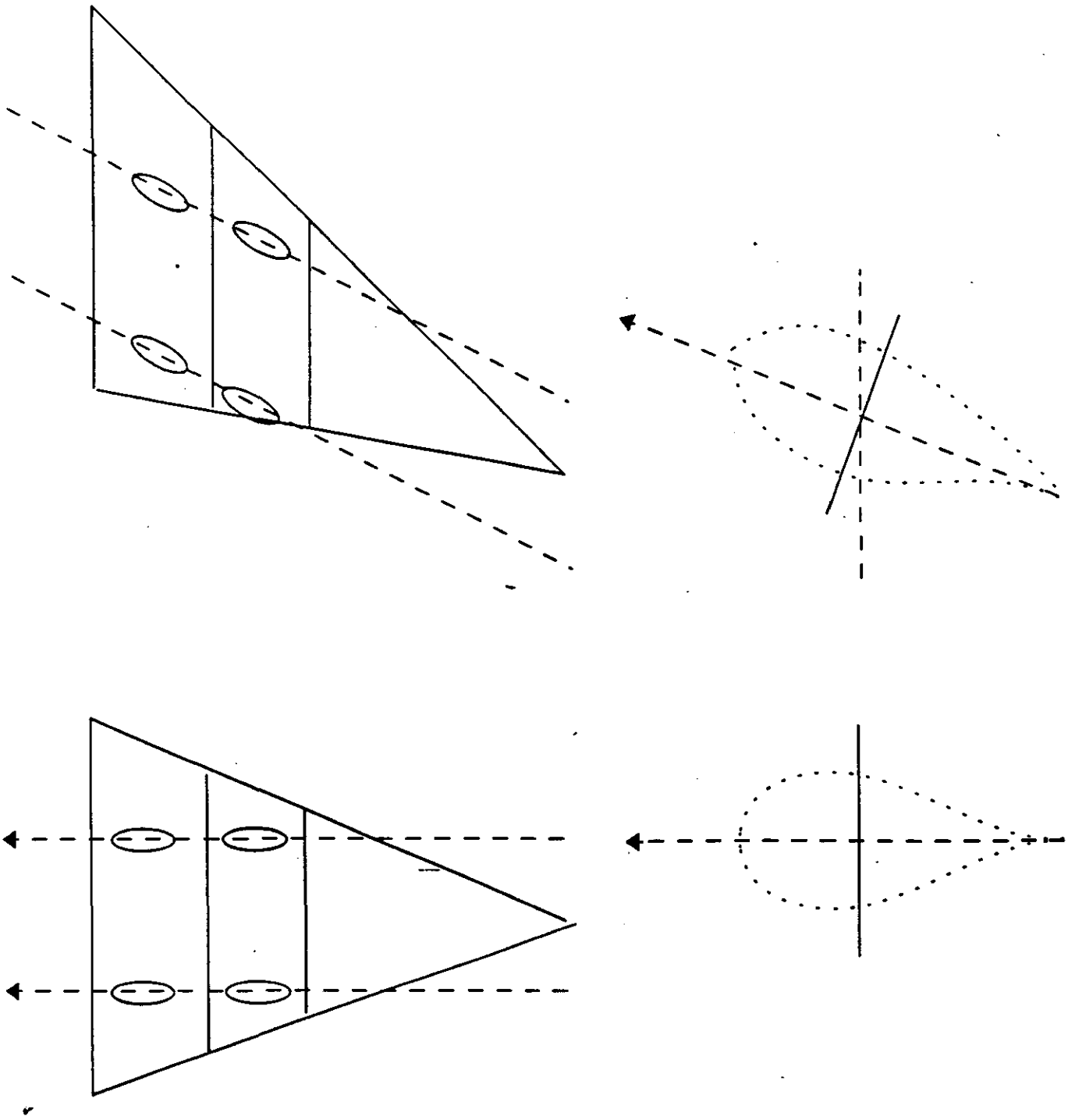

TO IMPROVE δZ, δΘ ?

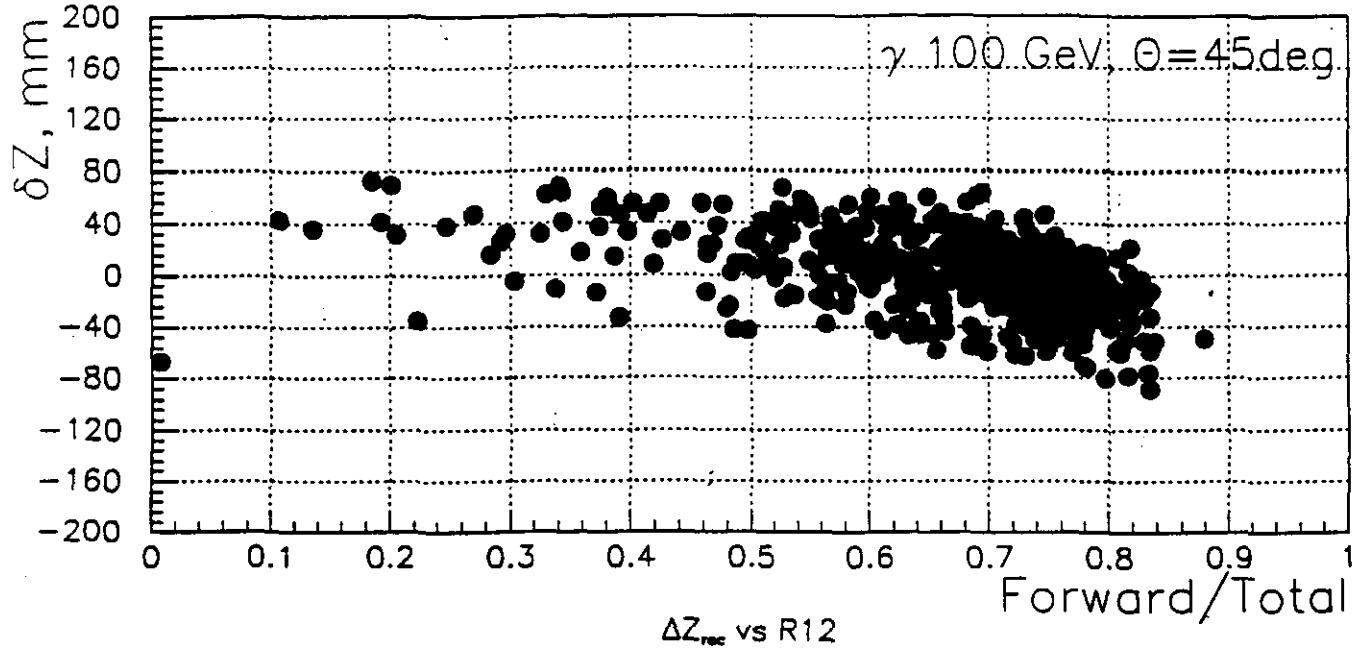

ΔZ_{rec} vs R12

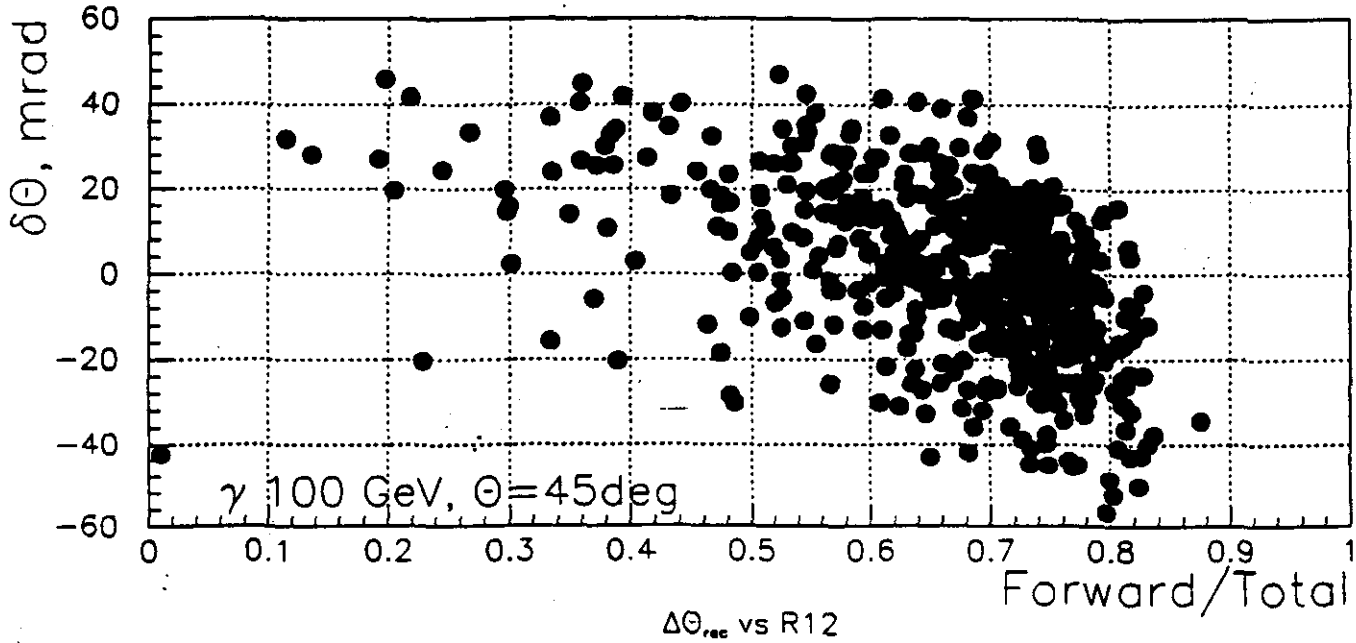

$\Delta\Theta_{rec}$ vs R12

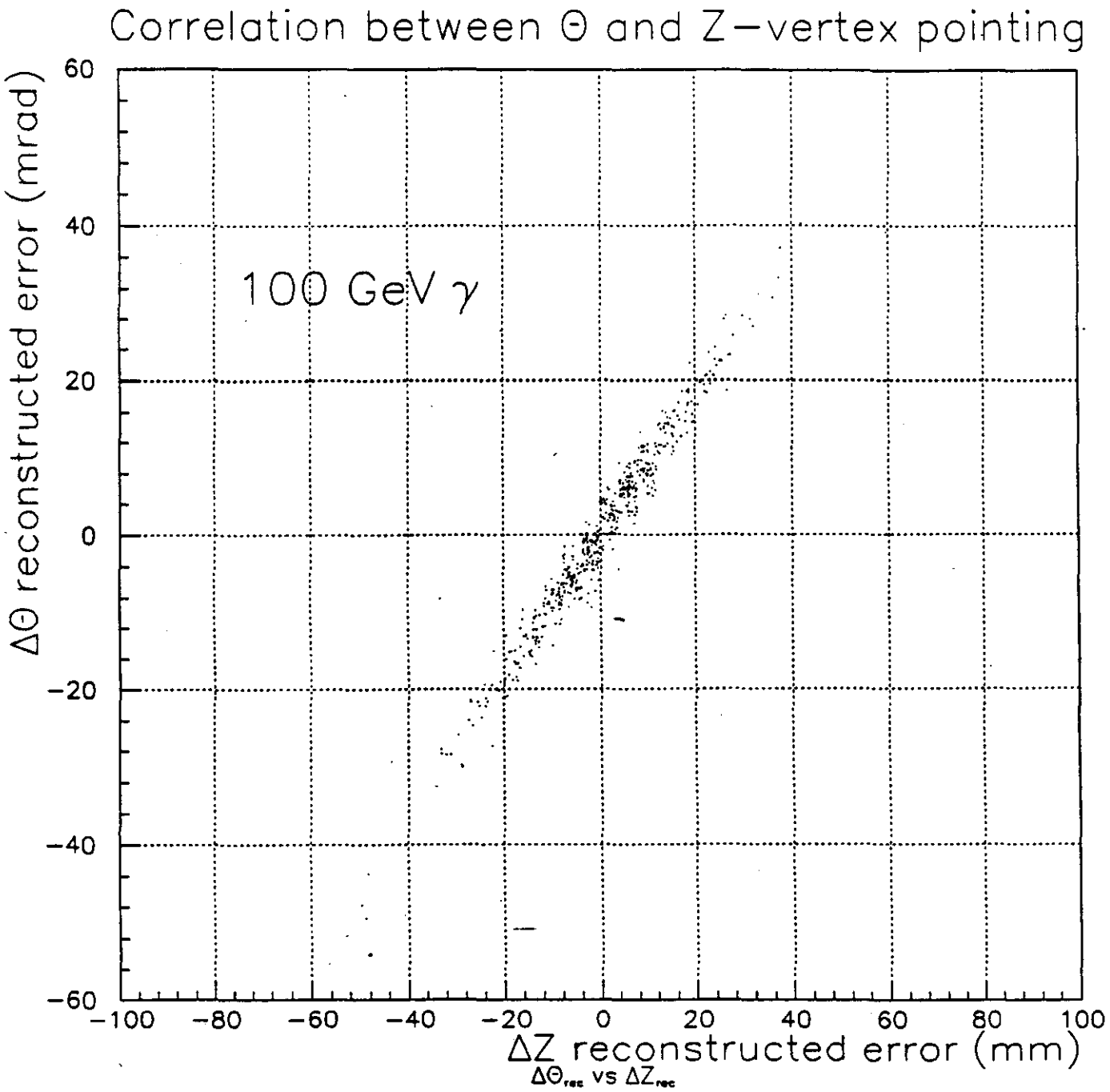
Correlation between Θ and Z−vertex pointing
100 GeV γ
ΔΘ reconstructed error (mrad)
ΔZ reconstructed error (mm)
ΔΘrec vs ΔZrec
60
40
20
0
−20
−40
−60
−100
−80
−60
−40
−20
0
20
40
60
80
100

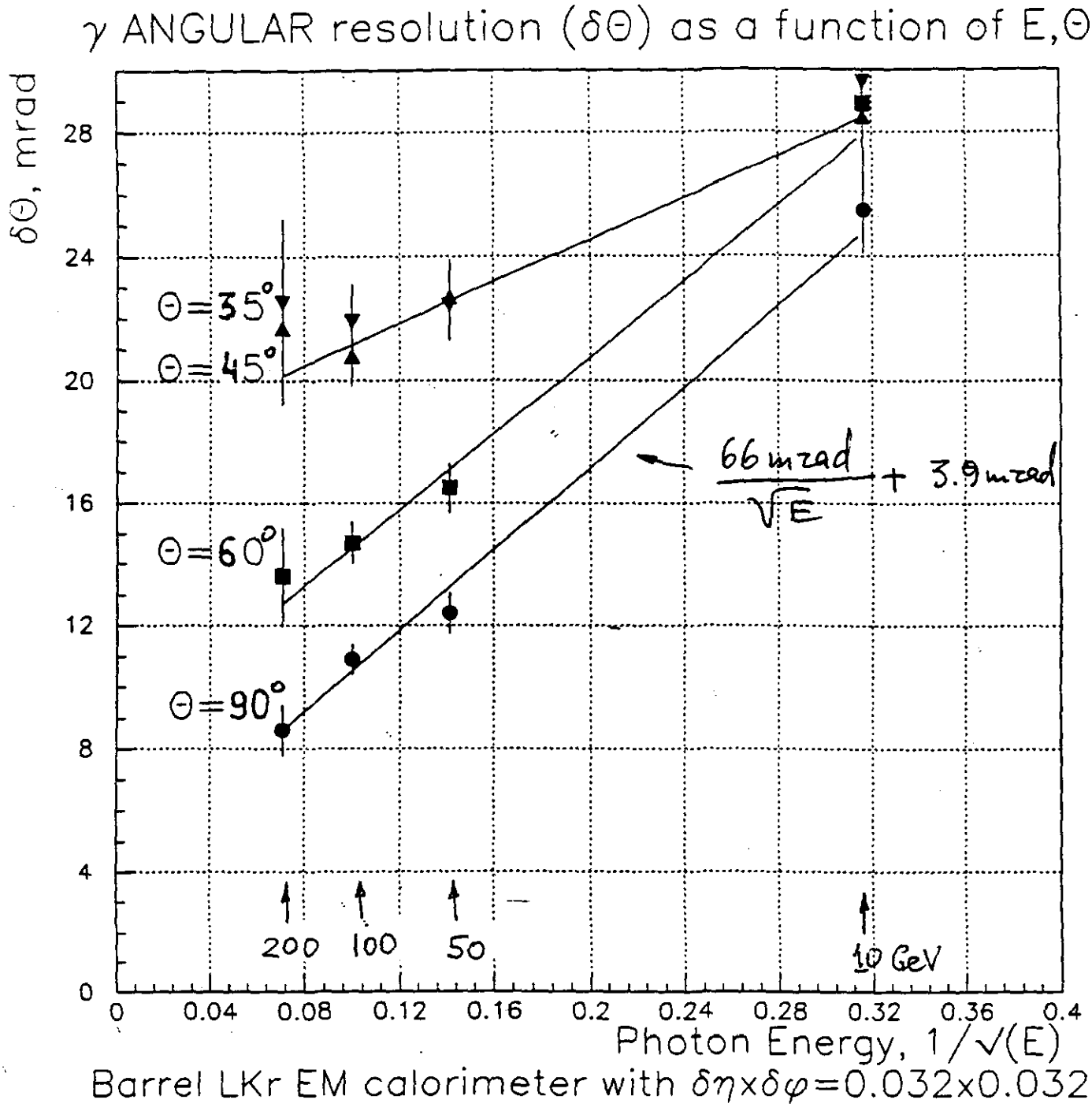
γ ANGULAR resolution (δΘ) as a function of E,Θ
δΘ, mrad
28
24
20
16
12
8
4
0
Θ=35°
Θ=45°
Θ=60°
Θ=90°
66 mrad / √E + 3.9 mrad
200
100
50
10 GeV
0
0.04
0.08
0.12
0.16
0.2
0.24
0.28
0.32
0.36
0.4
Photon Energy, 1/√(E)
Barrel LKr EM calorimeter with δη×δφ=0.032×0.032

Constant term in ANGULAR and Z−VERTEX resolution

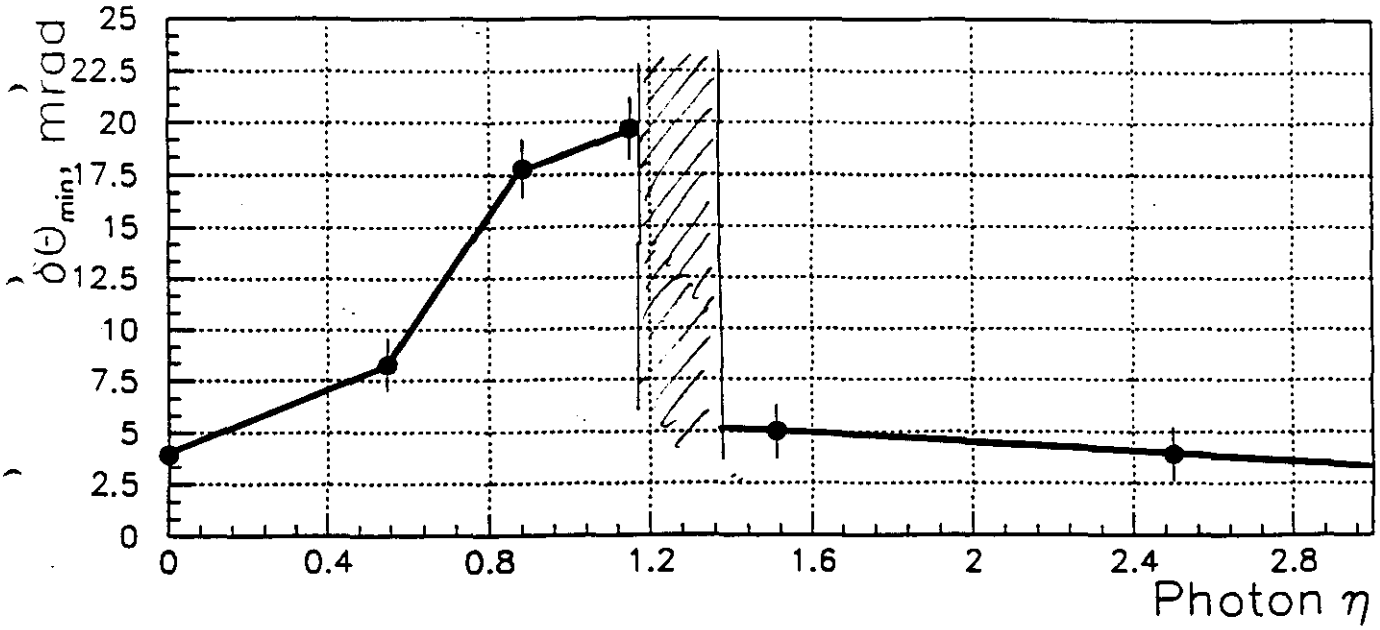

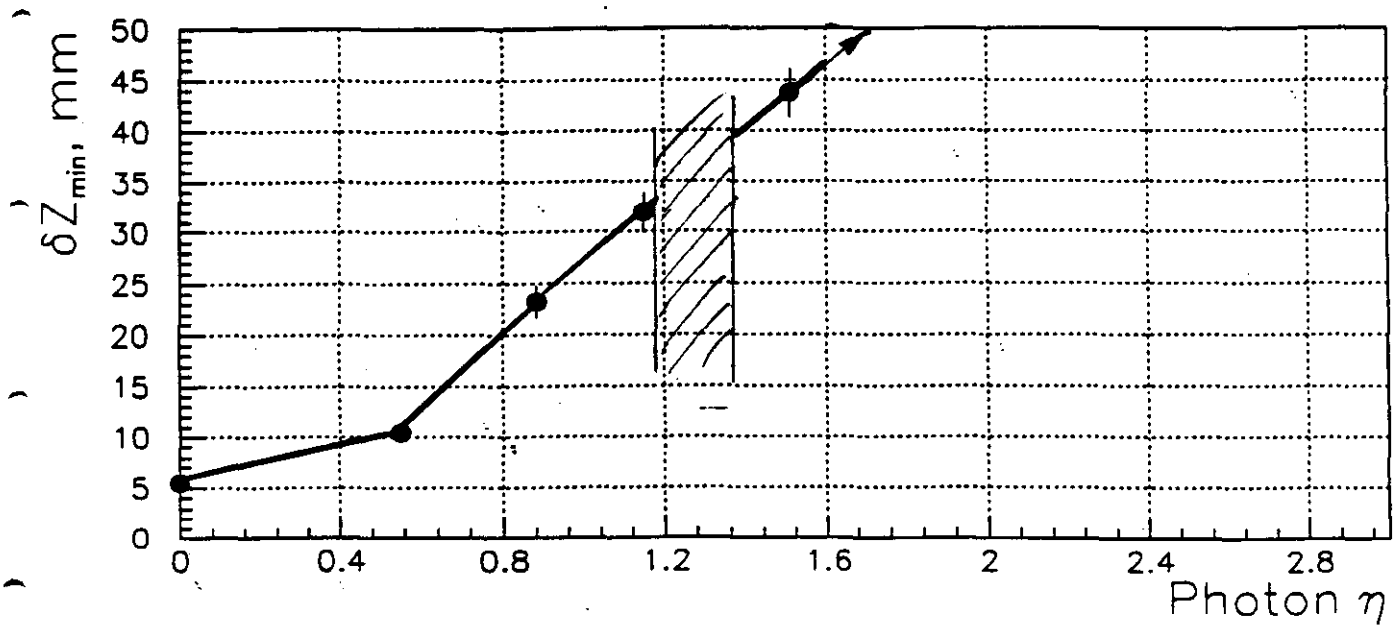

projective wall $\eta = 1.18 - 1.39$

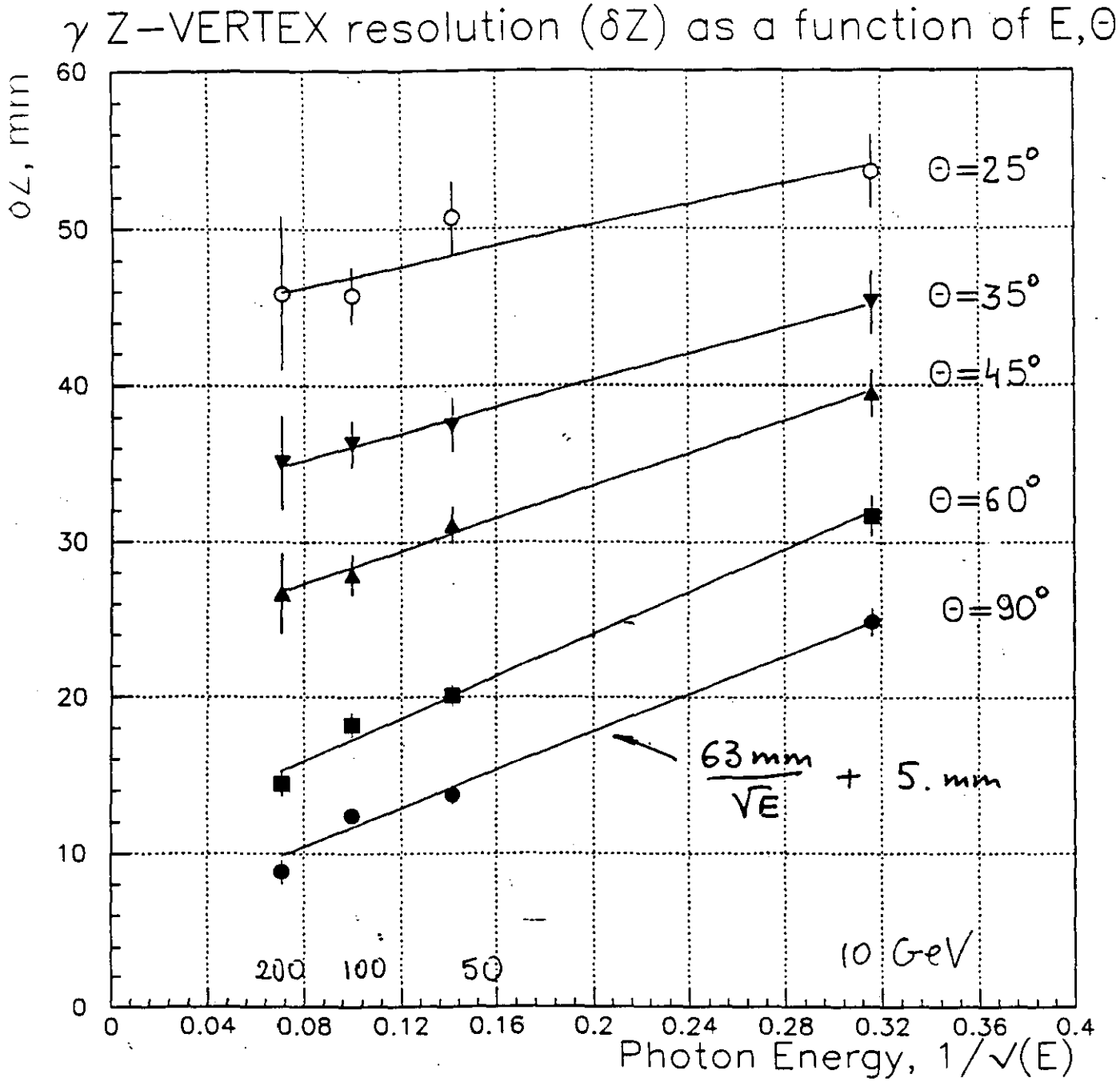

Barrel LKr EM calorimeter with $\delta\eta \times \delta\varphi = 0.032 \times 0.032$

"Stochastic" term in ANGULAR and Z-VERTEX resolution

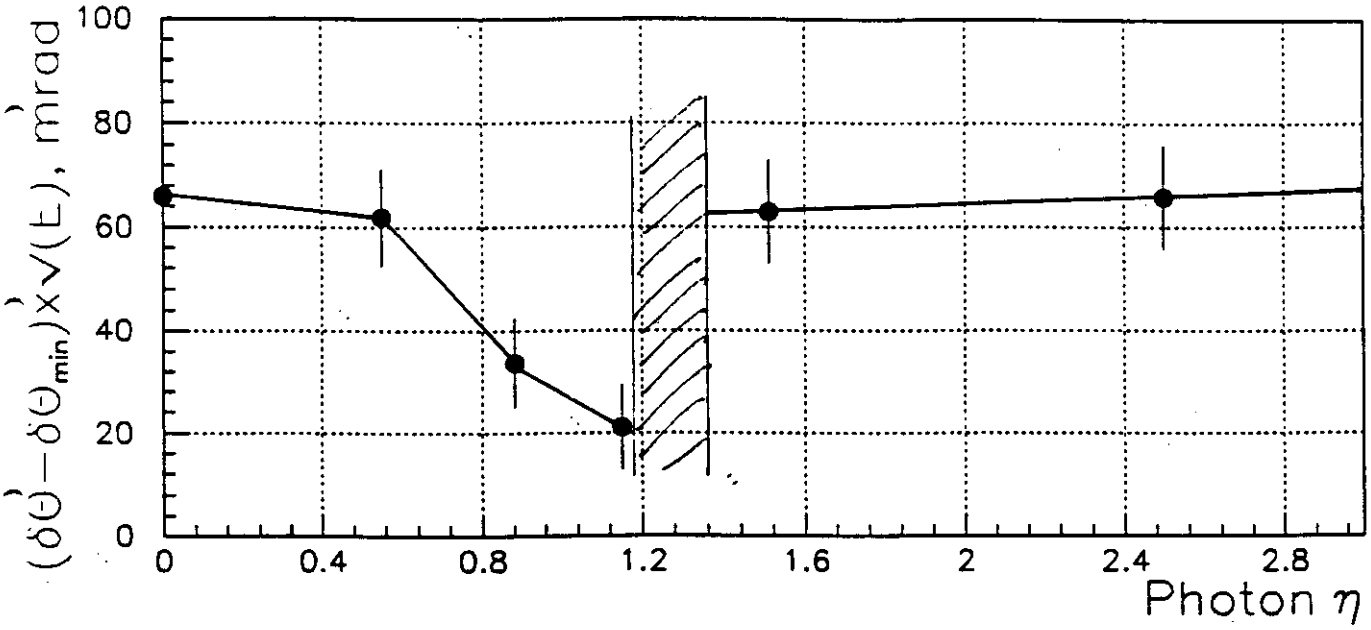

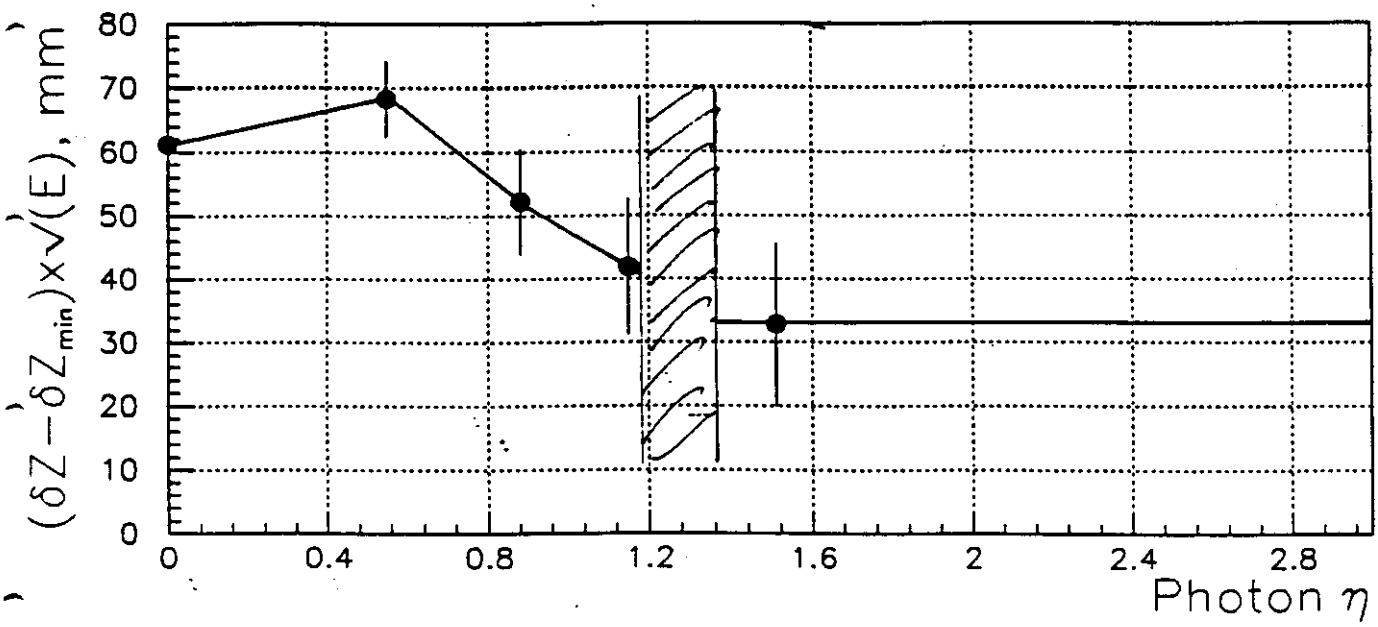

projective wall $\eta = 1.18 - 1.39$

LKr (Barrel)/LAr (Endcap), 10**33 Luminosity

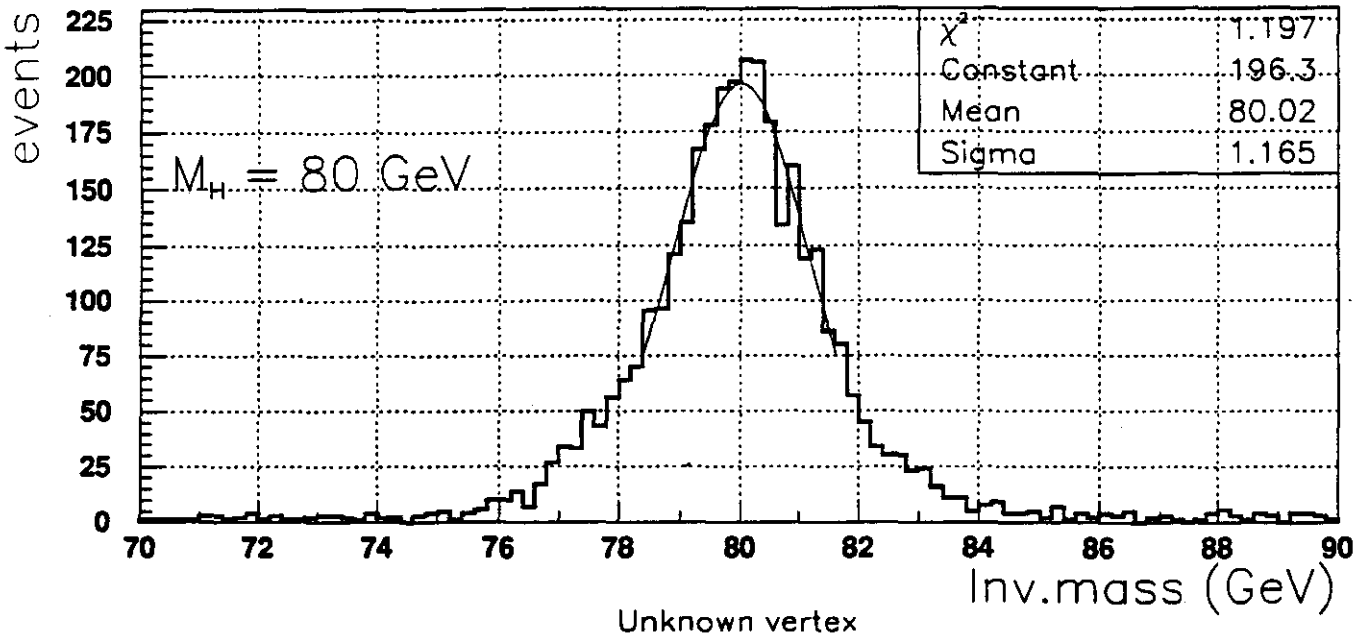

Unknown vertex

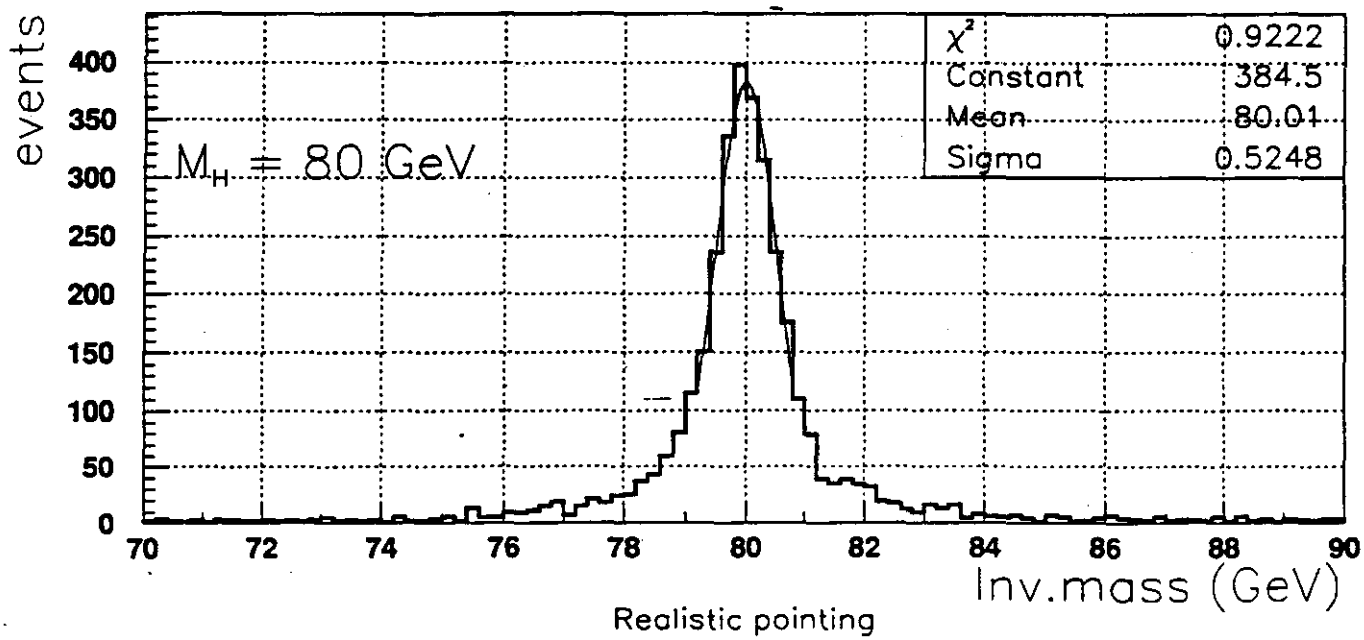

Realistic pointing

LKr (Barrel)/LAr (Endcap), 10**33 Luminosity

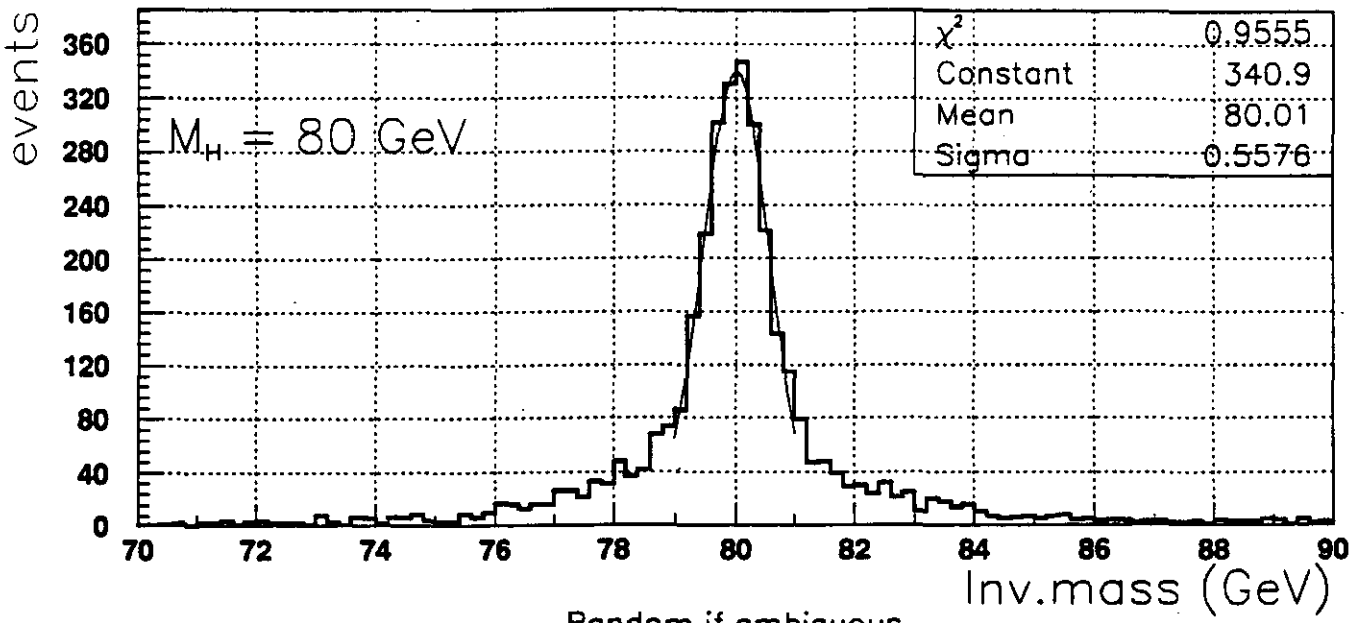

Random if ambiguous

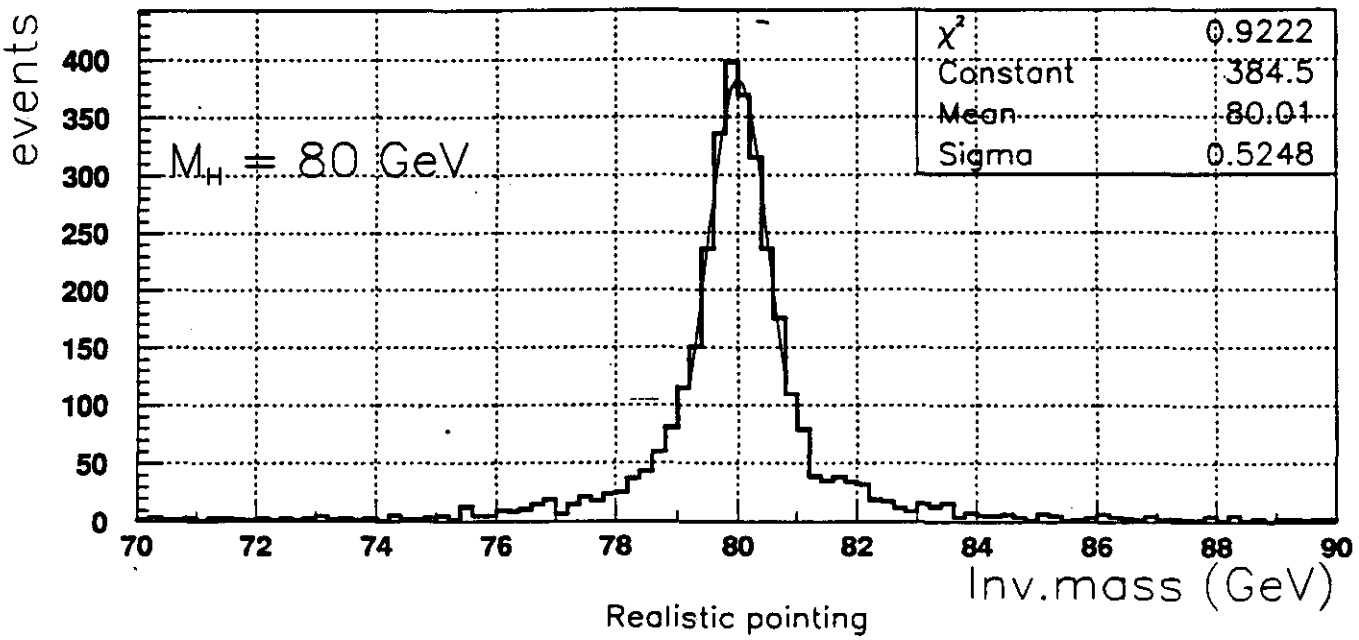

Realistic pointing

LKr (Barrel)/LAr (Endcap), 10**34 Luminosity

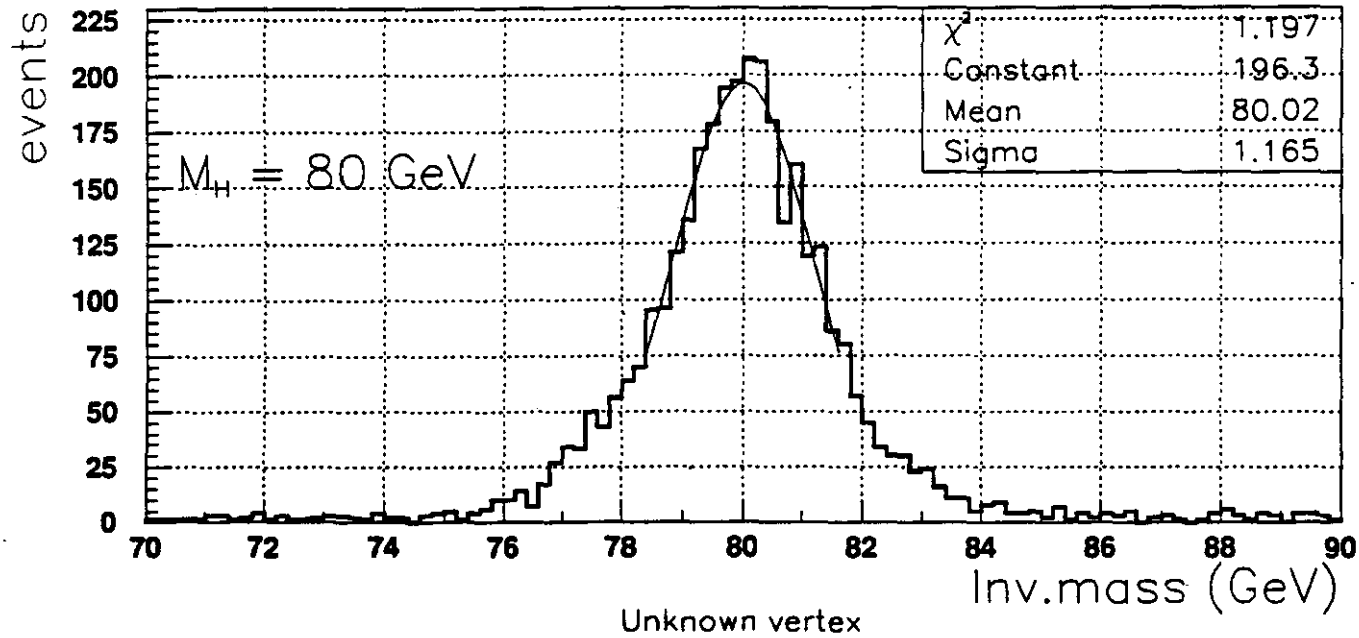

Unknown vertex

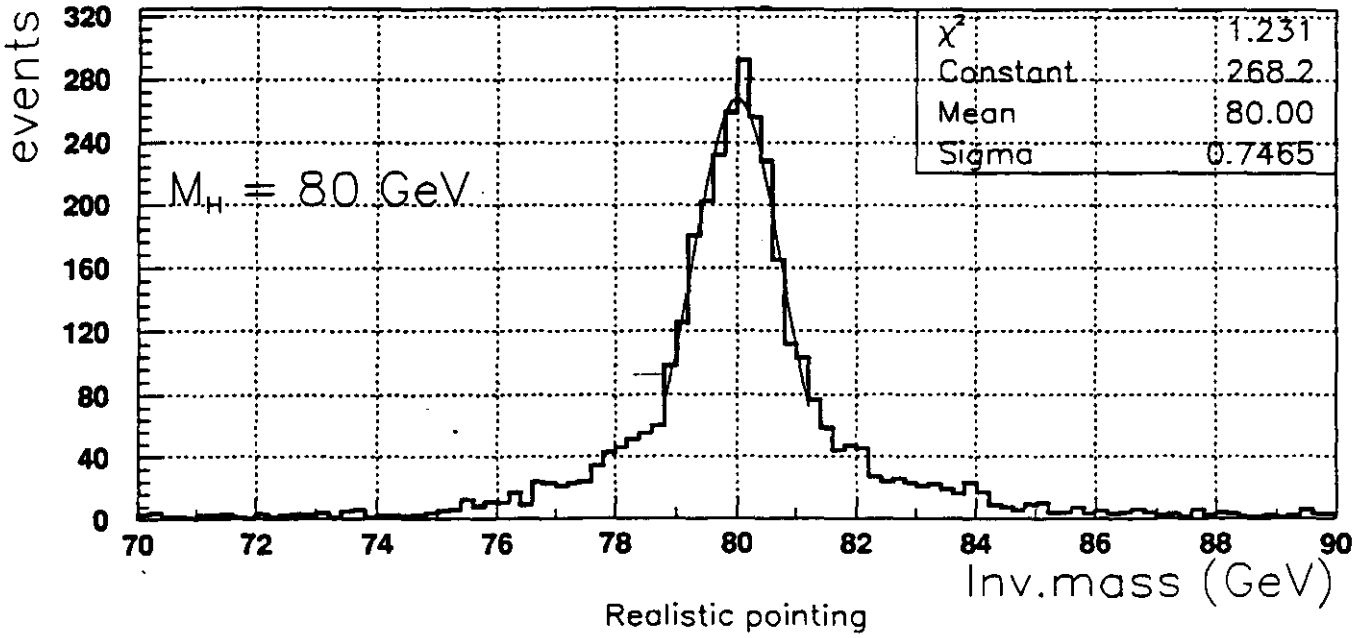

Realistic pointing

LKr (Barrel)/LAr (Endcap), 10**34 Luminosity

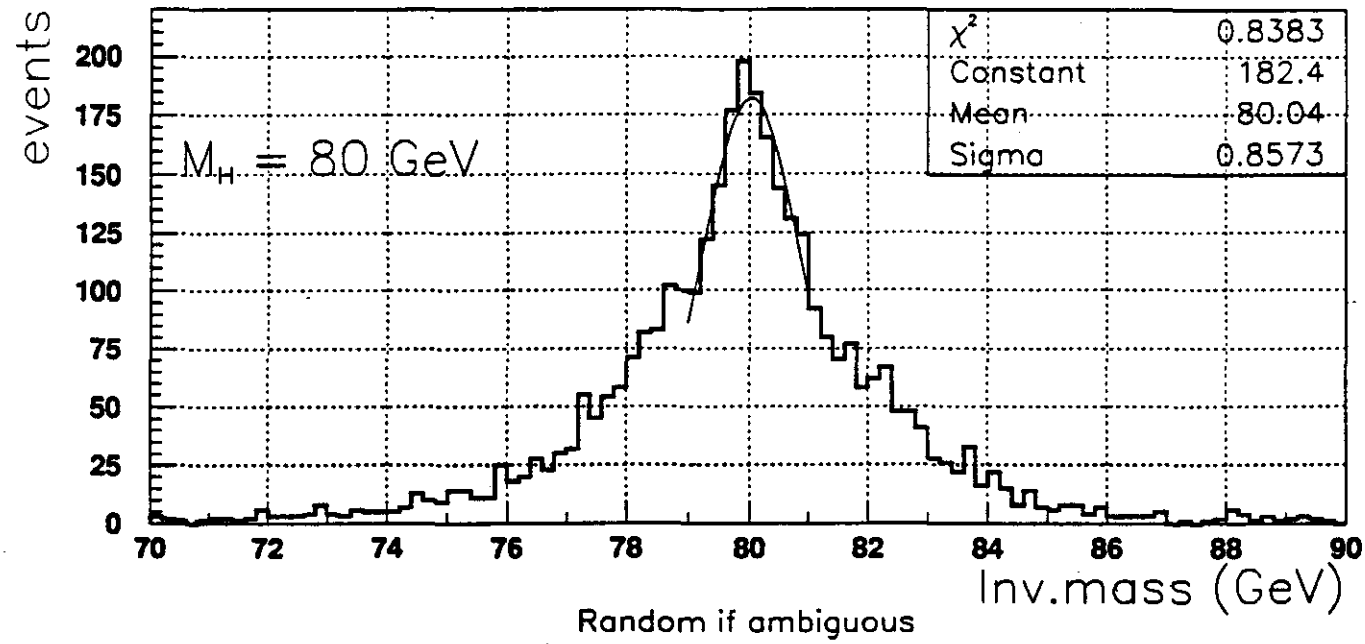

Random if ambiguous

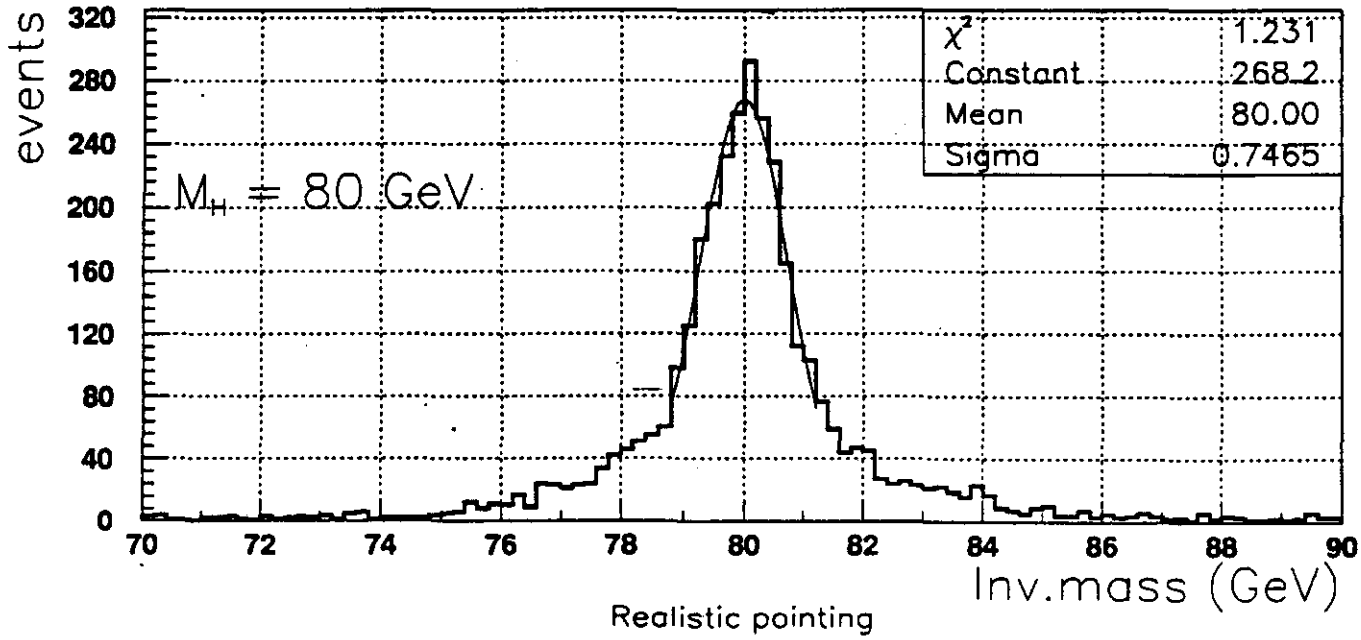

Realistic pointing

RECONSTRUCTION OF H0 MASS IN EM CALORIMETER

!!! ASSUMING THE SAME BACKGROUNDS !!!

$\left(\frac{S}{\sqrt{\sigma}}\right)^{-1}$

H0 mass = 80 GeV

	Sigma peak (GeV)	Nevents *	Time discovery factor *
1 H0 vertex only			
Ideal Calorimeter $\sigma/E = 5.5\%/\sqrt{E}$	0.42	100	1
Known vertex (parametrised resolution and dead regions included)	0.47	86	1.22
Unknown Vertex	1.17	78	2.13
Luminosity L = 10**33 , 1 H0 vertex is accompa by an average 1.6 MB			
Random vertex (if ambiguous)	0.56	65	1.77
Realistic pointing	0.53	69	1.47
Luminosity L = 10**34 , 1 H0 vertex is accompa by an average 16 MBE			
Random vertex (if ambiguous)	0.86	53	2.68
Realistic pointing	0.75	68	1.95

* Assuming for "Ideal" calorimeter 100 ev/peak (cuts and $\eta \in [-3;3]$ were applied)

** Assuming 1. for "Ideal" calorimeter

Howard Gordon

NOISE CALCULATIONS + MEASUREMENTS for LAr/Kr Calorimetry

(still evolving)

(In consultation with W.E. Cleland, V. Radeka, S. Rescia + E. Stern)

1) Measurement of thermal noise in "2mm" Accordion Tests

$t_p = 40ns$ 1.75kV, Ar not completely pure

		Baseline I	3x3	5x5
Ar	35 MeV/Tower	28	105	175
Kr	20 MeV/Tower		60	100

1.5kV not pure

1) dE/dx higher than Ar
2) preamp noise lower @ 120K

2) Cleland and Stern find $\sigma_E = 1.5\,GeV\,(A)^{0.76}$

$A = \Delta\eta \times \Delta\varphi$

eg $R = 0.6$ for "32ns gate" $\sigma_E = 3.3\,GeV$

3) $\sigma_T = \sqrt{\sigma_{TH}^2 + \sigma_{PU}^2}$ $\quad \sigma_{TH} \sim (1/t_p)^{3/2}$, $\sigma_{PU} = \sigma_E \sqrt{I_2 P/16ns}$

$\sim t_p^{1/2}$

σ_T (GeV) (t_p)(ns)

	Ar	Kr
0.08x0.08	0.154 (140)	0.128 (100)
R=0.45	3.8 (80)	3.14 (60)
R=0.60	5.7 (80)	4.6 (50)

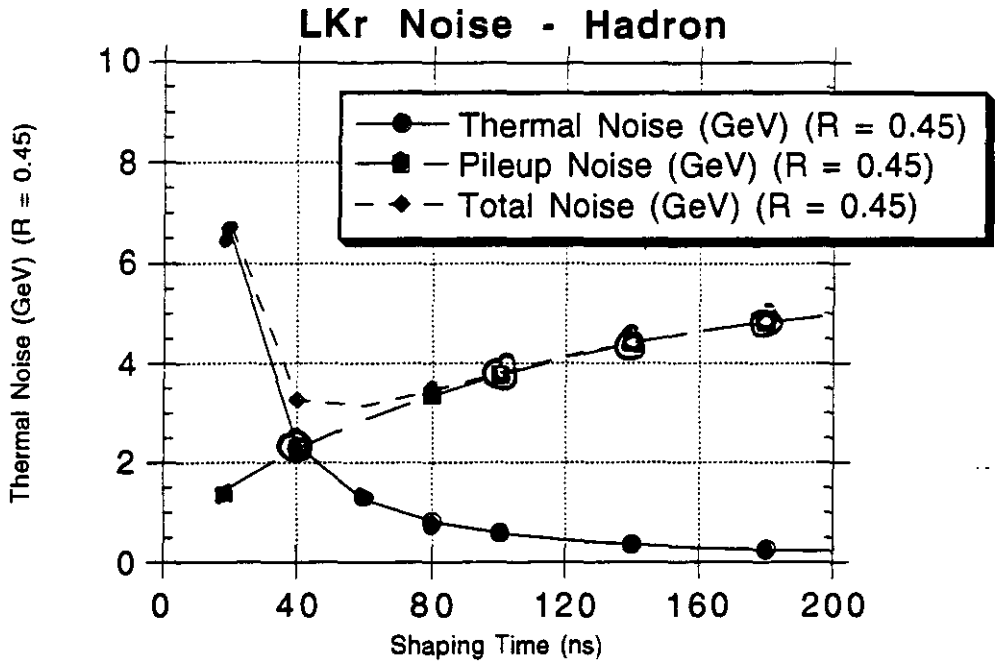
LKr Noise - Hadron
Thermal Noise (GeV) (R = 0.45)
Pileup Noise (GeV) (R = 0.45)
Total Noise (GeV) (R = 0.45)
Thermal Noise (GeV) (R = 0.45)
Shaping Time (ns)
0
2
4
6
8
10
0
40
80
120
160
200